Development of a Spatial Severity Model for the Quantification of Wildland Fire Effects in Coniferous Forests

A Dissertation
Presented in Partial Fulfillment of the Requirements for the
Degree of Doctorate of Philosophy
with a
Major in Natural Resources
in the
College of Graduate Studies
University of Idaho
by

Aaron M. Sparks

Major Professors: Crystal A. Kolden, Ph.D.; Alistair M. S. Smith, Ph.D.
Committee Members: Luigi Boschetti, Ph.D.; Dan M. Johnson, Ph.D.;
Mark A. Cochrane, Ph.D.
Department Administrator: Randall H. Brooks, Ph.D.

May 2017

Authorization to Submit Dissertation

This dissertation of Aaron M. Sparks, submitted for the degree of Doctor of Philosophy with a major in Natural Resources and titled "Development of a Spatial Severity Model for the Quantification of Wildland Fire Effects in Coniferous Forests," has been reviewed in final form. Permission, as indicated by the signatures and dates given below, is now granted to submit final copies to the College of Graduate Studies for approval.

Major Professor: _____ Date: _____
Crystal A. Kolden, Ph.D.

Co-Major Professor: _____ Date: _____
Alistair M. S. Smith, Ph.D.

Committee Members: _____ Date: _____
Luigi Boschetti, Ph.D.

_____ Date: _____
Daniel M. Johnson, Ph.D.

_____ Date: _____
Mark A. Cochrane, Ph.D.

Department Administrator: _____ Date: _____
Randall H. Brooks, Ph.D.

Abstract

Fire is an integral change agent in the Earth system and plays key roles in nutrient cycling, plant species distribution, atmospheric composition and ecosystem service function at temporal scales ranging from years to centuries and spatial scales ranging from micro to continental. Increased fire activity (intensity, frequency, and size) in North American forested ecosystems has been observed and predicted under warmer and drier climate conditions. As forested ecosystems serve as significant carbon sinks, there is an urgent need to improve our understanding of fire intensity impacts on forest productivity and recovery post-fire. The research within this dissertation is focused on advancing our current understanding by identifying mechanistic relationships between fire intensity and post-fire tree response (e.g. mortality, physiology, growth and vulnerability) that enable spatiotemporal characterization of fire effects. This research tested the hypothesis that increasing quantities, or 'doses', of fire intensity lead to predictable responses in terms of tree mortality or physiological function. This hypothesis was first tested using nursery grown *Pinus contorta* and *Larix occidentalis* seedlings subjected to highly controlled laboratory surface fires. A dose-response relationship was demonstrated between fire radiative energy and post-fire seedling mortality and physiological function. Additionally, this relationship was shown to be detectable using spectral indices common to plant physiology research. The dose-response hypothesis was further tested at the mature tree scale by using prescribed fires in mature *Pinus ponderosa* forest stands. Increasing levels of peak fire radiative power were observed to lead to reduced post-fire radial growth. Permanent defense structures, axial resin ducts, were found to increase in density, size, and area per growth ring post-fire regardless of fire intensity. Finally, observations from satellite based remote sensing were used to test the dose-response hypothesis at the landscape spatial scale. Similar to observations at the tree scale, satellite measures of forest productivity decreased with increasing fire radiative power. Species composition was demonstrated to influence the magnitude of productivity loss post-fire. Ultimately, the work in this dissertation demonstrates a framework to spatially characterize individual tree and forest condition post-fire, improving our understanding of the carbon cycle and ability to sustainably manage forests.

Acknowledgements

I would like to first express my gratitude to my co-major advisors, Crystal Kolden and Alistair Smith, for their guidance and support. Thank you for pushing me to excel beyond average and encouraging me to pursue research far 'down the rabbit hole'. I extend my gratitude to my committee members: Luigi Boschetti, Mark Cochrane, and Dan Johnson. Thank you for not 'sugar coating' anything. Your demanding questions and constructive criticism helped me become a better scientist.

A debt of thanks is owed to the 2014-2015 UI Research Crew for their help with fieldwork. I would undoubtedly still be 'counting sticks' if not for your hard work. Additionally, the prescribed fires that were central to this dissertation would not have been successful without planning and assistance from UI Experimental Forest staff-especially Rob Keefe and Brian Austin, Penny Morgan, Heather Heward, Zack Lyon, Connor Bell, and UI undergraduate students. Thank you office mates of Phinney 301 and McClure 219 for the enlightening, and entertaining, conversations that were had over many pints, poker chips, and powder days.

I also thank my family for their unwavering support. I'm not sure I would be in the position I am today without the strong work ethic instilled in me by my parents. I especially thank Amanda Argona for supporting and sharing this crazy chapter of life with me.

Most importantly, I thank the following organizations for funding this work: National Aeronautics and Space Administration (NASA), Idaho Space Grant Consortium, Joint Fire Science Program GRIN Award 16-2-01-09 and Award 13-1-05-7, and the National Science Foundation Hazards SEES award #1520873.

Dedication

A Dissertation Haiku:

To friends and colleagues

Who worked hard and played harder

We discovered life

Table of Contents

List of Figures

List of Tables

Chapter 1
Advancing Our Understanding of Fire Intensity Impacts on Tree Mortality, Physiology, Growth and Vulnerability

Introduction

Fire has been an integral part of life on Earth for millennia (Bowman et al. 2009). Fire plays key roles in nutrient cycling, plant species distribution, atmospheric composition and ecosystem service function at temporal scales ranging from years to centuries and spatial scales ranging from micro to continental. Increased fire activity (intensity, frequency, and size) in North American forested ecosystems has been observed and predicted under warmer and drier climate conditions (Balshi et al. 2009; Spracklen et al. 2009; IPCC 2013; Barbero et al. 2015; Abatzoglou and Williams 2016). As forested ecosystems serve as significant carbon sinks (IPCC 2013), there is an urgent need to improve our understanding of variable fire intensity impacts on forest productivity and recovery post-fire. Accurate characterization of post-fire forest condition is crucial for carbon accounting (Goetz et al. 2007; Goulden et al. 2011) and other ecosystem service assessments (Noss et al. 2006; Smith et al. 2014). Additionally, prediction of fire effects (e.g., tree mortality/decrease in physiological performance) is necessary for land-use planning and management (Moritz et al. 2014) such as the development of prescribed burn and wildland fire management plans (Butler and Dickinson 2010). While many fire effects models exist, few spatially quantify post-fire ecological and physiological characteristics, limiting our understanding of ecosystem carbon dynamics and our ability to manage landscapes pre- and post-fire (Reinhardt and Dickinson 2010).

Assessments of post-fire effects are important for immediate post-fire rehabilitation efforts (e.g., Burned Area Emergency Response, BAER) (Parsons 2003), decadal scale trajectories of ecosystem recovery (Hicke et al. 2003), and the projected impacts on the terrestrial carbon cycle (Hicke et al. 2003; Lentile et al. 2006; Goulden et al. 2011). Common metrics used for determining post-fire effects in ecosystems can be grouped under the term ‘burn severity’. Burn severity is loosely defined as the degree to which an ecosystem has changed due to a fire and encompasses both vegetation and soil effects (Key and Benson 2006). Biomass consumption, vegetation mortality, and soil infiltration/water

repellency are examples of common field metrics of burn severity (Lentile et al. 2006; Lewis et al. 2006). Burn severity assessments at local to regional scales are typically achieved using spectral reflectance indices derived from satellite remote sensing data before and following the fires (Lentile et al. 2006). These remotely sensed assessments can provide useful information regarding the areal extent of fires and vegetation cover change (Kolden et al. 2015; McCarley et al. 2017). However, current assessments and fire effects models provide little to no direct information regarding the physiological processes of trees or other surviving vegetation following wildfires (Smith et al. 2016), which is an important factor in determining effects on ecosystem services and post-fire land management planning.

Recent studies in plant physiology have observed that various tree physiology metrics respond to localized variations in heat (Butler and Dickinson 2010; Kavanagh et al. 2010; Michaletz et al. 2012) and increasing fire intensity from surface fires (Smith et al. 2016, 2017; Sparks et al. 2016, 2017). While research has not identified the dominant mode of heat transfer (e.g. conduction, convection, radiation) that drives post-fire vegetation physiological response and mortality, increasing quantities, or doses, of radiative flux metrics (e.g. fire radiative power, units: Watts; fire radiative energy, units: Joules) from surface fires have been linked with physiological responses in trees (Smith et al. 2016, 2017). Radiative flux metrics are useful in fire effects quantification as they are strongly related to common fire behavior metrics such as fireline intensity (Kremens et al. 2012; Sparks et al. 2017) as well as the total convective energy released during combustion (Freeborn et al. 2008; Butler et al. 2015), and they are some of the more easy-to-measure fire behavior metrics at large distances (e.g., airborne and satellite remote sensing) (Kremens et al. 2010). Coupling fire behavior-physiology observations to landscape-scale remote sensing could help to overcome the limitations associated with current severity assessments and promote quantitative measures that increase our understanding of carbon cycling and tree recovery and mortality post-fire (Smith et al. 2016).

In this dissertation I sought to explore and quantify links between fire intensity and tree physiological processes and growth at individual tree and landscape spatial scales (Figure 1). The analyses are supported by laboratory, field, and satellite data. These data, and any models that are produced, serve as a methodological framework that can either predict fire

effects using active fire observations from field/remotely sensed data, or characterize fire effects using post-fire remotely sensed data.

Scope and Objectives

The goal of this work was to advance our understanding of fire intensity impacts on tree mortality, physiology, growth and vulnerability and identify mechanistic relationships that enable spatiotemporal characterization of these effects. The tree species in this dissertation are limited to typical conifers found in the northwestern United States temperate forests. Figure 1 presents a conceptual diagram that highlights key findings and future work associated with this dissertation.

The main objectives of this work were to 1) quantify the linkages between fire intensity, physiology, and spectral response of tree seedlings in a laboratory setting using ground based remote sensing, 2) quantify the linkages between fire intensity, tree physiology, and post-fire vulnerability of mature trees in a forest stand using ground-based forest measurements and *in situ* remote sensing, and 3) understand how fire intensity affects post-fire productivity in conifer-dominated forested ecosystems using landscape remote sensing observations.

Chapter Summaries

The chapters in this dissertation are formatted according to the manuscript structure required for each journal.

Chapter 2 quantifies dose-response relationships between fire radiative energy and seedling growth and mortality. This chapter also explores the suitability of common spectral indices for detecting this relationship. This chapter answers the following questions: Is there a dose-response relationship between fire radiative energy and post-fire growth and mortality? Does increasing dose of radiative energy lead to increased mortality at extended time scales (1 year post-fire)? Can decreasing levels of physiological performance be detected using common spectral indices? Chapter 2 was published in *Remote Sensing* with Crystal Kolden, Alan Talhelm, Alistair Smith, Kent Apostol, Daniel Johnson, and Luigi Boschetti (Sparks et al. 2016).

Chapter 3 builds upon Chapter 2 and quantifies relationships between fire radiative metrics and mature *Pinus ponderosa* growth. This chapter answers the following questions: Is there a dose-response relationship between metrics of fire intensity and radiative flux and the post-fire mature tree growth? If yes, are the radiative heat flux metrics the same as those observed to produce dose-response relationships in seedlings and if not, why? Is there a dose-response relationship between metrics of fire intensity and fire radiative flux and mature tree defenses? Chapter 3 was published in the *International Journal of Wildland Fire* with Alistair Smith, Alan Talhelm, Crystal Kolden, Kara Yedinak, and Daniel Johnson (Sparks et al. 2017).

Chapter 4 uses landscape remote sensing observations to quantify relationships between fire intensity, estimated using fire radiative power, and forest productivity measurements. This chapter also presents a conceptual framework for spatiotemporal post-fire recovery assessments. This chapter answers the following questions: What are the relationships between fire radiative power and post-fire forest NPP at spatial scales of large wildland fires? How do these relationships vary over time? How do these relationships vary with species composition? Chapter 4 has been prepared for submission to *Journal of Geophysical Research* with Crystal Kolden, Alistair Smith, Luigi Boschetti, Dan Johnson, and Mark Cochrane.

Chapter 5 presents conclusions and questions to be addressed in future research.

References

Abatzoglou JT, Williams AP (2016) Impact of anthropogenic climate change on wildfire across western US forests. *Proceedings of the National Academy of Sciences* **113**, 11770-11775.

Balshi MS, McGuire AD, Duffy P, Flannigan M, Kicklighter DW, Melillo J (2009) Vulnerability of carbon storage in North American boreal forests to wildfires during the 21st century. *Global Change Biology* **15**, 1491-1510.

Barbero R, Abatzoglou JT, Larkin NK, Kolden CA, Stocks B (2015) Climate change presents increased potential for very large fires in the contiguous United States, *International Journal of Wildland Fire* **10**, 1071.

Bowman DMJS, Balch JK, Artaxo P, Bond WJ, Carlson JM, Cochrane MA, D'Antonio CM, DeFries RS, Doyle JC, Harrison SP, Johnston FH, Keeley JE, Krawchuk MA, Kull CA, Marston JB, Moritz MA, Prentice IC, Roos CI, Scott AC, Swetnam TW, van der Werf

GR, Pyne SJ (2009) Fire in the earth system, *Science* **324**, 5926, 481-484, DOI: 10.1126/science.1163886.

Butler BW, Dickinson MB (2010) Tree heating and injury in fires: developing process-based models, *Fire Ecology* **6**, 55-79.

Freeborn PH, Wooster MJ, Hao WM, Ryan CA, Nordgren BL, Baker SP, Ichoku C (2008) Relationships between energy release, fuel mass loss, and trace gas and aerosol emissions during laboratory biomass fires. *Journal of Geophysical Research: Atmospheres* **113** (D1).

Goetz SJ, Mack MC, Gurney KR, Randerson JT, Houghton RA (2007) Ecosystem responses to recent climate change and fire disturbance at northern high latitudes: observations and model results contrasting northern Eurasia and North America, *Environmental Research Letters* **2**, 045031.

Goulden ML, McMillan AMS, Winston GC, Rocha AV, Manies KL, Harden JW, Bond-Lamberty BP (2011) Patterns of NPP, GPP, respiration, and NEP during boreal forest succession, *Global Change Biology*, **17**, 855-871.

Hicke JA, Asner GP, Randerson JT, Tucker C, Los S, Birdsey R, Jenkins J, Field C (2002) Trends in North American net primary productivity derived from satellite observations, 1982–1998. *Global Biogeochemical Cycles* **16**, 2-1.

IPCC (2013). The Fifth Assessment Report (AR5) of the United Nations Intergovernmental Panel on Climate Change (IPCC), Climate Change 2013: The Physical Science Basis, IPCC WGI AR5. Tech. rep., Intergovernmental Panel on Climate Change (IPCC).

Kavanagh KL, Dickinson MB, Bova AS (2010) A way forward for fire-caused tree mortality prediction: modeling a physiological consequence of fire. *Fire Ecology* **6**, 80-94.

Key CH, Benson NC (2006) Landscape assessment. FIREMON: Fire effects monitoring and inventory system. *Gen. Tech. Rep. RMRS-GTR-164-CD*, Fort Collins, CO: US Department of Agriculture, Forest Service, Rocky Mountain Research Station.

Kolden CA, Smith AMS, Abatzoglou JT (2015) Limitations and utilisation of Monitoring Trends in Burn Severity products for assessing wildfire severity in the USA. *International Journal of Wildland Fire* **24**, 1023–1028.

Kremens R, Smith A, Dickinson M 2010 Fire Metrology: Current and Future Directions in Physics-Based Measurements *Fire Ecology* **6**, 13-35.

Kremens RL, Dickinson MB, Bova AS (2012) Radiant flux density, energy density and fuel consumption in mixed-oak forest surface fires. *International Journal of Wildland Fire* **21**, 722-730.

Lentile L, Holden Z, Smith A, Falkowski M, Hudak A, Morgan P, Lewis S, Gessler P, Benson N (2006) Remote sensing techniques to assess active fire characteristics and post-fire effects. *International Journal of Wildland Fire* **15**, 319. doi:10.1071/WF05097.

Lewis SA, Wu JQ, Robichaud PR (2006) Assessing burn severity and comparing soil water repellency, Hayman Fire, Colorado, *Hydrological Processes* **20**, 1-16.

McCarley TR, Kolden CA, Vaillant NM, Hudak AT, Smith AMS, Wing BM, Kellogg BS, Kreitler J (2017) Multi-temporal LiDAR and Landsat quantification of fire-induced changes to forest structure. *Remote Sensing of Environment*, in press.

Michaletz ST, Johnson EA, Tyree MT (2012) Moving beyond the cambium necrosis hypothesis of post-fire tree mortality: cavitation and deformation of xylem in forest fires. *New Phytologist* **194**, 254-263.

Moritz MA, Batllori E, Bradstock RA, Gill AM, Handmer J, Hessburg PF, Leonard J, McCaffrey S, Odion DC, Schoennagel T, Syphard AD (2014) Learning to coexist with wildfire, *Nature* **515**, 58-66.

Noss RF, Franklin JF, Baker WL, Schoennagel T, Moyle PB (2006) Managing fire-prone forests in the western United States, *Frontiers in Ecology and the Environment*, **4**, 481-487.

Parsons A (2003) Burned Area Emergency Rehabilitation (BAER), USDA USFS Regional BAER Coordinators 2003 Draft Report.

Reinhardt ED, Dickinson MB (2010) First-order fire effects models for land management: overview and issues, *Fire Ecology* **6**, 131-142.

Smith AMS, Kolden CA, Tinkham WT, Talhelm A, Marshall JD, Hudak AT, Boschetti L, Falkowski MJ, Greenberg JA, Anderson JW, Kliskey A, Alessa L, Keefe RF, Gosz J (2014) Remote Sensing the Vulnerability of Vegetation in Natural Terrestrial Ecosystems, *Remote Sensing of Environment* **154**, 322-337.

Smith AMS, Sparks AM, Kolden CA, Abatzoglou JT, Talhelm AF, Johnson DM, Boschetti L, Lutz JA, Apostol KG, Yedinak KM, Tinkham WT, Kremens RJ (2016) Towards a new paradigm in fire severity research using dose-response experiments, *International Journal of Wildland Fire* **25**, 158-166, doi: 10.1071/WF15130.

Smith AMS, Talhelm AF, Johnson DM, Sparks AM, Kolden CA, Yedinak KM, Apostol KG, Tinkham WT, Abatzoglou JT, Lutz JA, Davis AS, Pregitzer KS, Adams HD, Kremens RL (2017) Effects of fire radiative energy density doses on *Pinus contorta* and *Larix occidentalis* seedling physiology and mortality, *International Journal of Wildland Fire* **26**, 82-94, WF16077.

Sparks AM, CA Kolden, AF Talhelm, AMS Smith, KG Apostol, DM Johnson, L Boschetti (2016) Spectral indices accurately quantify changes in seedling physiology following fire: toward mechanistic assessments of post-fire carbon cycling, *Remote Sensing* **8**, 7, 572.

Sparks AM, Smith AMS, Talhelm AF, Kolden CA, Yedinak KM, Johnson DM (2017) Impacts of fire radiative flux on mature *Pinus ponderosa* growth and vulnerability to secondary mortality agents, *International Journal of Wildland Fire* **26**, 95-106, doi:10.1072/WF16139.

Spracklen DV, Mickley LJ, Logan JA, Hudman RC, Yevich R, Flannigan MD, Westerling AL (2009) Impacts of climate change from 2000 to 2050 on wildfire activity and carbonaceous aerosol concentrations in the western United States, *Journal of Geophysical Research: Atmospheres* **114**, (D20).

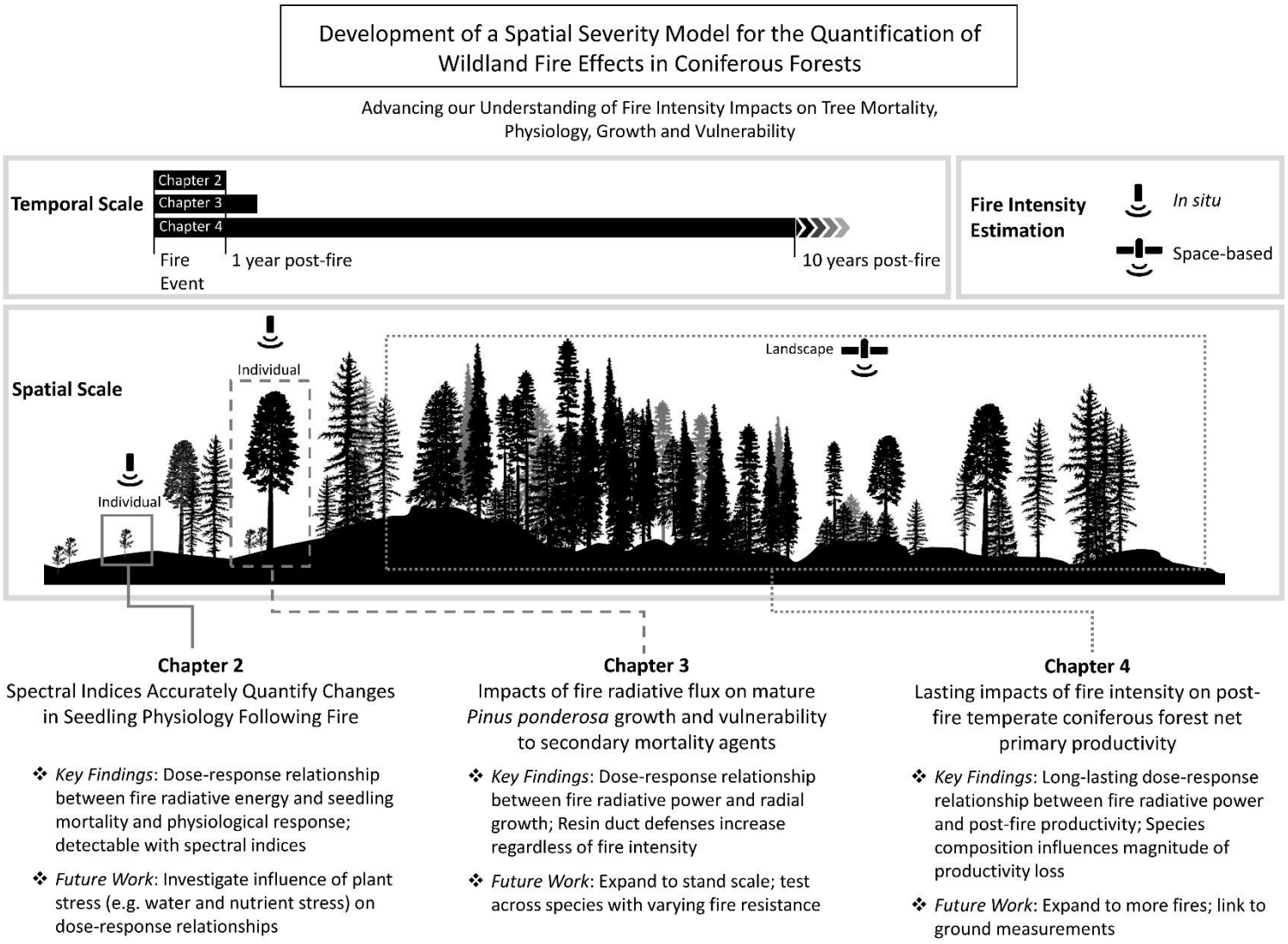

Figure 1. Dissertation conceptual diagram highlighting key findings and future work.

Chapter 2

Spectral Indices Accurately Quantify Changes in Seedling Physiology Following Fire: Towards Mechanistic Assessments of Post-Fire Carbon Cycling

Published in *Remote Sensing*:
Sparks, A.M., C.A. Kolden, A.F. Talhelm, A.M.S. Smith, K.G. Apostol, D.M. Johnson and L. Boschetti (2016), Spectral indices accurately quantify changes in seedling physiology following fire: toward mechanistic assessments of post-fire carbon cycling, *Remote Sensing*, 8, 7, 572.

Abstract

Fire activity, in terms of intensity, frequency, and total area burned, is expected to increase with a changing climate. A challenge for landscape-level assessment of fire effects, often termed burn severity, is that current remote sensing assessments provide very little information regarding tree/vegetation physiological performance and recovery, limiting our understanding of fire effects on ecosystem services such as carbon storage/cycling. In this paper, we evaluated whether spectral indices common in vegetation stress and burn severity assessments could accurately quantify post-fire physiological performance (indicated by net photosynthesis and crown scorch) of two seedling species, *Larix occidentalis* and *Pinus contorta*. Seedlings were subjected to increasing fire radiative energy density (FRED) doses through a series of controlled laboratory surface fires. Mortality, physiology, and spectral reflectance were assessed for a month following the fires, and then again at one year post-fire. The differenced Normalized Difference Vegetation Index (dNDVI) spectral index outperformed other spectral indices used for vegetation stress and burn severity characterization in regard to leaf net photosynthesis quantification, indicating that landscape-level quantification of tree physiology may be possible. Additionally, the survival of the majority of seedlings in the low and moderate FRED doses indicates that fire-induced mortality is more complex than the currently accepted binary scenario, where trees survive with no impacts below a certain temperature and duration threshold, and mortality occurs above the threshold.

Introduction

Recent evidence from North America of increased fire activity (intensity, frequency, and total area burned) due to anthropogenic climate change [1–3] underscores the need to improve our understanding of variable fire intensity impacts on ecosystem productivity at local to regional scales. Current assessments of the ecological impacts of fires, termed burn severity, investigate the degree to which an ecosystem has changed due to a fire [4] and typically encompass both vegetation and soil effects [5]. Biomass consumption, vegetation mortality, and soil infiltration/water repellency are field metrics used to quantify fire effects [6,7]. Burn severity at local to regional scales is typically characterized from bi-temporal spectral indices derived from satellite sensor remote sensing data that quantify change due to fire effects [6]. These remotely-sensed assessments can provide useful information regarding the areal extent of fires and vegetation cover change. However, current assessments provide little to no direct information regarding the physiological status of trees or other vegetation following fires [8], which is an important factor in determining effects on ecosystem services and post-fire land management planning.

The assessment of burn severity at landscape scales is widely achieved using methods employing spectral indices that use the red and infrared bands of the Landsat satellite sensor series. Differenced indices calculated using pre- and post-fire Landsat scenes are commonly used to improve change detection and visual contrast in burn severity assessments [9,10]. Specifically, the differenced Normalized Difference Vegetation Index (dNDVI), the differenced Normalized Burn Ratio (dNBR), and the Relativized differenced Normalized Burn Ratio (RdNBR) have been used to quantify area burned, burn severity, and recovery from continental to individual fire scales [6,10–14]. The majority of recent studies focus on dNBR- and RdNBR-based severity assessment [6,15]. However, dNBR- and RdNBR-based severity studies only serve as a proxy for changes in vegetation cover, char, and soils, and do not quantify tree mortality, tree physiological parameters relevant to carbon cycling (e.g., leaf area index, net ecosystem productivity), or recovery of physiological processes in the plants that survive the fire [6,8,16]. Importantly, such dNBR- and RdNBR-based severity assessments are not usually reported as quantitative spatial datasets, but rather as qualitative classes with values of unburned to low, moderate, and high severity [6,17]. Recent tree-scale research studies have observed that physiology metrics respond to variation in heat

associated with fires [8,18–20]. Coupling fire-physiology observations to landscape-scale remote sensing could help to overcome the limitations associated with current severity assessments and promote quantitative measures that increase our understanding of carbon cycling and mortality post-fire [8].

A prior study [8] provided greater detail on the problems associated with current severity assessment methods. That study [8] proposed that one potential approach to assessing burn severity could be achieved by incorporating biological sciences perspectives through the use of dose-response experiments, where fire radiative energy density (FRED: MJ m^{-2}) was the dose metric and plant carbon or water processes were proposed as potential response metrics. This proposed mechanistic approach to burn severity has the improved potential to link remote sensing datasets to ecosystem process models. Several other studies have used the FRED methodology as a pathway to characterize fire effects at both plot and landscape scales [21,22]. Increasing FRED doses have been observed to cause significant reductions in leaf-level net photosynthesis in Pinus contorta at four weeks post-fire [8]. This study called for further research to investigate these relations in other species, over a wider range of spectral indices, and at extended temporal scales.

Although the prior study [8] presented a potential framework for improving severity assessments from a mechanistic standpoint, it was only a short communication that did not investigate the potential for spectral indices and remote sensing in detail. The prior study [8] also only presented dNBR and dNDVI as examples, but did not evaluate other spectral indices that are known to have strong linkages with plant physiological function (e.g., the Photochemical Reflectance Index, PRI, [23]). This past study [8] also did not attempt to elucidate what physiological changes in the seedlings were responsible for the observed differences in the spectral indices over time. The earlier study [8] also only considered a single species, *Pinus contorta*, and a key question produced by their findings was whether the spectral changes associated with the increasing FRED doses would transfer across species.

Here, the main objectives are to build on the prior study [8] and test our hypotheses that, (1) increasing FRED dose leads to increased mortality one year post-fire; and (2) decreasing levels of seedling physiological performance caused by increasing FRED doses can be detected using common spectral indices, such as dNDVI, dPRI, and dNBR (Table 1). We

further hypothesized that dNDVI and dPRI would have the strongest linkages to physiological responses in the seedlings, as these spectral indices have well-documented successes in monitoring photosynthetic activity [24–27]. We tested the performance of dNBR as it is the most commonly used spectral index in the burn severity quantification literature [6,10,11,13,28–30]. To address the main objective, we examined how these three spectral indices changed as two physiologically different seedling species responded to increasing FRED levels. We then examined the post-fire trajectories of these three spectral indices for a month following the fires, and then again at one year post-fire.

Materials and Methods

Plant Materials

Details of seedling culture and growing conditions are reported in more detail in a prior study [8]. In total, 36 *Larix occidentalis* (western larch) and 36 *Pinus contorta* (lodgepole pine) seedlings were grown in an open-sided greenhouse at the University of Idaho Pitkin Forest Nursery in Moscow, ID, USA, using 3.8 L pots through two and a half growing seasons under natural light conditions. The *Pinus* and *Larix* seedlings were randomly divided into four groups of nine seedlings (control group and three levels of FRED), and kept in the greenhouse except during the fire combustion experiments. For both species, the seedlings averaged a height of approximately 0.6 m.

Experimental Fire Setup

Experiments were conducted at the indoor combustion laboratory associated with the Idaho Fire Initiative for Research and Education (IFIRE). From the fire science literature [31,32], it is well-accepted that the consumption of pure fuel beds of known type, loads, and moisture contents will release predictable amounts of FRED. Using data presented in [33] and following the methods described in [8], we determined the loads (kg m^{-2}) of dry (~0% fuel moisture content) *Pinus monticola* (western white pine) needles to produce total FRED "doses" of 0.4 MJ m^{-2} (low group), 0.8 MJ m^{-2} (moderate group), and 1.2 MJ m^{-2} (high group). A control group containing the same number of replicates was included that was not exposed to fire. These doses were created to simulate the range of fire behavior typically seen in surface fires across a range of global woodland ecosystems [21,34,35]. The needles used in the current experiment were collected from a *Pinus monticola* plantation located

adjacent to the University of Idaho, and were manually sorted to remove impurities. For each ignition, 1–2 g of 100-proof ethanol was added to the edge of the fuel bed and ignited to provide a uniformly spreading flaming front. Each burn occurred over approximately the same duration regardless of fuel load (229 ± 2.1 s) and was considered complete once smoldering combustion had ceased for at least 20 s.

Spectral Measurements

Spectral reflectance was collected from one week prior to the experiments until four weeks post-fire using an ASD FieldSpec Pro spectroradiometer with the mineral probe attachment (Analytical Spectral Devices, Boulder, CO, USA). This spectroradiometer has a spectral resolution of 3 nm between 350–1000 nm and 10 nm between 1000 and 2500 nm. Spectra were internally processed via linear interpolation to 1 nm resolution before any calculations were performed. Multiple (three-to-seven) pre-fire spectra were collected from both old (internodal) and new (apical bud) foliage on each seedling to create baseline spectral measurements for each tree, where each measurement averaged ten collections from the spectroradiometer. For each non-destructive spectral sample, ~5 cm^2 of foliage was positioned between a background object of known reflectance and the mineral probe attachment. The background reflectance was subtracted from each sample. Where possible, post-fire spectra were collected from the same locations as the pre-fire spectra. At 52 and 54 weeks post-fire, some of the trees were harvested for a companion study, leaving fewer trees for spectra collection. The location of the new foliage spectra was coincident with photosynthesis measurements (as described below). Between each seedling, a Spectralon panel calibration measurement was made to enable calculation of reflectance. All spectra were converted into band-equivalent reflectance [36,37] associated with Landsat 8 Operational Land Imager (OLI) (see [38] for specific wavelengths) for the calculation of the Normalized Burn Ratio (NBR: [30]) and the Normalized Difference Vegetation Index (NDVI: [39]). The Photochemical Reflectance Index (PRI: [23]) used the individual wavelengths of 531 and 570 nm. Table 1 outlines each spectral index calculated in this study. Photographs were also taken pre-fire- (−1 days) and post-fire (+1, 2, and 4 weeks) to obtain visual estimates of crown scorch, which was assessed following the methodology in [30]. Specifically, the proportion of the crown volume that is yellow-green or brown is visually compared to the total crown volume.

Seedling Physiology Measurements

To elucidate the potential physiological properties that cause the observed changes in the spectral indices, we draw on data from a related study [20]. That study collected additional seedling physiological metrics and sought to understand the underlying mechanisms associated with mortality and post-fire recovery. More detail of the methods can be found in [20] but the subset of metrics that are used in this study are briefly described here. Light-saturated (1100 mmol m^{-2} s^{-1} PPFD) gas exchange (photosynthesis) and chlorophyll fluorescence measurements were performed following standard protocols [40,41] using a LI-6400XT and 6400-05 LED light source and conifer chamber (LI-COR, Inc., Lincoln, NE, USA) one day prior to the burns and then at 1, 4, 7, 14, and 28 days following the burns on five randomly-selected plants in each dose group. Water potential was measured following standard protocols [42] at midday at the same sampling intervals as P_N using a Model 600 Pressure Chamber (PMS Instruments Company, Albany, OR, USA).

Statistical Analysis

Physiological and spectral differences were compared with ANOVA and, if significant, a Tukey's Honest Significant Difference test (HSD, $\alpha = 0.05$). Distributional assumptions required for ANOVA were graphically assessed and homogeneity of variances were verified using the Bartlett Test of Homogeneity of Variances [43]. Relationship 'goodness of fit' between dependent and independent variables was assessed using the coefficient of determination (r^2) and standard error of the estimate (SEE) from regression analysis.

Results

For both tree species, increasing FRED dose resulted in increasing crown scorch and decreasing physiological performance (Figure 1). We found positive, non-linear relationships between FRED dose and crown scorch at four weeks post-fire (Figure 1b, *Pinus*: $r^2 = 0.94$, SEE = 0.10, $p < 0.001$; *Larix*: $r^2 = 0.95$, SEE = 0.09, $p < 0.001$). In comparison, we observed negative linear relationships between crown scorch and PN at four weeks following the fire (Figure 1c) for *Pinus* ($r^2 = 0.44$, SEE = 2.1, $p < 0.01$) and *Larix* ($r^2 = 0.72$, SEE = 1.5, $p < 0.001$). Likewise, significant negative relationships were observed between crown scorch and stomatal conductance (Figure 1d, *Pinus*: $r^2 = 0.77$, $p < 0.001$, *Larix*: $r^2 = 0.45$, $p < 0.01$) for both species and leaf water potential for lodgepole pine

(*Pinus*: $r^2 = 0.56$, SEE = 0.08, $p < 0.001$). The dNDVI spectral index had significant positive relationships (i.e., greater deviation from baseline values as crown scorch increased) with crown scorch (data not shown, *Pinus*: $r^2 = 0.34$, $p < 0.001$; *Larix*: $r^2 = 0.24$, $p < 0.01$). Figure 2 displays example photos of crown scorch for each FRED dose group at four weeks post-fire.

The temporal trajectory of all spectral indices for the high FRED dose seedling group for both species generally displayed a slight increasing trajectory or no trend at all (Figure 3). An exception to this is the decrease in dNBR and dNDVI index values for *Larix* at three and four weeks post-fire. Several of the *Larix* produced small leaf buds that initially grew for a few days, but ultimately died. This could explain the slight decrease of spectral index values (toward pre-fire baseline values) of *Larix*. Both dNDVI and dPRI spectral index values for the low and moderate FRED doses displayed bell-shaped temporal trajectories with values peaking at two weeks post-fire. These values generally decreased at three and four weeks post-fire, possibly indicating partial recovery in both seedling species. The dNBR spectral index did not display as strong of a trend as dNDVI and dPRI in either species. All pre- and post-fire spectral reflectance data are contained within supplemental data (Table S1). At one year post-fire 100% of the *Pinus* and 67% of the *Larix* seedlings exposed to the 0.4 MJ m^{-2} dose survived. However, only 67% of the *Pinus* and 50% of the *Larix* seedlings exposed to the 0.8 MJ m^{-2} dose survived. All seedlings (over both species) exposed to 1.2 MJ m^{-2} died within one month post-fire. None of the control seedlings died during the observational period. The mortality of the two *Larix* seedlings in the low treatment was attributed to a potential interaction associated with poor pre-fire seedling vigor. For the trees that survived 52 and 54 weeks following the low and moderate intensity fires, all spectral indices returned to, or surpassed, their pre-fire baseline values (Figure 3). Even though some delayed mortality is present one year post-fire, these results still demonstrate a clear dose-response with higher delayed mortality in the larger 0.8 MJ m^{-2} dose groups.

Higher FRED dose resulted in increasing values (i.e., greater change from pre-fire baseline values) for all three differenced spectral indices across both species (Figure 3). Linear relationships between the differenced spectral indices and FRED were generally strongest (i.e., $r^2 > 0.50$ and SEE < 0.1) one to two weeks following the combustion experiments. The dNDVI spectral index had the strongest relationships ($r^2 = 0.73$–0.85) for

both species at these time periods. The dNBR spectral index had the weakest relationships over this same period (r^2 = 0.53–0.73).

Although the relationships between the differenced indices and FRED were strongest at 1–2 weeks following the burn, relationships between spectral indices and physiological performance were strongest four weeks post-fire (Figure 4c). Chlorophyll fluorescence was the only exception, where linear relationships were strongest one week post-fire. The dPRI spectral index had the strongest relationship with chlorophyll fluorescence one week post-fire (*Pinus*: r^2 = 0.76, SEE = 0.04, $p < 0.001$; *Larix*: r^2 = 0.36, SEE = 0.06, $p < 0.01$) for both species (Figure 4d). Linear relationships between the differenced spectral indices and PN were strongest at four weeks post-fire (Figure 4c). Among the differenced indices at this time point, dNDVI had stronger linear relationships with photosynthesis in both species (*Pinus*: r^2 = 0.70, SEE = 2.25, $p < 0.001$; *Larix*: r^2 = 0.38, SEE = 2.48, $p < 0.01$) than did dNBR (*Pinus*: r^2 = 0.65, SE = 2.4, $p < 0.001$; *Larix*: r^2 = 0.03, SEE = 3.12, $p = 0.57$) or dPRI (*Pinus*: r^2 = 0.60, SEE = 2.61, $p < 0.001$; *Larix*: r^2 = 0.35, SEE = 2.55, $p < 0.05$). Mean dNDVI values were significantly different ($p < 0.001$) between the control (−0.016) and high (0.457), control and low (0.172), control and moderate (0.209), low and high, and moderate and high FRED dose groups for *Pinus*. Additionally, mean dNDVI values were significantly different ($p < 0.001$) between the control (0.027) and moderate (0.142), control and high (0.349), low (0.053) and high, and low and moderate FRED dose groups for *Larix*.

Discussion

The strong relationship between dNDVI and P_N observed in these fire dose-response experiments supports the methodology of [8] and further demonstrates that spectral indices have the potential to improve burn severity quantification through the monitoring of plant physiological metrics. While many studies have tested the utility of spectral indices for quantifying broad burn severity metrics (i.e., canopy cover, soil color, etc.) [11,28,29,44], we were able link post-fire spectral indices and physiological responses in two functionally- and ecologically-distinct tree species.

While the links between vegetation physiological response and resulting post-fire reflectance are not well understood, this study provides evidence to suggest that these changes could be the result of significant photochemical and structural changes arising from

fire-caused damage and stress. Previous remote sensing vegetation studies have identified that red reflectance from living vegetation is largely driven by photosynthetic pigments (such as chlorophyll and carotenoids) and near-infrared (NIR) reflectance is driven by structural features (leaf thickness, intercellular space, and dimensions) and other factors, such as nitrogen content [26,45]. Since the dPRI spectral index uses reflectance wavelengths mostly influenced by leaf pigments [23,46], it is unsurprising that this index did not respond to the variations in photosynthesis that was not caused by differences in chlorophyll. In contrast, the use of both red and NIR reflectance in the calculation of dNDVI likely make this index a more integrative measure of changes in photosynthetic processes. The dNBR spectral index also uses a broader range of reflectance wavelengths than dPRI, but this index was not designed to assess physiological processes [30,47]. The NIR and shortwave infrared reflectance used by dNBR are apparently more influenced by water content and other compounds in a leaf than processes more directly related to photosynthesis [11]. While the overall spectral response was very similar between the two species, slight differences could be attributed to differences in leaf pigment composition or physiological response to stress [48].

Rather than chlorophyll fluorescence, changes in leaf structure could be driving the relationship between PN and dNDVI (Figure 4c). Changes in leaf structure have been observed to influence NIR in other vegetation types including herbaceous plants [49] and deciduous broadleaf trees [26]. High temperatures, such as those resulting from fires, can create structural deformations in leaf cell walls [19]. Similarly, model simulations suggest that the high air temperatures present during a fire could lead to extreme drops in water vapor pressure, causing cavitation in the foliage [50]. In our study, FRED doses caused clear damage to the seedling crowns and individual needles that were sampled for spectral and physiological measurements (Figure 1b–d). Generally, as the FRED dose increased, the proportion of needles with partial or complete scorch increased. Likewise, there were clear differences in the NIR reflectance between each FRED dose group (Figure 4a). Partial and/or complete heat damage could result in significant changes in both NIR reflectance and photosynthesis. In addition to chlorophyll and other pigments, photosynthesis requires adequate movement (conductance) of water, carbon dioxide (CO_2), nutrients, and plant biomolecules within and among cells. Although there was little evidence of increased water

stress, estimates of leaf intercellular CO_2 (Ci) indicated that the supply of CO_2 limited photosynthesis in these trees. Leaf conductance to CO_2 is highly influenced by leaf structure [51] and it is possible that we observed a strong relationship between dNDVI and P_N because dNDVI is responding to changes in leaf structure. However, studies have identified other factors, such as foliar nitrogen content, which were not measured in this study, that could be driving the relationship between dNDVI and PN [26,45,52].

The strong relationship we observed between dNDVI and changes in PN at the leaf level does not necessarily mean dNDVI can now be directly applied to the characterization of landscape-scale burn severity and effects on tree physiology; several limitations are obvious. First, we used a small sample size to correlate physiological metrics to spectral indices. This sample size (n = 15–20) varied depending on how quickly foliage from each seedling died and was shed. Second, trees in landscape-scale fires are likely to be under more stress (i.e., water and/or nutrient stress) than the seedlings in this study and, therefore, the relationship between reflectance and P_N potentially differs. Depending on environmental conditions, evergreen species can have periodic reductions in photosynthesis while light absorption remains constant [53,54], which could lead to large errors if a constant P_N-to-reflectance relationship is assumed. Multi-temporal field validation of the leaf-level dNDVI and P_N data is needed. In addition, there is evidence that spectral properties observed at the leaf and branch level scale poorly to the landscape level due to effects resulting from species composition mixing, shadows, and non-vegetated areas [25,27,55]. Despite these challenges, studies have reduced scaling problems in tropical forests by using a fusion of LiDAR-derived canopy cover estimates and high spatial resolution (<2 m pixel size) imagery [56]. Using this methodology, only spectral characteristics of canopy crowns are assessed, minimizing mixed pixel errors. A similar approach could be used with lower spatial resolution imagery (i.e., 30 m Landsat imagery) by integrating existing canopy cover products, such as the National Land Cover Database (NLCD) or the Landscape Fire and Resource Management Planning Tools Project (LANDFIRE) canopy cover products [57,58] or LiDAR data, to quantify errors associated with variable canopy cover.

The temporal trajectories of all three indices over the duration of this study suggests that caution should be used when using these indices for long-term severity characterization (i.e., >1 year), as all indices returned to their baseline (pre-fire) values for both species at one year

post-fire. This result has also been observed with studies using spectral indices to map burned area [36]. Specifically, burned area mapping accuracy derived from NBR and dNBR spectral indices was demonstrated to significantly decline in Southeastern U.S. ecosystems when satellite data more than two months post-fire was used [59]. While [59] were primarily concerned with an ecosystem dominated by *Pinus palustris* (longleaf pine), our findings agree with theirs in suggesting initial severity assessments may be preferred over extended assessments when using vegetation metrics (such as PN) as the burn severity metric.

The results of this and the prior studies [8] demonstrate that at one month post-fire a clear dose-response relationship between FRED and ecophysiology metrics is apparent. This study demonstrated that at one year post-fire the surviving seedlings of the 0.4 MJ m^{-2} and 0.8 MJ m^{-2} treatments were not significantly different from the control. Therefore, the compelling question that future research could seek to elucidate is how long (i.e., between one month and one year) does it take for the control and treatment groups to converge? In terms of plants within natural ecosystems (i.e., not nursery grown), additional questions include how seasonality and other environmental stressors, such as droughts and insects, impact this recovery trajectory.

This study serves as an example of how spectral data can be used to assess physiological function following wildland fires. For instance, these data could improve estimates of carbon assimilation loss due to damaged or consumed leaf area. The strong relationships between tree physiology and remote sensing spectral indices provides a significant step towards improving the characterization of wildland fire severity and carbon cycle dynamics across fires and regions.

Conclusions

Results from two physiologically-different conifer seedlings highlight the potential of spectral indices to predict fire effects related to carbon processes. The dNDVI spectral index outperformed other spectral indices used for vegetation stress and burn severity characterization in regard to leaf P_N quantification. In terms of how knowledge is advanced, this study provides the necessary spectral groundwork for the development of more sophisticated landscape-scale remote sensing assessments of how fires impact the terrestrial carbon cycle. Such research could help provide quantitative data on landscape fire

vulnerability [60] to help decision-makers mitigate the impact of fires on the environment [61]. Although promising, future work is, however, needed to examine how these relationships scale from individual trees to forest stands. Other spectral indices, such as dNBR, have been shown to be good at capturing broad change metrics, such as amount of live vegetation, vegetation moisture content, and changes in areal extent of exposed soil [11,28]. However, as the widely-used Monitoring Trends in Burn Severity (MTBS) product [62] (delineated using dNBR) is usually the result of arbitrary thresholds [17], this research provides a path toward the development of more quantitative and mechanistic severity metrics.

Importantly, the survival of low and moderate FRED seedlings after one year post-fire confirms an immediate post-fire dose-response relationship and not short-term variation followed by delayed mortality. This further reaffirms that fire-induced mortality is more complex than the binary scenario where trees survive with no impacts below a certain temperature and duration threshold, and mortality occurs above the threshold [8]. In terms of burn severity for these two species, the return of all spectral indices from surviving seedlings to their pre-fire baselines at 52 and 54 weeks post-fire indicates that initial severity assessments conducted utilizing post-fire data from the same growing season as the fire may be more useful at quantifying severity (in terms of P_N) than extended assessments that utilize data from the following growing season. Further study is clearly needed to determine if these relationships hold for older, larger trees, and other plant species.

Acknowledgments

Seedlings were grown at the University of Idaho's Center for Forest Nursery and Seedling Research and combustion experiments were conducted within the Idaho Fire Initiative for Research and Education (IFIRE) combustion laboratory. This work was partially funded by the National Aeronautics and Space Administration (NASA) under award NNX11AO24G and the National Science Foundation under award IOS-1146751 to Dan Johnson. Partial support for Alan Talhelm was provided by the National Science Foundation under award DEB-1251441. Partial funding for this research for Aaron Sparks, Alistair Smith, and Crystal Kolden was provided by the National Science Foundation under Hazards SEES award DMS-1520873. Alistair Smith received partial support from the

National Science Foundation award IIA-1301792. Aaron Sparks was additionally funded through the Idaho Space Grant Consortium. The views expressed in this paper are those of the authors and do not necessarily represent the views or policies of the U.S. Environmental Protection Agency.

References

1. Van der Werf, G.R.; Randerson, J.T.; Giglio, L.; Collatz, G.J.; Kasibhatla, P.S.; Arellano, A.F., Jr. Inter-annual variability in global biomass burning emissions from 1997 to 2004. Atmos. Chem. Phys. 2006, 6, 3423–3441.

2. Moritz, M.A.; Batllori, E.; Bradstock, R.A.; Gill, A.M.; Handmer, J.; Hessburg, P.F.; Leonard, J.; McCaffrey, S.; Odion, D.C.; Schoennagel, T.; et al. Learning to coexist with wildfire. *Nature* **2014**, *515*, 58–66.

3. Barbero, R.; Abatzoglou, J.T.; Larkin, N.K.; Kolden, C.A.; Stocks, B. Climate change presents increased potential for very large fires in the contiguous United States. *Int. J. Wildland Fire* **2015**, *10*, 1071.

4. Morgan, P.; Hardy, C.C.; Swetnam, T.W.; Rollins, M.G.; Long, D.G. Mapping fire regimes across time and space: Understanding coarse and fine-scale fire patterns. *Int. J. Wildland Fire* **2001**, *10*, 329–342.

5. Keeley, J.E. Fire intensity, fire severity and burn severity: A brief review and suggested usage. *Int. J. Wildland Fire* **2009**, *18*, 116–126.

6. Lentile, L.B.; Holden, Z.A.; Smith, A.M.S.; Falkowski, M.J.; Hudak, A.T.; Morgan, P.; Lewis, S.A.; Gessler, P.E.; Benson, N.C. Remote sensing techniques to assess active fire characteristics and post-fire effects. *Int. J. Wildland Fire* **2006**, *15*, 319–345.

7. Lewis, S.A.; Wu, J.Q.; Robichaud, P.R. Assessing burn severity and comparing soil water repellency, Hayman Fire, Colorado. *Hydrol. Process.* **2006**, *20*, 1–16.

8. Smith, A.M.S.; Sparks, A.M.; Kolden, C.A.; Abatzoglou, J.T.; Talhelm, A.F.; Johnson, D.M.; Boschetti, L.; Lutz, J.A.; Apostol, K.O.; Yedinak, K.M.; et al. Towards a new paradigm in fire severity research using dose-response experiments. *Int. J. Wildland Fire* **2016**, *25*, 158–166.

9. Key, C.H. Ecological and sampling constraints on defining landscape fire severity. *Fire Ecol.* **2006**, 2, 34–59.

10. Hudak, A.T.; Morgan, P.; Bobbitt, M.J.; Smith, A.M.S.; Lewis, S.A.; Lentile, L.B.; Robichaud, P.R.; Clark, J.T.; McKinley, R.A. The relationship of multispectral satellite imagery to immediate fire effects. *Fire Ecol*. **2007**, *3*, 64–90.

11. Miller, J.; Thode, A. Quantifying burn severity in a heterogeneous landscape with a relative version of the delta Normalized Burn Ratio (dNBR). *Remote Sens. Environ*. **2007**, *109*, 66–80.

12. Heward, H.; Smith, A.M.S.; Roy, D.P.; Tinkham, W.T.; Hoffman, C.M.; Morgan, P.; Lannom, K.O. Is burn severity related to fire intensity? Observations from landscape scale remote sensing. *Int. J. Wildland Fire* **2013**, *9*, 910–918.

13. Birch, D.S.; Morgan, P.; Kolden, C.A.; Hudak, A.T.; Smith, A.M.S. Is proportion burned severely related to daily area burned? *Environ. Res. Lett*. **2014**, *9*, 064011.

14. Sparks, A.M.; Boschetti, L.; Smith, A.M.S.; Tinkham, W.T.; Lannom, K.O.; Newingham, B.A. An accuracy assessment of the MTBS burned area product for shrub–steppe fires in the northern Great Basin, United States. *Int. J. Wildland Fire* **2015**, *24*, 70–78.

15. Morgan, P.; Keane, R.E.; Dillon, G.K.; Jain, T.B. Challenges of assessing fire and burn severity using field measures, remote sensing and modelling. *Int. J. Wildland Fire* **2014**, *23*, 1045–1060.

16. Hicke, J.; Asner, G.; Kasischke, E.; French, N.; Randerson, J.; Collatz, J.; Stocks, B.; Tucker, C.; Los, S.; Field, C. Postfire response of North American boreal forest net primary productivity analyzed with satellite observations. *Glob. Chang. Biol*. **2003**, *9*, 1145–1157.

17. Kolden, C.A.; Smith, A.M.S.; Abatzoglou, J.T. Limitations and utilisation of Monitoring Trends in Burn Severity products for assessing wildfire severity in the USA. *Int. J. Wildland Fire* **2015**, *24*, 1023–1028.

18. Butler, B.; Dickinson, M.B. Tree injury and mortality in fires: Developing process-based models. *Fire Ecol*. **2010**, *6*, 55–79.

19. Michaletz, S.; Johnson, E.; Tyree, M. Moving beyond the cambium necrosis hypothesis of post-fire tree mortality: Cavitation and deformation of xylem in forest fires. *New Phytol.* **2012**, *194*, 254–263.

20. Smith, A.M.S.; Talhelm, A.F.; Johnson, D.M.; Sparks, A.M.; Yedinak, K.M.; Apostol, K.G.; Tinkham, W.T.; Kolden, C.A.; Abatzoglou, J.A.; Lutz, J.A.; et al. Impacts of fire radiative energy density dose on lodgepole pine and western larch seedling physiology and mortality. *Int. J. Wildland Fire* **2016**, doi:10.1071/WF16077.

21. Kremens, R.J.; Dickinson, M.B.; Bova, A.S. Radiant flux density, energy density and fuel consumption in mixed-oak forest surface fires. *Int. J. Wildland Fire* **2012**, *21*, 722–730.

22. Hudak, A.T.; Dickinson, M.B.; Bright, B.C.; Kremens, R.L.; Loudermilk, E.L.; O'Brien, J.J.; Hornsby, B.S.; Ottmar, R.D. Measurements relating fire radiative energy density and

surface fuel consumption-RxCADRE 2011 and 2012. *Int. J. Wildland Fire* **2015**, doi:10.1071/WF14159.

23. Gamon, J.; Peñuelas, J.; Field, C. A narrow-waveband spectral index that tracks diurnal changes in photosynthetic efficiency. *Remote Sens. Environ*. **1992**, *41*, 35–44.

24. Sellers, P.J.; Tucker, C J.; Collatz, G J.; Los, S.O.; Justice, C.O.; Dazlich, D.A.; Randall, D.A. A global 1 by 1 NDVI data set for climate studies. Part 2: The generation of global fields of terrestrial biophysical parameters from the NDVI. *Int. J. Remote Sens.* **1994**, *15*, 3519–3545.

25. Friedl, M.A.; Davis, F.W.; Michaelsen, J.; Moritz, M.A. Scaling and uncertainty in the relationship between the NDVI and land surface biophysical variables: An analysis using a scene simulation model and data from FIFE. *Remote Sens Environ*. **1995**, *54*, 233–246.

26. Ollinger, S.V. Sources of variability in canopy reflectance and the convergent properties of plants. *New Phytol*. **2011**, *189*, 375–394.

27. Masek, J.; Hayes, D.; Hughes, M.; Healey, S.; Turner, D. The role of remote sensing in process-scaling studies of managed forest ecosystems. *For. Ecol. Manag*. **2015**, *355*, 109–123.

28. Brewer, C.; Winne, J.; Redmond, R.; Opitz, D.; Mangrich, M. Classifying and mapping wildfire severity. *Photogramm. Eng. Remote Sens*. **2005**, *71*, 1311–1320.

29. Cocke, A.; Fulé, P.; Crouse, J. Comparison of burn severity assessments using Differenced Normalized Burn Ratio and ground data. *Int. J. Wildland Fire* **2005**, *14*, 189–198.

30. Key, C.H.; Benson, N.C. Landscape Assessment FIREMON: Fire Effects Monitoring and Inventory System, 1-55; USDA Forest Service General Technical Report, RMRS-GTR-164-CD; USDA Forest Service: Ogden, UT, USA, 2006.

31. Wooster, M.J.; Roberts, G.; Perry, G.L.W.; Kaufman, Y.J. Retrieval of biomass combustion rates and totals from fire radiative power observations: FRP derivation and calibration relationships between biomass consumption and fire radiative energy release. J. *Geophys. Res. Atmos*. **2005**, *110*, D24.

32. Kremens, R.J.; Smith, A.M.S.; Dickinson, M.B. Fire metrology: current and future directions in physics-based measurements. *Fire Ecol*. **2010**, *6*, 13–35.

33. Smith, A.M.S.; Tinkham, W.T.; Roy, D.P.; Boschetti, L.; Kremens, R.J.; Kumar, S.; Sparks, A.M.; Falkowski, M.J. Quantification of fuel moisture effects on biomass consumed derived from fire radiative energy retrievals. *Geophys. Res. Lett*. **2013**, *40*, 6298–6302.

34. Sackett, S.S.; Haase, S.M. Fuel loadings in southwestern ecosystems of the United States. In Proceedings of the Symposium on Fire on Madrean. Province Ecosystems; USDA Forest Service, General Technical Report RM-GTR-289; USDA Forest Service: Ogden, UT, USA, 1996; pp. 187–192.

35. Shea, R.W.; Shea, B.W.; Kauffman, J.B.; Ward, D.E.; Haskins, C.I.; Scholes, M.C. Fuel biomass and combustion factors associated with fires in savanna ecosystems of South Africa and Zambia. *J. Geophys. Res*. **1996**, *101*, 23551–23568.

36. Trigg, S.; Flasse, S. Characterizing the spectral-temporal response of burned savannah using in situ spectroradiometry and infrared thermometry. *Int. J. Remote Sens*. **2000**, *21*, 3161–3168.

37. Smith, A.M.S.; Wooster, M.J.; Drake, N.A.; Dipotso, F.; Falkowski, M.J.; Hudak, A.T. Testing the potential of multi-spectral remote sensing for retrospectively estimating fire severity in African Savannahs. *Remote Sens. Environ*. **2005**, *97*, 92–115.

38. Roy, D.P.; Wulder, M.A.; Loveland, T.R.; Allen, R.G.; Anderson, M.C.; Helder, D.; Irons, J.R.; Johnson, D.M.; Kennedy, R.; Scambos, T.A.; et al. Landsat-8: Science and product vision for terrestrial global change research. *Remote Sens. Environ*. **2014**, *145*, 154–172.

39. Rouse, J.W.; Haas, R.H.; Schell, J.A.; Deering, D.W.; Harlan, J.C. Monitoring the Vernal Advancements and Retrogradation of Natural Vegetation; NASA/GSFC, Final Report: Greenbelt, MD, USA, 1974; p. 137.

40. Glenn, E.P.; Cardann, P.; Thompson, T.L. Seasonal effects of shading on growth of greenhouse lettuce and spinach. *Sci. Hortic*. **1984**, *24*, 231–239.

41. Schoettle, A.W.; Smith, W.K. Interrelationships among light, photosynthesis and nitrogen in the crown of mature Pinus contorta ssp. latifolia. *Tree Physiol.* **1999**, *19*, 13–22.

42. Andrews, S.F.; Flanagan, L.B.; Sharp, E.J.; Cai, T. Variation in water potential, hydraulic characteristics and water source use in montane Douglas-fir and lodgepole pine trees in southwestern Alberta and consequences for seasonal changes in photosynthetic capacity. *Tree Physiol*. **2012**, *32*, 146–160.

43. Bartlett, M.S. Properties of sufficiency and statistical tests. *Proc. R. Soc. Lond. Ser. A* **1937**, *160*, 268–282.

44. Lentile, L.B.; Smith, A.M.S.; Hudak, A.;T. Morgan, P.; Bobbitt, M.J.; Lewis, S.A.; Robichaud, P.R. Remote sensing for prediction of 1-year post-fire ecosystem condition. *Int. J. Wildland Fire* **2009**, 18, 594–608.

45. Peñuelas, J.; Filella, I. Visible and near-infrared reflectance techniques for diagnosing plant physiological status. *Trends Plant Sci*. **1998**, *3*, 151–156.

46. Carter, G.; Knapp, A. Leaf optical properties in higher plants: linking spectral characteristics to stress and chlorophyll concentration. *Am. J. Bot.* **2001**, *88*, 677–684.

47. García, M.J. Caselles Mapping burns and natural reforestation using thematic Mapper data. *Geocarto Int*. **1991**, *6*, 31–37.

48. Wong, C.Y.; Gamon, J.A. Three causes of variation in the photochemical reflectance index (PRI) in evergreen conifers. *New Phytol*. **2015**, *206*, 187–195.

49. Sinclair, T.; Schreiber, M.; Hoffer, R. Diffuse reflectance hypothesis for the pathway of solar radiation through LEAVES1. *Agron. J.* **1973**, *65*, 276–283.

50. Kavanagh, K.; Dickinson, M.B.; Bova, A.S. A way forward for fire-caused tree mortality prediction: modeling a physiological consequence of fire. *Fire Ecol.* **2010**, *6*, 80–94.

51. Flexas, J.; Barbour, M.; Brendel, O.; Cabrera, H.; Carriquí, M.; Díaz-Espejo, A.; Douthe, C.; Dreyer, E.; Ferrio, J.; Gago, J.; et al. Mesophyll diffusion conductance to CO2: An unappreciated central player in photosynthesis. *Plant Sci.* **2012**, *193*, 70–84.

52. Gamon, J.A.; Field, C.B.; Goulden, M.L.; Griffin, K.L. Relationships between NDVI, canopy structure, and photosynthesis in three Californian vegetation types. *Ecol. Appl*. **1995**, *5*, 28–41.

53. Peñuelas, J.; Garbulsky, M.; Filella, I. Photochemical reflectance index (PRI) and remote sensing of plant CO2 uptake. *New Phytol*. **2011**, *191*, 596–599.

54. Grace, J.; Nichol, C.; Disney, M.; Lewis, P.; Quaife, T.; Bowyer, P. Can we measure terrestrial photosynthesis from space directly, using spectral reflectance and fluorescence? *Glob. Chang. Biol*. **2007**, *13*, 1484–1497.

55. Williams, D. A comparison of spectral reflectance properties at the needle, branch, and canopy level for selected Conifer species. *Remote Sens. Environ*. **1991**, *35*, 79–93.

56. Asner, G.; Martin, R.; Anderson, C.; Knapp, D. Quantifying forest canopy traits: Imaging spectroscopy versus field survey. *Remote Sens. Environ*. **2015**, *158*, 15–27.

57. Zhu, Z.; Vogelmann, J.; Ohlen, D.; Kost, J.; Chen, X.; Tolk, B.; Rollins, M. Mapping existing vegetation composition and structure for the LANDFIRE prototype project. In *The LANDFIRE Prototype Project: Nationally Consistent and Locally Relevant Geospatial Data and Tools for Wildland Fire Management*; USDA Forest Service Gen. Tech. Rep. RMRS-GTR-175; US Department of Agriculture, Forest Service, Rocky Mountain Research Station: Fort Collins, CO, USA, **2006**; pp. 197–215.

58. Homer, C.G.; Dewitz, J.A.; Yang, L.; Jin, S.; Danielson, P.; Xian, G.; Coulston, J.; Herold, N.D.; Wickham, J.D.; Megown, K. Completion of the 2011 National Land Cover Database for the conterminous United States-Representing a decade of land cover change information. *Photogram. Eng. Remote Sens.* **2015**, *81*, 345–354.

59. Picotte, J.; Robertson, K. Timing constraints on remote sensing of wildland fire burned area in the southeastern US. *Remote Sens.* **2011**, *3*, 1680–1690.

60. Smith, A.M.S.; Kolden, C.A.; Tinkham, W.T.; Talhelm, A.F.; Marshall, J.D.; Hudak, A.T.; Boschetti, L.; Falkowski, M.J.; Greenberg, J.A.; Anderson, J.W.; et al. Remote sensing the vulnerability of vegetation in natural terrestrial ecosystems. *Remote Sens. Environ.* **2014**, *154*, 322–337.

61. Smith, A.M.S.; Kolden, C.A.; Paveglio, T.; Cochrane, M.A.; Mortitz, M.A.; Bowman, D.M.J.S.; Hoffman, C.M.; Lutz, J.; Queen, L.P.; Hudak, A.T.; et al. The science of firescapes: Achieving fire resilient communities. *BioScience* **2016**, *66*, 130–146.

62. Eidenshink, J.; Schwind, B.; Brewer, K.; Zhu, Z.L.; Quayle, B.; Howard, S. A project for monitoring trends in burn severity. *Fire Ecol.* **2007**, *3*, 3–21.

Tables

Table 1. Spectral indices assessed in this study.

Spectral Index	Formulation
NDVI	$\rho_{NIR} - \rho_r / \rho_{NIR} + \rho_r$
dNDVI	$NDVI_{prefire} - NDVI_{postfire}$
NBR	$\rho_{NIR} - \rho_{SWIR} / \rho_{NIR} + \rho_{SWIR}$
dNBR	$NBR_{prefire} - NBR_{postfire}$
PRI	$\rho_{531} - \rho_{570} / \rho_{531} + \rho_{570}$
dPRI	$PRI_{prefire} - PRI_{postfire}$

ρ_{NIR} = sensor near-infrared reflectance, ρ_r = sensor red reflectance, and ρ_{SWIR} = sensor shortwave infrared reflectance. For PRI, ρ_{531} and ρ_{570} denote reflectance from specific spectral wavelengths (μm).

Figures

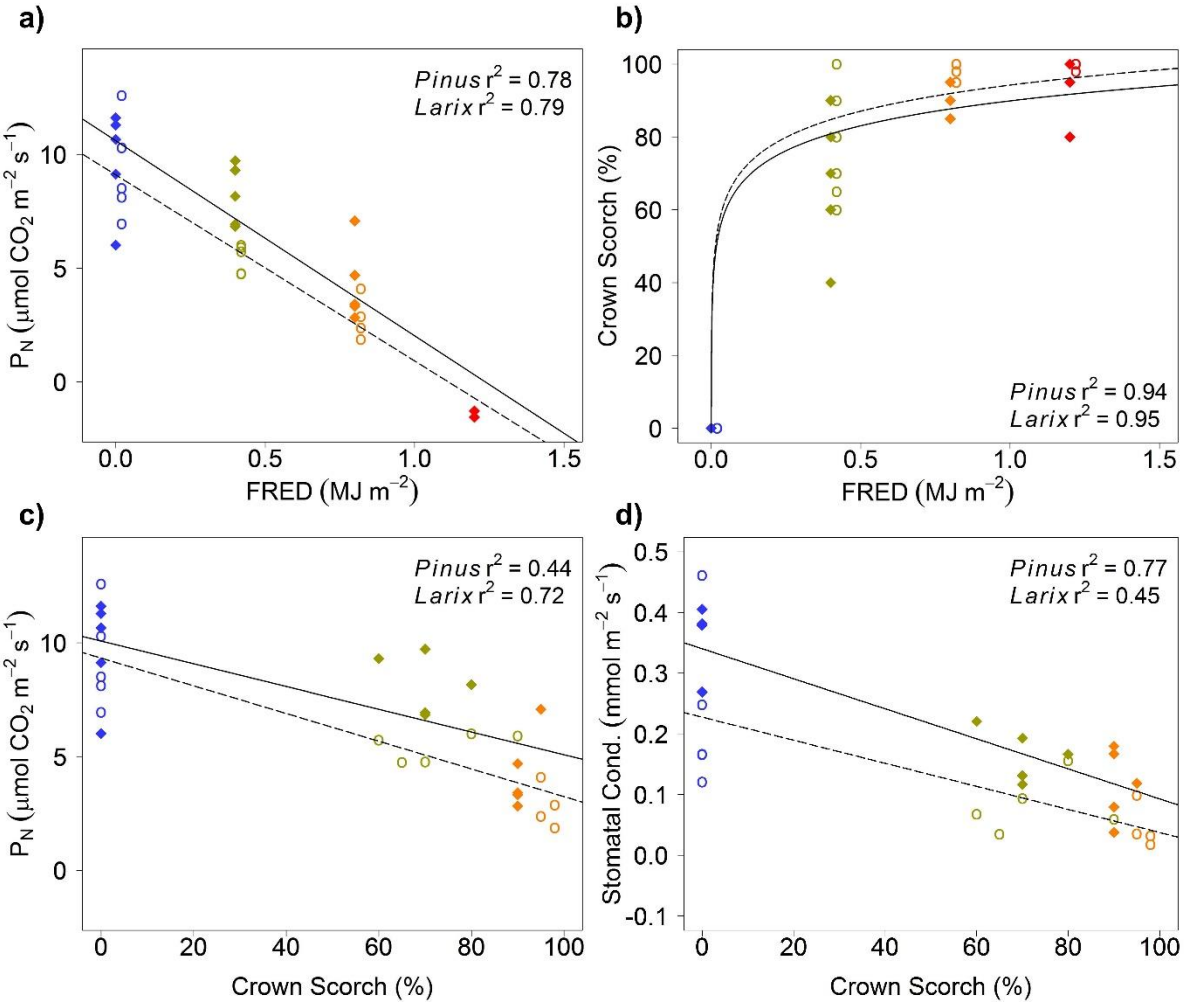

Figure 1. Increasing FRED dose leads to increasing crown scorch and lower leaf physiological performance. Scatterplots display four week post-fire data with colors representing FRED doses: blue = control, yellow = 0.4 MJ m^{-2}, orange = 0.8 MJ m^{-2}, and red = 1.2 MJ m^{-2}, and solid markers representing *Pinus* and open markers representing *Larix*. The solid and dotted lines represent predicted values for *Pinus* and *Larix* four weeks post-fire, respectively. Sub-plots are as follows: (a) leaf P_N predicted from FRED (adapted from [8] to include a comparison with *Larix*) and (b) crown scorch predicted from FRED; (c) P_N predicted from crown scorch; and (d) stomatal conductance predicted from crown scorch.

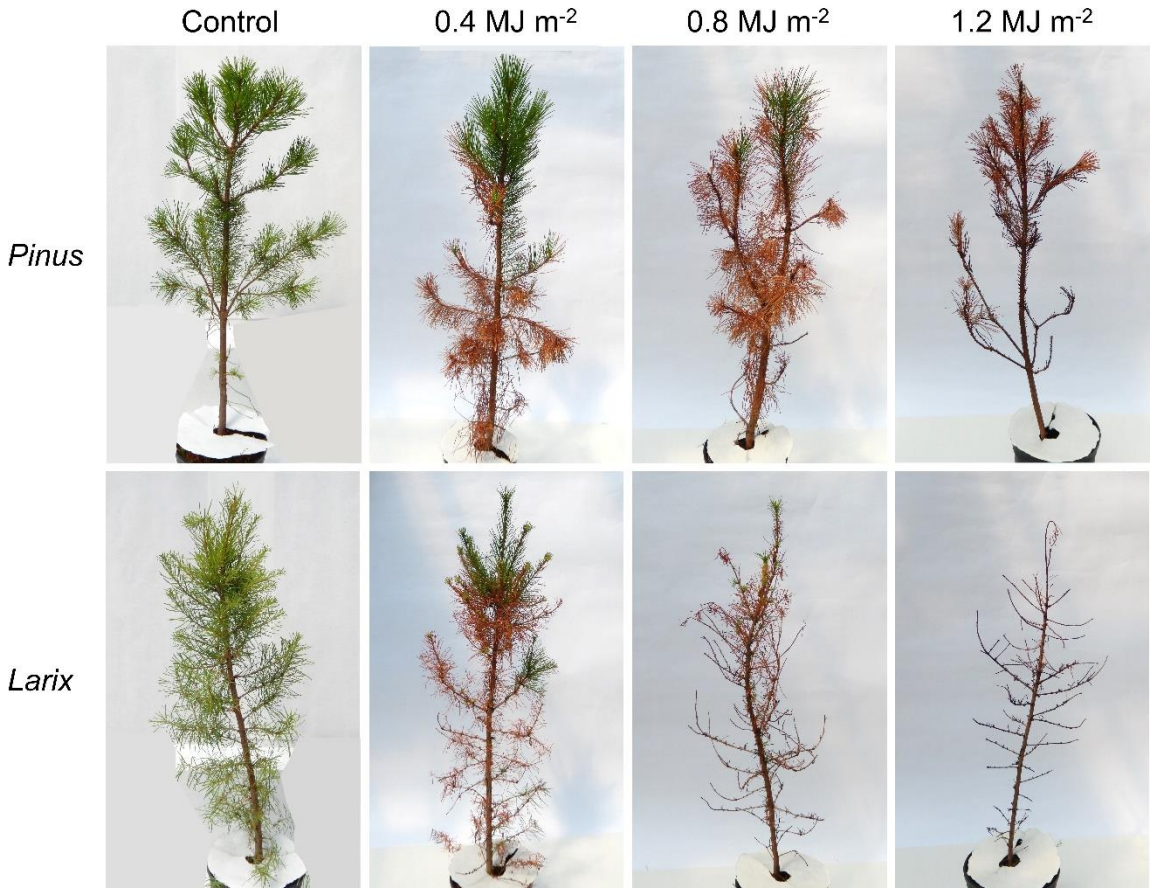

Figure 2. Crown scorch increased with FRED dose for both species. Photographs display overall seedling condition four weeks post-fire.

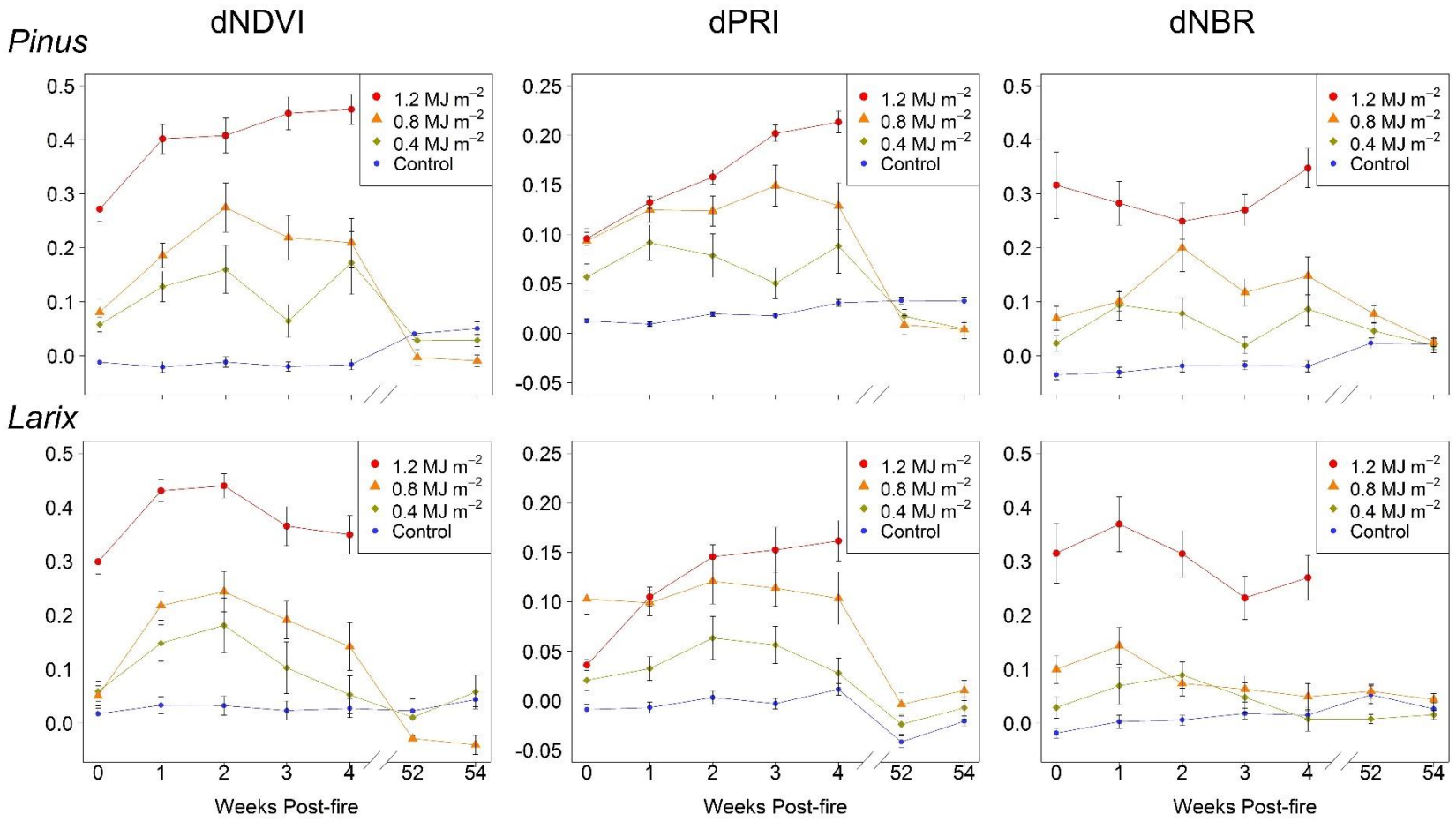

Figure 3. Differenced spectral indices display greater change with increasing FRED dose. Temporal trajectories of the three differenced spectral indices are displayed from one day to four weeks and at 52 and 54 weeks post-fire for *Pinus contorta* (top row) and *Larix occidentalis* (bottom row). Error bars represent standard error (1 day–4 weeks n = 9, 52 and 54 weeks n = 3–6).

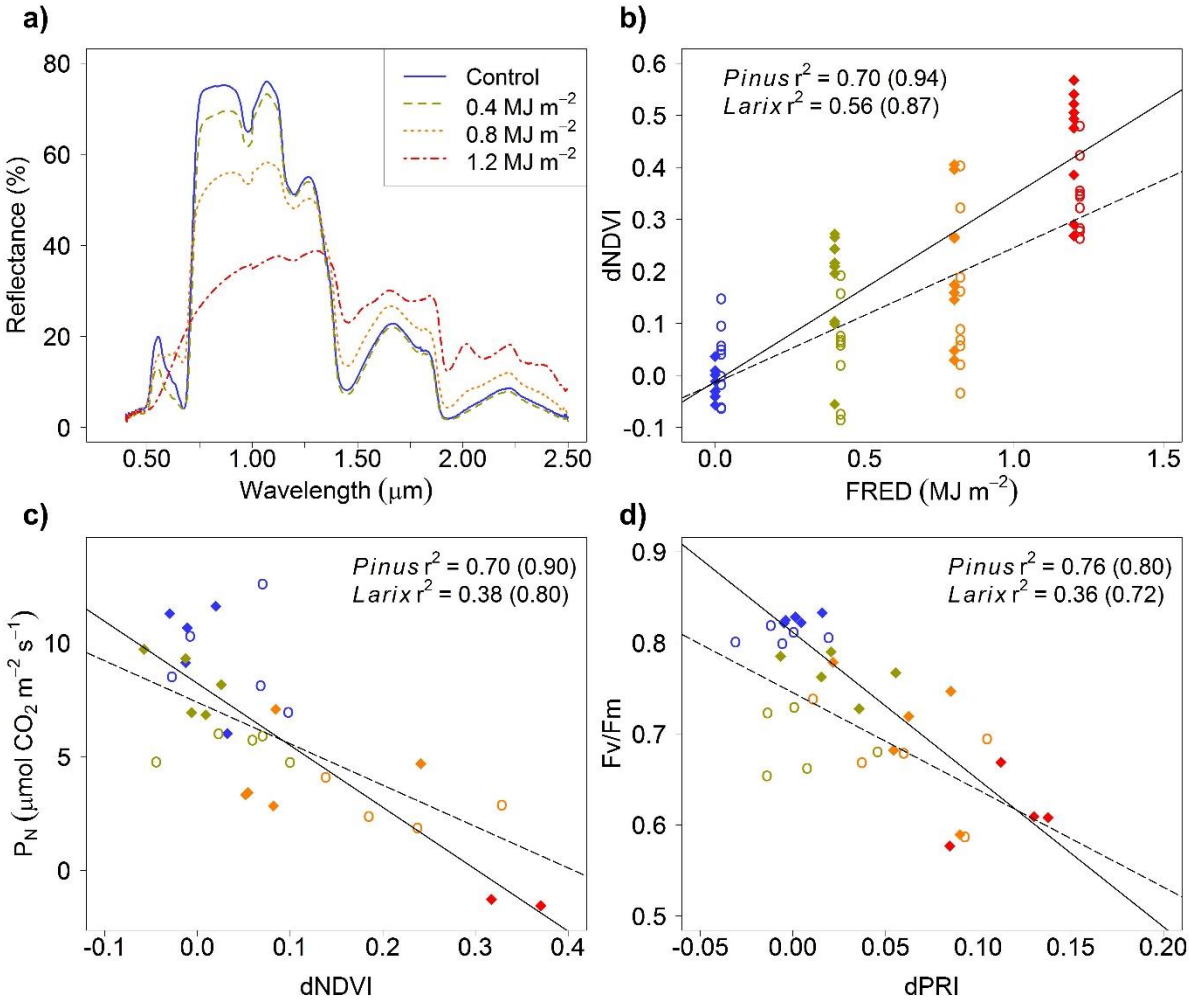

Figure 4. Spectral indices are strongly influenced by FRED dose and provide relatively accurate quantification of leaf physiological performance. Scatterplots display post-fire data with colors representing FRED doses: blue = control, yellow = 0.4 MJ m^{-2}, orange = 0.8 MJ m^{-2}, and red = 1.2 MJ m^{-2}, and solid markers representing *Pinus* and open markers representing *Larix*. The solid and dotted lines represent predicted values for *Pinus* and *Larix*, respectively. Regression fits of mean values are in parentheses. Sub-plots are as follows: (a) average spectral reflectance of *Pinus* FRED dose groups from ~0.4–2.5 μm; (b) dNDVI predicted from FRED four weeks post-fire (adapted from [8] to include a comparison with *Larix*); (c) P_N predicted from dNDVI four weeks post-fire (adapted from [8] to include a comparison with *Larix*); and (d) chlorophyll fluorescence predicted from dPRI one week post-fire.

Chapter 3

Impacts of fire radiative flux on mature *Pinus ponderosa* growth and vulnerability to secondary mortality agents

Published in *International Journal of Wildland Fire*:
Sparks, A.M., A.M.S. Smith, A.F. Talhelm, C.A. Kolden, K.M. Yedinak and D.M. Johnson (2017), Impacts of fire radiative flux on mature *Pinus ponderosa* growth and vulnerability to secondary mortality agents, *International Journal of Wildland Fire* 26, 95-106, doi:10.1072/WF16139.

Abstract

Recent studies have highlighted the potential of linking fire behavior to plant ecophysiology as an improved route to characterizing severity, but research to date has been limited to laboratory-scale investigations. Fine-scale fire behavior recorded during prescribed fires has been identified as a strong predictor of post-fire tree recovery and growth, but most studies report fire behavior metrics averaged over the entire fire. Additionally, previous research has found inconsistent effects of low-intensity fire on mature *Pinus ponderosa* growth. In this study, fire behavior was quantified at the tree scale and compared with post-fire radial growth and axial resin duct defenses. Results show a clear dose-response relationship between peak fire radiative flux density (FRFD: W m^{-2}) and post-fire *Pinus ponderosa* radial growth. Unlike in previous laboratory research on seedlings, there was no dose-response relationship observed between fire radiative energy density (FRED: J m^{-2}) and post-fire mature tree growth in the surviving trees, potentially indicating the importance of heat transfer modes in characterizing these relationships. These results may also suggest that post-fire impacts on growth of surviving seedlings and mature trees require modes of heat transfer to impact plant canopies. This study demonstrates that increased resin duct defense is induced regardless of fire intensity, which may decrease *Pinus ponderosa* vulnerability to secondary mortality agents.

Introduction

Low-intensity surface fires have a well-documented role in maintaining healthy ponderosa pine (*Pinus ponderosa* Dougl. ex Laws.) forests (Agee, 1998; Heyerdahl *et al.* 2001; Baker, 2009). Surface fires can reduce susceptibility to high-intensity, stand replacing fires by consuming surface fuels, thinning understory trees and shrubs, and increasing canopy base height of dominant trees (Steele *et al.* 1986; Busse *et al.* 2000; Strom and Fule 2007). Changes in climate and widespread fire exclusion have led to fuel accumulation and forest structural changes resulting in higher intensity fires across the western United States (Stephens *et al.* 2009). To counter this trend, management efforts have included low-intensity prescribed fires as a tool to help return these forests to characteristic stand densities and fuel loadings (Agee and Skinner 2005). The resulting range of surface fire intensity (wildfire to prescribed fire) in *Pinus ponderosa* forests is large, and varies considerably depending on the fuel complex structure, ignition pattern, burning conditions, slope, and other factors (Alexander and Cruz 2012). High variability in fire intensity, coupled with secondary mortality agents such as bark beetles and disease, have resulted in considerable uncertainties in identifying the causes and magnitudes of tree vulnerability, recovery, and mortality post-fire. While many fire effects models exist, none spatially quantify post-fire ecological and physiological characteristics, limiting our understanding of ecosystem carbon dynamics and our ability to manage landscapes pre- and post-fire (Reinhardt and Dickinson 2010; Smith *et al.* 2016).

The effects of fire on tree growth and physiology are a consequence of the transfer of heat into the roots, bole, and crown (Michaletz and Johnson 2007). Heat-induced cell necrosis can reduce growth by damaging apical and lateral meristems and can eventually lead to tree mortality. Many empirical studies have linked visual assessments of crown and bole damage with post-fire tree mortality and recovery (Ryan and Reinhardt 1988; Mantgem *et al.* 2003; Hood *et al.* 2007). Unfortunately, most studies have failed to link fire behavior with post-fire vegetation response (Smith *et al.* 2016). This is illustrated in Table 1, which shows widely differing *Pinus ponderosa* growth and physiology responses despite similar treatments, tree size and ages, and post-fire sampling times. Research that has tried to link heat transfer with vegetation response has mainly focused on localized cell death, such as through stem girdling and cell deformation (Bova and Dickinson 2005; Michaletz *et al.*

2012). For instance, Michaletz *et al.* (2012) observed heat-induced xylem conduit wall deformation and cavitation, which they hypothesized could lead to reduced xylem conductivity and tree mortality. Other studies have applied hot water baths to excised branch segments as a proxy for fire (West *et al.* 2016). However, these studies are limited in their inference because they do not replicate natural fire conditions where large sections of plants are exposed to heat (Smith *et al.* 2016). Further, the constant heat flux created by the application of a heater, controlled flame, or water bath is limited in relevance to the sporadic short duration heat pulses that are experienced in a wildland fire (Kremens *et al.* 2010). Physiologically, the application of heat to a plant module or portion of the stem provides insight into cellular and molecular processes, but may miss both compensatory responses that allow plants to maintain physiological function at an organismal scale (Trifilò *et al.* 2011) and potential synergistic effects that could result from damage to multiple portions of the plant.

Fire damage to boles and crowns can reduce photosynthetic potential and phloem transport and increase immediate (within 2 years post-fire) *Pinus ponderosa* vulnerability to secondary mortality agents, such as *Dendroctonus ponderosae* (mountain pine beetle) (Davis *et al.* 2012). Primary tree defense to bark beetle attacks consists of resin duct systems that can transport resin vertically through axial ducts in the sapwood and radially through ducts in the sapwood and phloem (Lieutier 2002; Hood and Sala 2015a). In pines, resin ducts are crucial during beetle attack and serve as physical barriers that are toxic to both the beetles and the symbiotic fungi introduced by the beetles (Lieutier 2002; Hood and Sala 2015a). Resin duct systems can be classified as defenses that are either constitutive, which are pre-formed before damage, or induced, which are activated by injury or pest colonization (Lieutier 2002). There is growing evidence that trees with greater resin duct defenses (i.e., resin duct size and proportional area of growth ring) have a greater chance of surviving beetle attack than trees with lesser defenses (Kane and Kolb 2010; Ferrenberg *et al.* 2014; Hood *et al.* 2015a). Resin duct properties have been demonstrated to be more important than growth for predicting tree survival (Kane and Kolb 2010; Hood *et al.* 2015b).

Low-intensity surface fires have been observed to increase the size and production of resin ducts and enhance resin flow in *Pinus ponderosa* (Feeney *et al.* 1998; Perrakis and Agee 2006; Davis *et al.* 2012; Hood *et al.* 2015a). This increase in resin duct defense can

persist for years post-fire, increasing constitutive defenses and long-term resistance to pest attack (Hood *et al.* 2015a). Hood *et al.* (2015a) hypothesized that non-lethal fire damage could serve as a cue for trees to increase defense capacity in preparation for beetle attacks that are common post-fire (Hood and Bentz 2007; Davis *et al.* 2012). In the studies we have identified (Table 1), the induction of increased resin duct defense in *Pinus ponderosa* following wildfire is relatively universal. However, none of these studies related spatial variation in fire behavior to differences in resin duct formation, leaving relationships between fire intensity and post-fire changes in tree defenses largely unknown.

Recent studies have highlighted the utility of using radiative heat flux metrics that quantify fire energy as a route to characterize fire behavior and predict post-fire tree mortality, growth, and physiological function. Radiation typically represents only ~11-17% of the total heat flux (Freeborn *et al.* 2008; Smith *et al.* 2013; Kremens *et al.* 2012), however, it is relatively easy to measure (Kremens *et al.* 2010) and is strongly correlated to other heat flux components (Freeborn *et al.* 2008). Kremens *et al.* (2012) and Hudak *et al.* (2016) used Fire Radiative Flux Density (FRFD: W m^{-2}) to characterize fire behavior in oak woodland and longleaf pine forests, respectively. Satellite derived fire radiative power (FRP: W) has been used to predict changes in burn severity spectral indices at landscape scales (Heward *et al.* 2013) and FRP products derived from the Moderate Resolution Imaging Spectrometer (MODIS) are widely used in the assessment of fire regimes (Giglio 2007; Roberts *et al.* 2009; Archibald *et al.* 2010; Andela *et al.* 2015) and regional and global fire emissions (Mebust *et al.* 2011; Kaiser *et al.* 2012; Konovalov *et al.* 2014). Recent studies have observed dose-response relationships in *Pinus contorta* (lodgepole pine) and *Larix occidentalis* (western larch) seedlings to increasing doses of fire radiative energy density (FRED: J m^{-2}). Specifically, under controlled nursery and laboratory conditions, FRED dose resulted in decreasing photosynthesis and diameter at root collar in surviving trees (Smith *et al.* 2016, in review) and increased mortality at extended temporal scales (Sparks *et al.* 2016). These studies indicate that there is a strong link between measures of radiative heat flux and vegetation response and mortality. However, there is a need to investigate such linkages on larger trees and under field burning conditions. In larger trees we would expect that defensive traits, such as crown base height and bark thickness, would result in reduced impacts of heat flux dose on the post-fire recovery and mortality (Wade, 1993). Trees burning

within the natural environment (not within a laboratory) would also be expected to be more resistant given they have adapted to environmental conditions and variability. Consequently, in this study we sought to answer the following questions:

1) Is there a dose-response relationship between metrics of fire intensity and radiative flux and the post-fire mature tree growth? If yes, are the radiative heat flux metrics the same as those observed to produce dose-response relationships in seedlings and if not, why?
2) Is there a dose-response relationship between metrics of fire intensity and fire radiative flux and mature tree defenses?

Methods

Site Description and Experimental Design

The University of Idaho Experimental Forest (UIEF) is located on the Palouse Range, approximately 20 km northeast of Moscow, Idaho. The UIEF is characterized by a mixed-conifer temperate forest. Dominant tree species within the UIEF include, *Psuedotsuga menziesii* (Douglas-fir), *Abies grandis* (grand fir), *Thuja plicata* (western red cedar), and *Pinus ponderosa* (ponderosa pine). Mean summer temperatures over the 1981-2010 time period were 16.4 ºC and mean summer precipitation was 97.5 mm (annual precipitation was 658.1 mm)(Arguez *et al.* 2010).

Three even-aged, *Pinus ponderosa* dominated stands were chosen for this study, ranging in elevation from ~880-950 m (Figure 1). The three stands were planted in 1982 following clearcut and broadcast burn treatments and have understories dominated by *Physocarpus malvaceus* (ninebark) and *Symphoricarpos albus* (snowberry). In June 2014, approximately two hectares of each stand was mechanically thinned using a boom-mounted brushing head on a CAT 320B excavator (Caterpillar Inc., Peoria, IL, USA). All understory shrubs were chipped and the overstory *Pinus ponderosa* was thinned to a target spacing of 6 m and chipped (see Figure 2 for pre-burn conditions). The thinning decreased basal area (m^2 ha^{-1}) of trees >5 cm diameter at breast height (DBH) by an average of 12.1 m^2 ha^{-1} across all three stands (Table 2). Likewise, stand density (tree ha^{-1}) of trees >5 cm DBH was reduced by an average of 655 trees ha^{-1} across all three stands (Table 2).

Prescribed burns were conducted on two consecutive days in late October, 2014 in one-half of each stand to reduce surface fuel loadings. Prior to the prescribed burns, nine 5 m by

7 m rectangular plots were selected from a 60-plot grid established as part of an ongoing study (Figure 3). The nine plots were deliberately selected to exhibit a wide variability of slopes, aspects, fuel loading, and moisture content to facilitate a large range of potential fire behavior conditions. Temperature during burning operations on both days ranged from 16-20 °C, with the highest temperature occurring at the start of operations and the lowest temperature occurring at the end of operations. Likewise, relative humidity ranged from 26-52% both days. Surface winds were 1.6-4.8 km h^{-1} during burning operations. Plots were ignited with a drip torch on the downhill side to establish a uniform head fire flaming front, with ignition lines separated by ~8m.

Fire Behavior and Fuel Consumption

Fireline intensity was calculated using the low heat of combustion for *Pinus ponderosa* chipped woody material and needles. To calculate the heat yield of the fuel consumed in each plot, we followed the calculations presented in Van Wagner (1972) for woody fuels and subtracted the heat loss deductions due to bound and free water. Specifically, a deduction of 1,264 kJ kg^{-1} was subtracted from high heat of combustion estimates obtained through bomb calorimetry. Fuel depth and loading of fine and coarse woody debris (1, 10, 100, 1000 hour fuels), duff, and litter were obtained through destructive quadrat (0.5 m by 0.5 m) sampling in the four corners of each plot. Following collection, the fuels were sorted and oven dried to obtain dry fuel loading (detailed in Table 3). Litter and 1, 10, and 100 hour fuel samples (n=5) were collected immediately before plot ignition just outside each plot, sealed in plastic bags, and oven dried to obtain fuel moisture content. Ignition operation logistics did not permit the collection of litter and 1 hour fuel moisture samples in plots 1 and 2. Consumption was estimated following Kreye *et al.* (2013). Specifically, a systematic grid of nine steel pins were installed in each instrumented plot in order to measure the average depth of pin exposed post-fire. This method was used as there were strong linear relationships (r^2=0.66, SE=3.52, $p<0.001$) between woody fuel depth and total fuel load derived from 62 individual quadrats. These relationships have also been observed in similar chipped fuelbeds (Reiner *et al.* 2009). To enable the calculation of rate of spread, video cameras (Samsung HMX-F90 HD Camcorder, Samsung Electronics America Inc., Ridgefield Park, NJ, USA) were positioned at each of the plots such that the plot corner pin flags and center of the plot were visible. The average rate of spread for each plot was

calculated by analyzing the time to travel between different sets of reference points (n=10). As all of the plots had some slope and were ignited from the bottom, the direction of spread was predominately uphill and in-line with reference points.

We used the definition of flame length described by Johnson (1992) due to its ease of use and interpretation, where flame length is the distance from the center of the burning bed on the surface to the tip of the continuous flame in the direction of the travelling fire front. The center towers were marked with graduated height intervals to create reference points to aid in the assessment of flame length. Flame lengths were observed and recorded by field observers and were validated through examination of still-frame video data, analyzed at 10 s intervals. Flame residence time was derived from the video data and was calculated as the total time that plots maintained continuous flaming combustion (Cheney 1990). Smoldering time was estimated to be the difference between the total duration of radiometer signal above average pre-fire values and flame residence time.

Fire radiative flux density (FRFD: W m^{-2}) was calculated using observations from dual-band infrared radiometers and methodology detailed in Kremens *et al.* (2012). The dual-band infrared radiometers were affixed on instrument towers 5.2 m above the center of each plot and recorded data at 0.1 Hz from pre-ignition to fire extinction. The size of the burning plot exceeded the radiometer field of view, thus minimizing edge effects. We calculated fire radiative energy density (FRED: J m^{-2}) as the time integral of FRFD observations for each plot. For non-instrumented plots, FRED was modeled using the combustion factor (kg J^{-1}) derived from linear regression analysis between observed FRED and fuel consumption (r^2 = 0.92, SEE = 0.991, $p < 0.001$). Effects of variable FRED dose duration (J m^{-2} hr^{-1}) are not well-researched (Smith *et al.* 2016) and so we also calculated FRED normalized by total burn duration for each plot (average FRFD per unit time: $FRFD_{\mu}$). $FRFD_{\mu}$ was obtained by dividing FRED by the total duration of radiometer signal above average pre-fire values.

Tree Growth and Resin Ducts

In March 2016, a mortality and tree health survey was conducted in all prescribed burning stands. Live/dead status, DBH, and overall stem and crown condition were recorded for each tree. Additionally, we collected 5 mm increment cores at ~1.37 m above the ground from all (n=31) trees within the nine 5 by 7 m study plots. Additional cores (n=31) were also collected from trees in randomly selected control plots of the unburned half of each stand

(see Figure 1 for control plot locations). Cores were prepared for cross-dating following standard methodology (Speer, 2010). Ring widths were measured to the nearest 1 μm using a Nikon (Nikon Instruments Inc., Melville, NY, USA) SMZ800 microscope equipped with a Velmex micrometer and Metronics digital readout (Velmex Inc., Bloomfield, NY, USA). Ring widths were used to calculate relative growth (% deviation from mean 3-year pre-fire growth), calculated as $[(Growth_{yrX} - Growth_{avgPrefire}) / Growth_{avgPrefire}]$. Images of each core were obtained using a SPOT Idea 5 MP camera and SPOT Imaging Microscopy Imaging Software version 5.2 (Diagnostic Instruments, Inc, Sterling Heights, MI, USA). Images were acquired at a resolution (0.741 pixels μm^{-1}) where individual earlywood and latewood tracheid cells were clearly visible. This resolution was considered adequate as the resin ducts in this study were, on average, 30 and 90 times greater in size compared to earlywood and latewood cells, respectively. Axial resin duct size was obtained using ImageJ 1.50b (U.S. National Institutes of Health, Bethesda, MD, USA) following methodology presented in Hood *et al.* (2015a).

Statistics

Growth and resin duct metric differences between burned and control trees were compared with ANOVA, and if significant, a Tukey's Honest Significant Difference test ($\alpha = 0.05$) was employed. Growth and resin duct metric differences were also analyzed by peak FRFD, FRED, and $FRFD_{\mu}$ class to determine if there was a dose-response relationship. Data were organized into classes using equal-width bins for each radiative energy flux metric. Distributional assumptions required for ANOVA were graphically assessed and homogeneity of variances were verified using the 'Bartlett Test of Homogeneity of Variances' (Bartlett 1937). Relationship 'goodness of fit' between dependent and independent variables was assessed using the coefficient of determination (r^2) and standard error of the estimate (SEE) from regression analysis.

Results

Fire behavior, consumption, and radiative flux measurements for each plot are summarized in Table 3 and typical fire behavior is shown in Figure 2. Although some plots displayed very active fire behavior (high rate of spread and long flame length), most plots were dominated by smoldering combustion. On average, smoldering dominated combustion

represented 97.3% of the total burn duration. Similar to studies in other ecosystems (Kremens *et al.* 2012), we observed linear relationships between peak FRFD and fireline intensity. Peak FRFD was linearly related with both fireline intensity (r^2 = 0.96, SE=284.6, $p<0.001$) and fireline intensity derived from flame length (r^2 = 0.86, SE=59.7, $p<0.001$). Two trees died within the plots, one with 17.8 cm DBH and one with 22.1 cm DBH. These trees died in plots with FRED ranging from 0.2 to 5.4 MJ $m^{-2}$and had no obvious signs of bark beetle attack (e.g. pitch tubes, beetle larvae galleries) ~1.5 years after the burns. Due to the fact that only two trees died within the burn plot boundaries during the study period (Figure 3), we had little statistical power to detect a relationship between fire behavior and tree mortality.

There were no significant differences in pre-fire relative growth between burned and control trees. Relative growth was lower for burned trees compared to control trees 1 year post-fire (Figure 4a). Additionally, there was a clear dose-response between peak FRFD and 1-year post-fire relative growth (Figure 4b). There were no significant differences between pre-fire peak FRFD groups and only control and high peak FRFD groups were significantly different from each other in 2015. Generally, trees exposed to higher doses of peak FRFD experienced lower relative growth compared to those exposed to lower peak FRFD dose and control trees. There was a weak linear relationship between relative growth and peak FRFD (r^2=0.23, SE=29.7, $p<0.001$). There were no obvious dose-response relationships between $FRFD_{\mu}$ or FRED and relative growth. Only relative growth for control (11.5 ± 5.2%) and low (-20.8 ± 9.3%) FRED groups and control (11.9 ± 5.2%) and low (-19.7 ± 10.7%) $FRFD_{\mu}$ groups were significantly different from each other (Figure 4c). There were no significant linear relationships between relative growth and FRED or $FRFD_{\mu}$.

The only significant differences in duct metrics pre-fire were between control (1.7 ± 0.25 ducts yr^{-1}) and high (1 ± 0.0 ducts yr^{-1}) FRED duct production groups and control (0.013 ± 0.0008 mm^2) and high (0.024 ± 0.0092 mm^2) FRED total duct area groups in 2011. Unlike relative growth, there were differences in resin duct metrics in 2014 but not 2015 (Figure 5). Duct production (ducts yr^{-1}), mean duct size (mm^2 $duct^{-1}$), and total duct area (mm^2) in 2014 were higher in burned trees compared to control trees (Figure 5a-c). Unlike relative growth, there were no apparent dose-response relationships between peak FRFD, FRED, or $FRFD_{\mu}$ and any of the duct metrics. In 2014, duct production and total duct area were lower in the

control group than in the low $FRFD_{\mu}$ groups (Figure 5d,f). Mean duct size was lower in the control group than in the low and moderate $FRFD_{\mu}$ groups in 2014 (Figure 5e). There were no significant effects of burn status (control, burn) or radiative heat metrics on resin duct size, production, or area in 2015.

Discussion

Sources of variability in post-fire Pinus ponderosa *growth*

There is considerable variability in reported fire effects on *Pinus ponderosa* growth metrics (Table 1). This variation even occurs across research conducted in the same region and with trees of similar size and age. For example, in central Arizona, basal area increment has been observed to both decrease (Sutherland *et al.* 1991) and increase (Feeney *et al.* 1998) relative to control trees ~1-2 years post-fire. Likewise, in the Bitterroot Mountains in western Montana, radial wood growth has been observed to increase (Fajardo *et al.* 2007) or not be significantly different (Sala *et al.* 2005) relative to control trees ~9-10 years post-fire. Variability in growth metrics could be due to differences in water availability and other environmental factors between studies. Our findings suggest that this variability could be attributed to fine scale spatial variability in fire intensity. It is clear that both FRED and FRFD can vary by many orders of magnitude in low-intensity wild- and prescribed-fires. The peak FRFD data observed in this study were within the typical range observed in past studies. Specifically, peak FRFD in prescribed fires have been observed to range from ~4-20 kW m^{-2} in mixed oak forests (Kremens *et al.* 2012), 0-15 kW m^{-2} in longleaf pine forests (Hudak *et al.* 2016), 13.5-48.6 kW m^{-2} in hardwood/loblolly pine forests (Cannon *et al.* 2014), and 1.7-16.3 kW m^{-2} in chipped ponderosa pine forests (this study). While most studies in Table 1 recorded an 'average' fire intensity metric for the entire burn, none quantified fire intensity spatially, and thus could not link within-study variation in post-fire tree response to differences in fire intensity experienced by the trees. Smith *et al.* (2016) used a dose-response methodology with *Pinus contorta* seedlings and found strong relationships between FRED dose and photosynthesis. As FRED dose increased, there was a linear decrease in photosynthesis four weeks post-fire. Likewise, they observed decreasing tree diameter at root collar with increasing FRED.

Heat Transfer Mode and Dose-Response

Unlike Smith *et al.* (in review) we did not observe a dose-response between FRED and changes in post-fire diameter growth in these mature *Pinus ponderosa* trees. There are several factors that could account for this disparity, including: (i) variability in microsite environmental conditions, (ii) the trees in our study were much larger and had more fire resistant traits (thicker bark, higher crown base height) and (iii) compared to the flaming-dominated combustion in the other study, combustion in these burns was smoldering-dominated.

Variability in microsite environmental conditions such as water and light availability could be the result of differences in slope position. These conditions could influence the radial growth and mask any dose-response relationships like those seen in prior studies. These differences could also have led to variation in the degree of heat exposure around the boles and the degree to which flames interacted vertically with each tree (i.e. bole scorch on lee-ward sides).

Diameter and bark thickness have been observed to be strong predictors of post-fire conifer survival, with larger diameter and bark thickness increasing the probability of survival (Ryan and Reinhardt 1988; Stephens and Finney 2002). Whereas the previous dose-response studies used seedlings with thin bark and low crown base height (<0.2 m) and observed crown scorch from 40-100% (Sparks *et al.* 2016), the *Pinus ponderosa* trees in our study ranged from 13.2-33.0 cm in DBH and had an average crown base height of 6.4 ± 0.3 m.

Relative to the controlled laboratory burns conducted by Smith *et al.* (2016) and Sparks *et al.* (2016), the burns in our study produced larger FRED values (up to 13.7 MJ m^{-2}). However, compared to the artificially constructed fuelbeds in the laboratory burns, combustion of the chipped fuelbeds was much more dominated by smoldering (>97% of total burn duration on average) and occurred over a much longer period of time (11.9 hours on average). Distributing the FRED dose over a longer duration may have reduced the amount of damage caused by the fires. However, the smoldering-dominated combustion could have led to below-ground damage of tree root systems and reductions in fine roots, which could result in reduced growth (Swezy and Agee 1990). The dose-response relationship between peak FRFD and relative growth (Figure 4b) may be indicative of

damage to the tree crowns caused by convective heat fluxes. Similarly, the past studies of FRED doses on seedlings (Smith et al. 2016, in review) involved flames in contact with the entire plant leaving it open to speculation on what mode of heat transfer was responsible for the observed effects. The use of FRED in these studies was only used due to its ease in repeatability and the radiative heat flux itself was not assumed to necessarily be the cause of the observed effects. In the current study, while flames did not conduct heat to foliage through direct contact, maximum flame lengths reached >1.5 m in several of the plots, which could deliver substantial convective heat flux to the crown via high temperature gases rising above the flames. These heat fluxes could cause necrosis in foliage and buds (Michaletz *et al.* 2007) and extreme drops in vapor pressure, which could lead to structural deformation in xylem cell walls (Michaletz *et al.* 2012), cavitation in foliage (Kavanagh *et al.* 2010), and consequently decrease tree growth.

Vulnerability to Secondary Mortality Agents

The data from our study and others (Table 1) suggest that low-intensity fires serve as a cue for *Pinus ponderosa* to increase their resin duct defenses. The majority of studies surveyed observed post-fire increases in resin duct defenses (Feeney *et al.* 1998; Perrakis and Agee 2006; Davis *et al.* 2012; Hood *et al.* 2015a) despite an enormous range of reported fire intensity. Likewise, we observed no dose-response relationship between radiative heat transfer metrics (peak FRFD, FRED, $FRFD_{\mu}$) and resin duct metrics. The increase in resin duct production that occurs after fire could be a direct physiological response to fire or it could be indirect response to fire induced by changes in resource (light, water, nutrient) availability that are associated with fire. Other studies have hypothesized that smoke exposure could serve as a cue for increased production of defensive compounds (Calder *et al.* 2010). While Calder et al. (2010) found decreases in photosynthesis, they did not find significant differences in defensive compound production between trees exposed to 20 minutes of smoke and control trees. The control trees in our stands were in close proximity (~20-55 m) to the burn plots and could have received some smoke exposure, however, we do not have sufficient data to conclude that the smoke exposure experienced by the burned and control trees increased or decreased resin duct metrics. In addition to direct fire effects, other studies have found that resin duct area in *Pinus ponderosa* increases under higher temperature and precipitation (Hood *et al.* 2015a). For our study area, mean summer

temperatures increased from 2011-2015, however, precipitation decreased over this period. Average departure in mean summer (JJA) temperature from the 30 year normal (1981-2010)(Arguez *et al.* 2010) was +1.9ºC in the three years prior to the burn experiments and +3.5 ºC in the two years post. The percent of normal summer precipitation averaged 19% in the three years prior to the burn experiments and 11% in the two years post. In our study, the increase in all resin duct metrics in the burn treatments could also be due to the pulse of nutrients that typically follows combustion of surface fuels (Certini 2005).

Limitations and Future Work

We acknowledge that our study has some limitations. First, we have relatively small sample sizes for higher doses of peak FRFD, FRED, and $FRFD_{\mu}$ compared to lower doses and control samples. Future studies could manipulate surface fuel loading and moisture content so that even sample sizes are maintained. Second, in an attempt to create a wide range of fire intensity, our plots were set up on slightly different slopes and aspects, creating increased potential for different growing conditions between the sampled trees pre- and post-fire. Studies continuing this research should strive for more uniform stand conditions to help control for environmental variation.

Conclusions

Our study demonstrates that quantification of fine-scale fire behavior (e.g. flaming versus smoldering combustion) are crucial components for quantifying post-fire tree growth. These results also highlight the utility of peak FRFD for characterizing post-fire growth in *Pinus ponderosa* and its potential for landscape-scale application (e.g. MODIS derived FRP). More research is needed to test the applicability of this dose-response relationship in different age classes and species. This study also highlights the need for more research into heat flux dose duration (e.g. vegetation response to large dose distributed over a long time versus large dose distributed over a short time). Our observations also suggest that non-lethal surface fires, regardless of intensity, have potential to significantly increase resin duct defenses of *Pinus ponderosa* post-fire. This study extended the prior dose-response studies on seedlings (Sparks *et al.* 2016; Smith *et al.* 2016) through investigating whether radiative heat flux doses leads to predictable responses in post-fire growth and vulnerability to

secondary agents. Ultimately, this research furthers the argument to advance fire severity research through connecting doses of the fire heat flux to plant ecophysiology responses.

Acknowledgements

Partial funding for this research for Sparks, Kolden, and Smith was provided by the National Science Foundation under Hazards SEES award #1520873. Sparks was additionally funded through the Idaho Space Grant Consortium and Joint Fire Science Program GRIN Award 16-2-01-09 and Award 13-1-05-7. This work is based on work that is supported by the National Institute of Food and Agriculture, U.S. Department of Agriculture, McIntire Stennis project under 1004149. The views expressed in this paper are those of the authors and do not necessarily reflect the views or policies of the U.S. Environmental Protection Agency.

References

Agee JK (1998) The landscape ecology of western forest fire regimes. *Northwest Science* **72**, 17, 24-34.

Alexander ME, Cruz MG (2012) Interdependencies between flame length and fireline intensity in predicting crown fire initiation and crown scorch height. *International Journal of Wildland Fire* **21**, 2, 95-113.

Andela N, Kaiser JW, van der Werf GR, Wooster MJ (2015) New fire diurnal cycle characterizations to improve fire radiative energy assessments made from MODIS observations. *Atmospheric Chemistry and Physics* **15**, 8831-8846.

Archibald S, Scholes R, Roy D, Roberts G, Boschetti L (2010) Southern African fire regimes as revealed by remote sensing. *International Journal of Wildland Fire* **19**, 861. doi:10.1071/WF10008.

Arguez A, Durre I, Applequist S, Squires M, Vose R, Yin X, Bilotta R (2010) NOAA's U.S. Climate Normals (1981-2010). NOAA National Centers for Environmental Information. doi:10.7289/V5PN93JP [9/30/2016].

Baker WL (2009) *Fire ecology in Rocky Mountain landscapes*, Island Press.

Bartlett MS (1937) Properties of sufficiency and statistical tests. *Proceedings of the Royal Society of London Series A* **160**, 268–282.

Bova AS, Dickinson MB (2005) Linking surface-fire behavior, stem heating, and tissue necrosis. *Canadian Journal of Forest Research* **35**, 4, 814-822.

Busse D, Simon A, Riegel M (2000) Tree-growth and understory responses to low-severity prescribed burning in thinned Pinus ponderosa forests of central Oregon. *Forest Science* **46**, 2, 258-268.

Calder WJ, Lifferth G, Moritz MA, Clair SBS (2010) Physiological effects of smoke exposure on deciduous and conifer tree species. *International Journal of Forestry Research*, **2010**. 438930, 1-7, doi: 10.115/2010/438930.

Cannon J, O'Brien J, Loudermilk E, Dickinson M, Peterson C (2014) The influence of experimental wind disturbance on forest fuels and fire characteristics. *Forest Ecology and Management* **330**, 294–303.

Certini G (2005) Effects of fire on properties of forest soils: a review. *Oecologia* **143**, 1, 1-10.

Cheney NP (1990) Quantifying bushfires. *Mathematical and Computer Modelling* **13**, 12, 9-15.

Davis RS, Hood S, Bentz BJ (2012) Fire-injured ponderosa pine provide a pulsed resource for bark beetles. *Canadian Journal of Forest Research* **42**, 12, 2022-2036.

Fajardo A, Graham JM, Goodburn JM (2007) Ten-year responses of ponderosa pine growth, vigor, and recruitment to restoration treatments in the Bitterroot Mountains, Montana, USA. *Forest Ecology and Management* **243**, 1, 50-60.

Feeney SR, Kolb TE, Covington WW, Wagner MR (1998) Influence of thinning and burning restoration treatments on presettlement ponderosa pines at the Gus Pearson Natural Area. *Canadian Journal of Forest Research* **28**, 1295–1306. doi:10.1139/x98-103.

Ferrenberg S, Kane JM, Mitton JB (2014) Resin duct characteristics associated with tree resistance to bark beetles across lodgepole and limber pines. *Oecologia* **174**, 4, 1283-1292.

Giglio L (2007) Characterization of the tropical diurnal fire cycle using VIRS and MODIS observations. *Remote Sensing of Environment* **108**, 407-421.

Hatten J, Zabowski D, Ogden A, Theis W, Choi B (2012) Role of season and interval of prescribed burning on ponderosa pine growth in relation to soil inorganic N and P and moisture. *Forest Ecology and Management* **269**, 106–115, doi:10.1016/j.foreco.2011.12.036.

Heward H, Smith AMS, Roy DP, Tinkham WT, Hoffman CM, Morgan P, Lannom KO (2013) Is burn severity related to fire intensity? Observations from landscape scale remote sensing. *International Journal of Wildland Fire* **22**, 7, 910-918, doi:10.1071/WF12087.

Heyerdahl EK, Brubaker LB, Agee JK (2001) Spatial controls of historical fire regimes: a multiscale example from the interior west USA. *Ecology* **82**, 3, 660-678.

Hood S, Bentz B (2007) Predicting postfire Douglas-fir beetle attacks and tree mortality in the northern Rocky Mountains. *Canadian Journal of Forest Research* **37**, 6, 1058-1069.

Hood S, McHugh C, Ryan K, Reinhardt E, Smith S (2007) Evaluation of a post-fire tree mortality model for western USA conifers. *International Journal of Wildland Fire* **16**, 679. doi:10.1071/WF06122.

Hood S, Sala A, Heyerdahl EK, Boutin M (2015a) Low-severity fire increases tree defense against bark beetle attacks. *Ecology* **96**, 7, 1846-1855.

Hood S, Sala A (2015b) Ponderosa pine resin defenses and growth: metrics matter. *Tree Physiology* doi:10.1093/treephys/tpv098.

Hudak AT, Dickinson MB, Bright BC, Kremens RL, Loudermilk EL, O'Brien JJ, Hornsby BS and Ottmar RD (2016) Measurements relating fire radiative energy density and surface fuel consumption-RxCADRE 2011 and 2012. *International Journal of Wildland Fire* **25**, 25-37, doi:10.1071/WF14159.

Kaiser JW, Heil A, Andreae MO, Benedetti A, Chubarova N, Jones L, Morcrette J, Razinger M, Schultz MG, Suttie M, Werf GR (2012) Biomass burning emissions estimated with a global fire assimilation system based on observed fire radiative power. *Biogeosciences* **9**, 527554. doi:10.5194/bg-9-527-2012.

Kane JM, Kolb TE (2010) Importance of resin ducts in reducing ponderosa pine mortality from bark beetle attack. *Oecologia* **164**, 3, 601-609.

Kavanagh K, Dickinson M, Bova A (2010) A Way Forward for Fire-Caused Tree Mortality Prediction: Modeling a Physiological Consequence of Fire. *Fire Ecology* **6**, 80-94.

Konovalov IB, Berezin EV, Ciais P, Broquet G, Beekmann M, Hadji-Lazaro J, Clerbaux C, Andreae MO, Kaiser JW, Schulze ED (2014) Constraining CO2 emissions from open biomass burning by satellite observations of co-emitted species: a method and its application to wildfires in Siberia. *Atmospheric Chemistry and Physics* **14**, 10383-10410.

Kremens RL, Smith AMS, Dickinson MB (2010) Fire Metrology: Current and Future Directions in Physics-Based Measurements. *Fire Ecology* **6**, 13-35. doi:10.4996/fireecology.0601013.

Kremens RL, Dickinson MB, Bova A (2012) Radiant flux density, energy density and fuel consumption in mixed-oak forest surface fires. *International Journal of Wildland Fire* **21**, 722-730. doi:10.1071/WF10143.

Landsberg JD, Cochran PH, Finck MM, Martin RE (1984) Foliar nitrogen content and tree growth after prescribed fire in ponderosa pine. USDA Forest Service Research Note, PNW-412, USDA Forest Service, Ogden, UT, USA.

Lieutier F (2002) Mechanisms of resistance in conifers and bark beetle attack strategies. In *Mechanisms and deployment of resistance in trees to insects*. Springer, Netherlands, doi:10.1007/0-306-47596-0_2.

Mantgem PJV, Stephenson NL, Mutch LS, Johnson VG, Esperanza AM, Parsons DJ (2003) Growth rate predicts mortality of Abies concolor in both burned and unburned stands. *Canadian Journal of Forest Research* **33**, 6, 1029-1038.

Mebust AK, Russell AR, Hudman RC, Valin LC, Cohen RC (2011) Characterization of wildfire NOx emissions using MODIS fire radiative power and OMI tropospheric NO2 columns. *Atmospheric Chemistry and Physics* **11**, 5839-5851.

Michaletz ST, Johnson EA (2007) How forest fires kill trees: a review of the fundamental biophysical processes. *Scandinavian Journal of Forest Research* **22**, 6, 500-515.

Michaletz S, Johnson E, Tyree M (2012) Moving beyond the cambium necrosis hypothesis of post-fire tree mortality: cavitation and deformation of xylem in forest fires. *New Phytologist* **194**, 254–263.

Perrakis D, Agee JK (2006) Seasonal fire effects on mixed-conifer forest structure and ponderosa pine resin properties. *Canadian Journal of Forest Research* **36**, 1, 238-254, doi:10.1139/x05-212.

Reinhardt ED, Dickinson MB (2010) First-order fire effects models for land management: overview and issues. *Fire Ecology* **6**, 131-142.

Reiner AL, Vaillant NM, Fites-Kaufman J, Dailey SN (2009) Mastication and prescribed fire impacts on fuels in a 25-year old ponderosa pine plantation, southern Sierra Nevada. *Forest Ecology and Management* **258**, 2365-2372.

Roberts G, Wooster MJ, Lagoudakis E (2009) Annual and diurnal African biomass burning temporal dynamics. *Biogeosciences* **6**, 849-866, doi:10.5194/bg-6-849-2009.

Ryan KC, Reinhardt ED (1988) Predicting postfire mortality of seven western conifers. *Canadian Journal of Forest Research* **18**, 10, 1291-1297.

Sala A, Peters GD, McIntyre LR, Harrington MG (2005) Physiological responses of ponderosa pine in western Montana to thinning, prescribed fire and burning season. *Tree Physiology* **25**, 3, 339-348.

Six DL, Skov K (2009) Response of bark beetles and their natural enemies to fire and fire surrogate treatments in mixed-conifer forests in western Montana. *Forest Ecology and Management* **258**, 5, 761-772.

Smith AMS, Sparks AM, Kolden CA, Abatzoglou JT, Talhelm AF, Johnson DM, Boschetti L, Lutz JA, Apostol KO, Yedinak KM, Tinkham WT (2016) Towards a new paradigm in fire severity research using dose-response experiments. *International Journal of Wildland Fire* **25**, 2, 158–166.

Smith AMS, Talhelm AF, Johnson DM, Sparks AM, Yedinak KM, Apostol KG, Tinkham WT, Kolden CA, Abatzoglou JA, Lutz JA, Davis AS, Pregitzer KS, Adams HD, Kremens RL (in review) Impacts of fire radiative energy density dose on lodgepole pine and western larch seedling physiology and mortality. *International Journal of Wildland Fire* doi:10.1071/WF16077.

Sparks AM, Kolden CA, Talhelm AF, Smith AMS, Apostol KG, Johnson DM, Boschetti L (2016) Spectral indices accurately quantify changes in seedling physiology following fire: towards mechanistic assessments of post-fire carbon cycling. *Remote Sensing* **8**, 7, 572, doi:10.3390/rs8070572.

Speer JH (2010) Fundamentals of tree ring research. University of Arizona Press, Tucson, AZ, USA.

Steele R, Arno SF, Geier-Hayes K (1986) Wildfire patterns change in central Idaho's ponderosa pine-Douglas-fir forest. *Western Journal of Applied Forestry* **1**, 1, 16-18.

Stephens SL, Finney MA (2002) Prescribed fire mortality of Sierra Nevada mixed conifer tree species: effects of crown damage and forest floor combustion. *Forest Ecology and Management* **162**, 2, 261-271.

Stephens SL, Moghaddas JJ, Edminster C, Fiedler CE, Haase S, Harrington M, Keeley JE, Knapp EE, McIver JD, Metlen K, Skinner CN (2009) Fire treatment effects on vegetation structure, fuels, and potential fire severity in western US forests. *Ecological Applications* **19**, 2, 305-320.

Strom BA, Fulé PZ (2007) Pre-wildfire fuel treatments affect long-term ponderosa pine forest dynamics. *International Journal of Wildland Fire* **16**, 1, 128-138.

Sutherland EK, Covington WW, Andariese S (1991) A model of ponderosa pine growth response to prescribed burning. *Forest Ecology and Management* **44**, 2, 161-173.

Swezy DM, Agee JK (1991) Prescribed-fire effects on fine-root and tree mortality in old-growth ponderosa pine. *Canadian Journal of Forest Research* **21**, 5, 626-634.

Trifilò P, Nardini A, Raimondo F, Gullo MAL, Salleo S (2011) Ion-mediated compensation for drought-induced loss of xylem hydraulic conductivity in field-growing plants of Laurus nobilis. *Functional Plant Biology* **38**, 7, 606-613.

Van Wagner CE (1972) Heat of combustion, heat yield, and fire behavior, Information Report, PS-X-35, Petawawa Forest Experiment Station, Canadian Forest Service, Ontario.

Wade DD (1993) Thinning young loblolly pine stands with fire. *International Journal of Wildland Fire* **3**, 3, 169-178.

Wallin KF, Kolb TE, Skov KR (2003) Effects of crown scorch on ponderosa pine resistance to bark beetles in northern Arizona. *Environmental Entomology* **32**, 3, 652-661.

West AG, Nel JA, Bond WJ, Midgley JJ (2016) Experimental evidence for heat plume-induced cavitation and xylem deformation as a mechanism of rapid post-fire tree mortality. *New Phytologist* doi:10.1111/nph.13979.

Wyant JG, Laven RD, Omi PN (1983) Fire effects on shoot growth characteristics of ponderosa pine in Colorado. *Canadian Journal of Forest Research* **13**, 4, 620-625.

Tables

Table 1 (continued on next page). Summary of previous work on *Pinus ponderosa* growth and physiology responses to fire. Fire behavior metrics include: I = fireline intensity, FL = flame length. Growth or other physiological metrics include: DBH = diameter at breast height, BAI = basal area increment, A = photosynthesis, pre-dawn Ψ = pre-dawn water potential. Notation: ns = non-significant. State acronyms include: Colorado (CO), Arizona (AZ), Idaho (ID), and Utah (UT).

Location	Approx. age	Approx. DBH (cm)	Treatments	Fire behavior
Growth Metrics				
Rocky Mtns, CO	-	21-34	Burn (fall), no burn, control	Avg. I: 20 kW m^{-1}
Central OR	45	25	Burn (high fuel consumption), burn (moderate fuel consumption), control	FL (m): 0.3-0.5 (mod), 0.6-1.0 (high) ROS (m min^{-1}): 2-4.6 (mod), 0.3-0.6 (high)
Central AZ	50-190	20-40	Burn (fall), control	FL < 0.4 m
Central AZ	115-423	16-41	Thin, thin + burn (fall), control	FL: 0.15 m (0.6 max)
South-central OR	-	-	Burn (spring), control	I: 4.2-48 kW m^{-1}, FL: 0.15-0.46 m
Central AZ	-	26 ± 1.1	Thin + burn (spring)	FL: 0.3-0.6 m (2.5 max)
Bitterroot Mtns, MT	70	25-31	Thin, thin + burn (spring & fall), control	-
Bitterroot Mtns, MT	20-250	-	Thin, thin + burn (spring), control	-
Blue Mtns, OR	80-100	-	Burn (spring), burn (fall), control	FL: 0.6 m
North-central ID	34	23 ± 0.6	Thin + burn (fall), Thin control	FL: 0.2-1.1 m, I: 83-2712 kW m^{-1}
Resin Metrics				
Central AZ	115-423	16-41	Thin, thin + burn (fall), control	FL 0.15 m (0.6 max)
Central AZ	-	26 ± 1.1	Thin + burn (spring)	FL 0.3-0.6 m (2.5 max)
Crater Lake NP, OR	-	94 ± 22.4	Burn (spring), burn (fall), control	FL 0.18-0.6 m (spring), 0.3-0.9 m (fall)
Western MT	-	>25	Thin, thin + burn (spring), burn (spring), control	FL 0.2-2.7 m
MT, ID	-	21.5-46.6	Wildfire (fall), burn (spring)	-
MT, UT	-	29.5	Wildfires	-
North-central ID	34	23 ± 0.6	Thin + burn (fall), Thin control	FL: 0.2-1.1 m, I: 83-2712 kW m^{-1}

Table 1 (continued from last page). Summary of previous work on *Pinus ponderosa* growth and physiology responses to fire. Fire behavior metrics include: I = fireline intensity, FL = flame length. Growth or other physiological metrics include: DBH = diameter at breast height, BAI = basal area increment, A = photosynthesis, pre-dawn Ψ = pre-dawn water potential. Notation: ns = non-significant. State acronyms include: Colorado (CO), Arizona (AZ), Idaho (ID), and Utah (UT).

Growth or Physiological Metric	**Increase (+) Decrease (-)**	**Sampling Time (yr post-fire)**	**Reference**
Fasicle length, bud size	+	1	Wyant *et al.* 1983
Needle mass, foliar nitrogen, tree height, basal area	-	1,4	Landsberg *et al.* 1984
BAI	- ns	<2 8	Sutherland *et al.* 1991
A, BAI pre-dawn Ψ	+ -	1,2	Feeney *et al.* 1998
Basal area, crown length	-	2-4	Busse *et al.* 2000
A, pre-dawn Ψ	+	<1	Wallin *et al.* 2003
A, Radial wood growth	ns	9	Sala *et al.* 2005
BAI	+	10	Fajardo *et al.* 2007
BAI	ns	1-2	Hatten *et al.* 2012
Relative wood growth	-	1.5	*This study*
Resin flow	+	1,2	Feeney *et al.* 1998
Resin production	-	<1	Wallin *et al.* 2003
Resin flow	+	1,2	Perrakis and Agee 2006
Resin flow	+	1,2 months	Six and Skov 2009
Resin flow	+	0.25 - 3	Davis *et al.* 2012
Resin duct size and area	+	1,2	Hood *et al.* 2015
Resin duct size and area	+	1.5	*This study*

Table 2. Stand characteristics pre- and post-thinning (mean ± SE).

Timeframe	Stand	DBH (cm)	Height (m)	Basal Area (m^2 ha^{-1})	Density (trees ha^{-1})
Pre-thinning	A	14.9 ± 0.7	9.4 ± 0.4	24.6 ± 1.4	1325.0 ± 89.7
	B	17.6 ± 0.6	10.9 ± 0.2	32.8 ± 2.6	1208.3 ± 79.3
	C	19.0 ± 1.4	10.6 ± 0.9	24.0 ± 3.5	700.0 ± 56.4
Post-thinning	A	18.2 ± 0.9	11.0 ± 0.5	10.6 ± 1.1	383.3 ± 20.7
	B	21.8 ± 0.9	12.9 ± 0.4	14.6 ± 1.5	391.7 ± 45.2
	C	21.7 ± 1.4	11.8 ± 0.8	20.0 ± 3.5	491.7 ± 62.1

Table 3 (continued on next page). Pre-fire fuel characteristics and fire behavior, consumption, and radiative flux metrics derived from videography and infrared radiometers. FL = flame length, ROS = rate of spread, I = fireline intensity, FRFD = Fire Radiative Flux Density, FRED = Fire Radiative Energy Density, and $FRFD_{\mu}$ = average Fire Radiative Flux Density.

Plot	Fuel Load ($kg\ m^{-2}$)			Fuel Moisture Content (%)				Litter + Duff Depth (cm)	Total Consumption ($kg\ m^{-2}$)
	Litter	Duff	Wood	Litter	1 hour	10 hour	100 hour		
1	0.8	1.6	3.9	-	-	9	15	7.9	4.2
2	1.2	4.4	2.8	-	-	12	18	8.4	2.2
3	2.3	5.1	14.5	13	23	28	41	5.7	6.6
4	0.3	8.3	2.8	40	26	26	53	7.3	1.6
5	1.0	1.0	5.8	22	22	23	22	8.1	3.0
6	1.4	4.2	3.9	20	26	27	57	5.2	4.7
7	0.3	1.3	1.5	16	18	19	28	4.7	1.8
8	0.2	2.2	2.9	14	16	19	37	8.4	2.3
9	0.4	2.4	2.4	14	19	27	54	7.8	1.7

Table 3 (continued from last page). Pre-fire fuel characteristics and fire behavior, consumption, and radiative flux metrics derived from videography and infrared radiometers. FL = flame length, ROS = rate of spread, I = fireline intensity, FRFD = Fire Radiative Flux Density, FRED = Fire Radiative Energy Density, and $FRFD_{\mu}$ = average Fire Radiative Flux Density.

FL (m)	ROS ($m\ min^{-1}$)	I ($kW\ m^{-1}$)	Flame Residence Time (hr)	Smoldering Time (hr)	$FRFD_{peak}$ ($kW\ m^{-2}$)	FRED ($MJ\ m^{-2}$)	$FRFD_{\mu}$ ($MJ\ m^{-2}\ hr^{-1}$)
0.30	0.50	734	0.37	6.52	5.96	6.00	0.87
0.23	0.45	324	0.15	17.68	3.62	1.99	0.11
0.30	0.37	637	0.34	14.16	2.16	9.75	0.68
0.30	0.27	83	0.12	1.24	1.69	0.17	0.15
0.79	0.55	346	0.25	10.47	3.81	2.41	0.22
1.07	2.22	2516	0.14	8.78	11.74	4.36	0.49
1.02	6.00	2712	0.08	22.03	16.27	4.09	0.19
0.61	0.80	460	0.13	11.87	2.79	1.94	0.04
0.61	2.40	1099	0.20	12.35	5.70	2.94	0.23

Figures

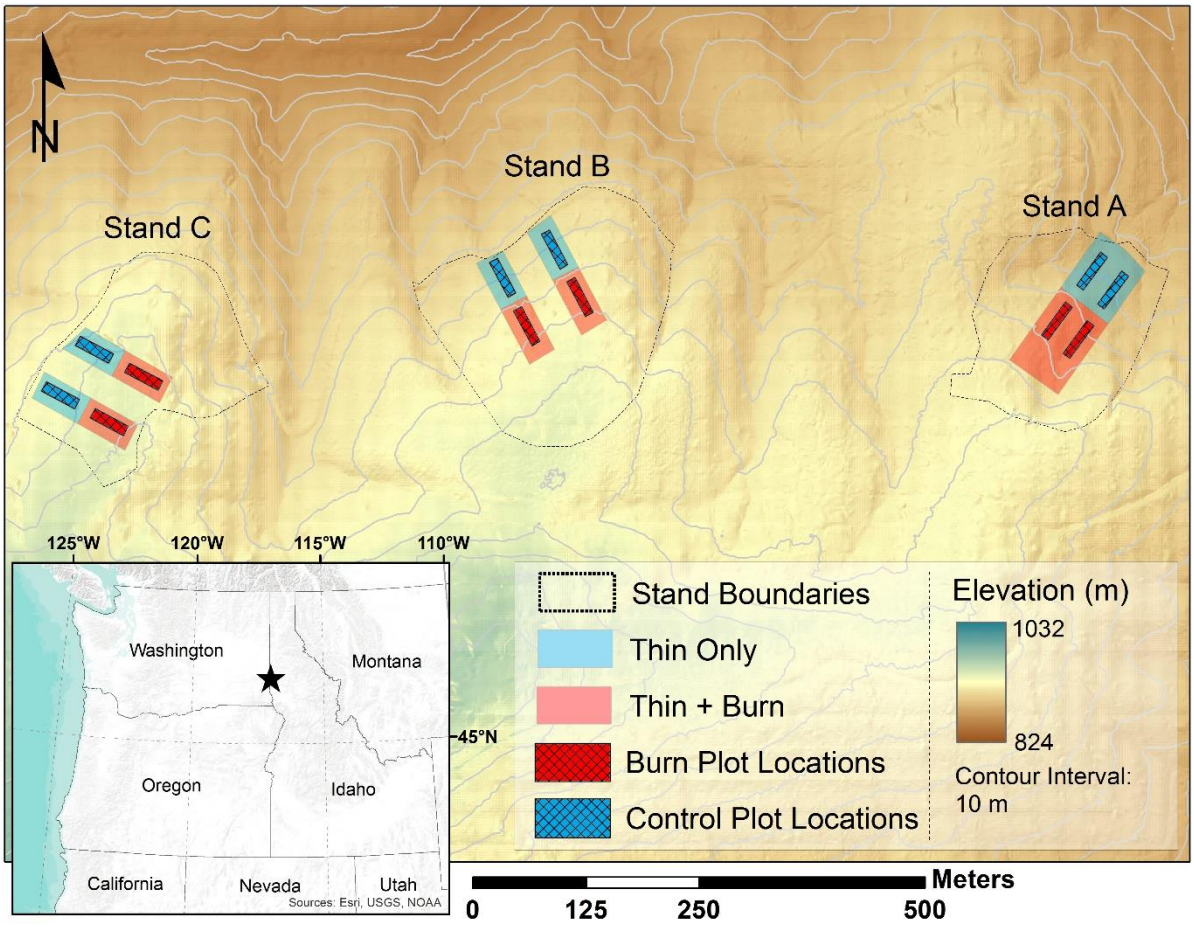

Figure 1. Location of the treatment units and plot locations within the three *Pinus ponderosa* stands at the University of Idaho Experimental Forest near Moscow, Idaho.

Figure 2. Fuelbed conditions pre-, during, and post-fire for plots with Fire Radiative Energy Density (FRED) ranging from minimum observed values (bottom row) to maximum observed values (top row).

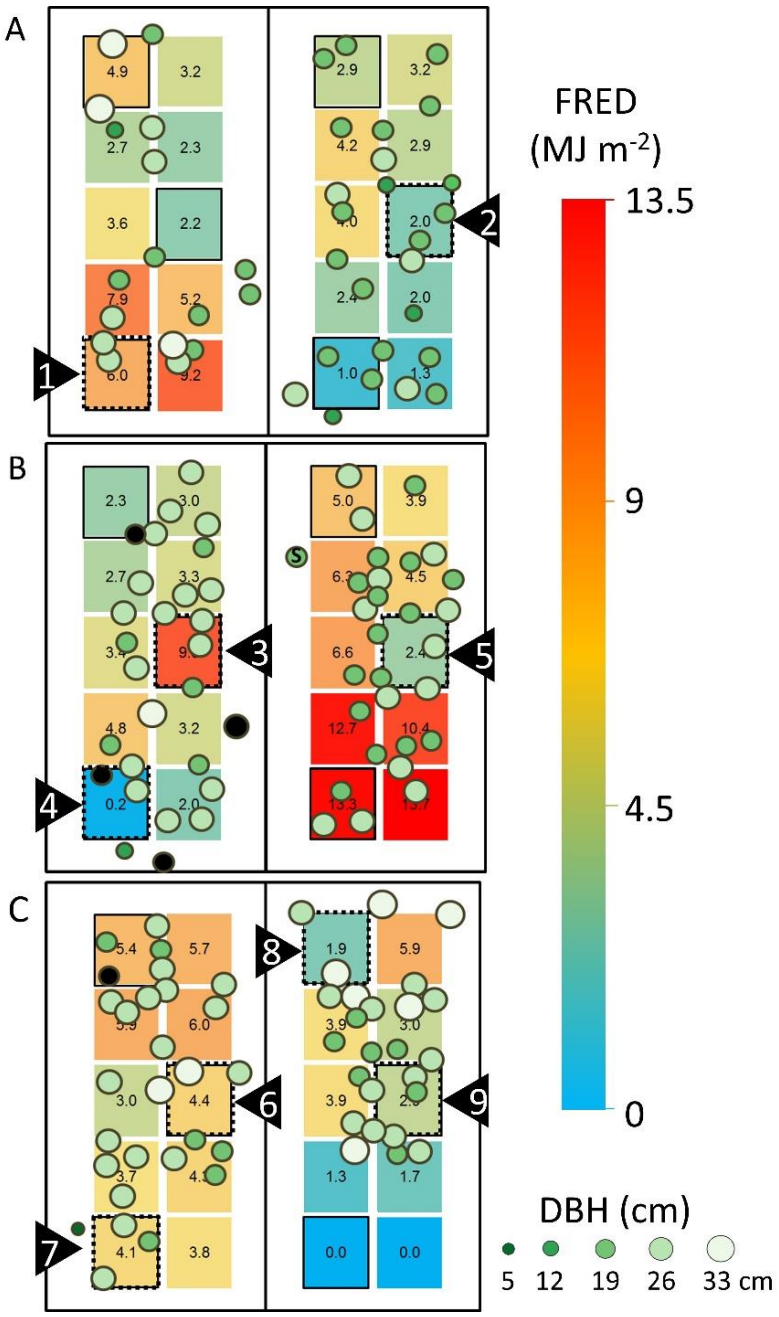

Figure 3. Stem map of *Pinus ponderosa* by diameter at breast height (DBH) class with observed and modeled Fire Radiative Energy Density (FRED) (stands A-C). Numbered plots (1-9) with dotted outlines indicate where consumption and Fire Radiative Flux Density (FRFD) were measured. Solid plot outlines indicate plots where fuel consumption was measured and FRED was modeled. Consumption and FRED were modeled for plots with no outlines. Trees outside of the plots, but within 2 m are shown for illustrative purposes. Black and 's' trees indicate dead and stressed trees, respectively.

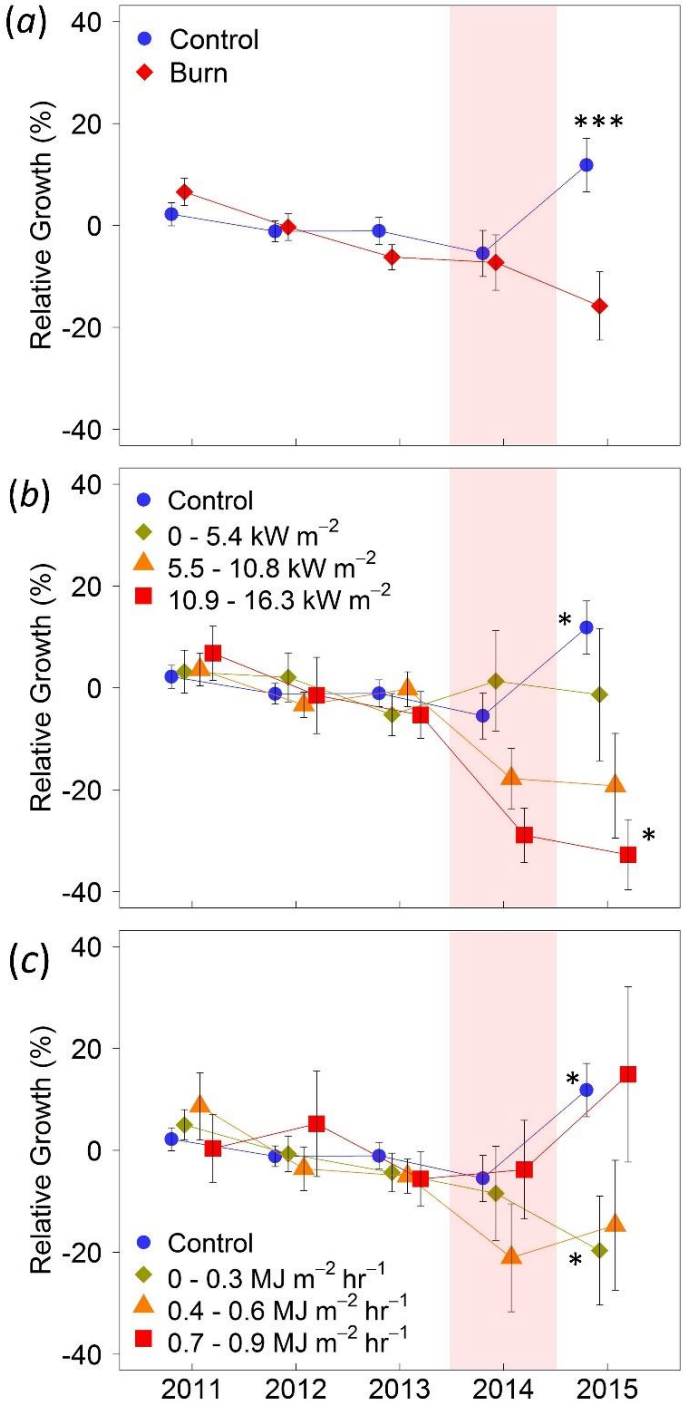

Figure 4. *Pinus ponderosa* relative radial growth (mean ± SE) by treatment (a), Fire Radiative Flux Density (FRFD) class (b) and normalized average Fire Radiative Flux Density ($FRFD_{\mu}$) class (c). Relative radial growth is calculated as [($Growth_{yrX}$ – $Growth_{avgPrefire}$) / $Growth_{avgPrefire}$]. Red highlight indicates year that prescribed fires were conducted. Asterisks indicate significant differences: * p<0.05; ** p<0.01; *** p<0.001.

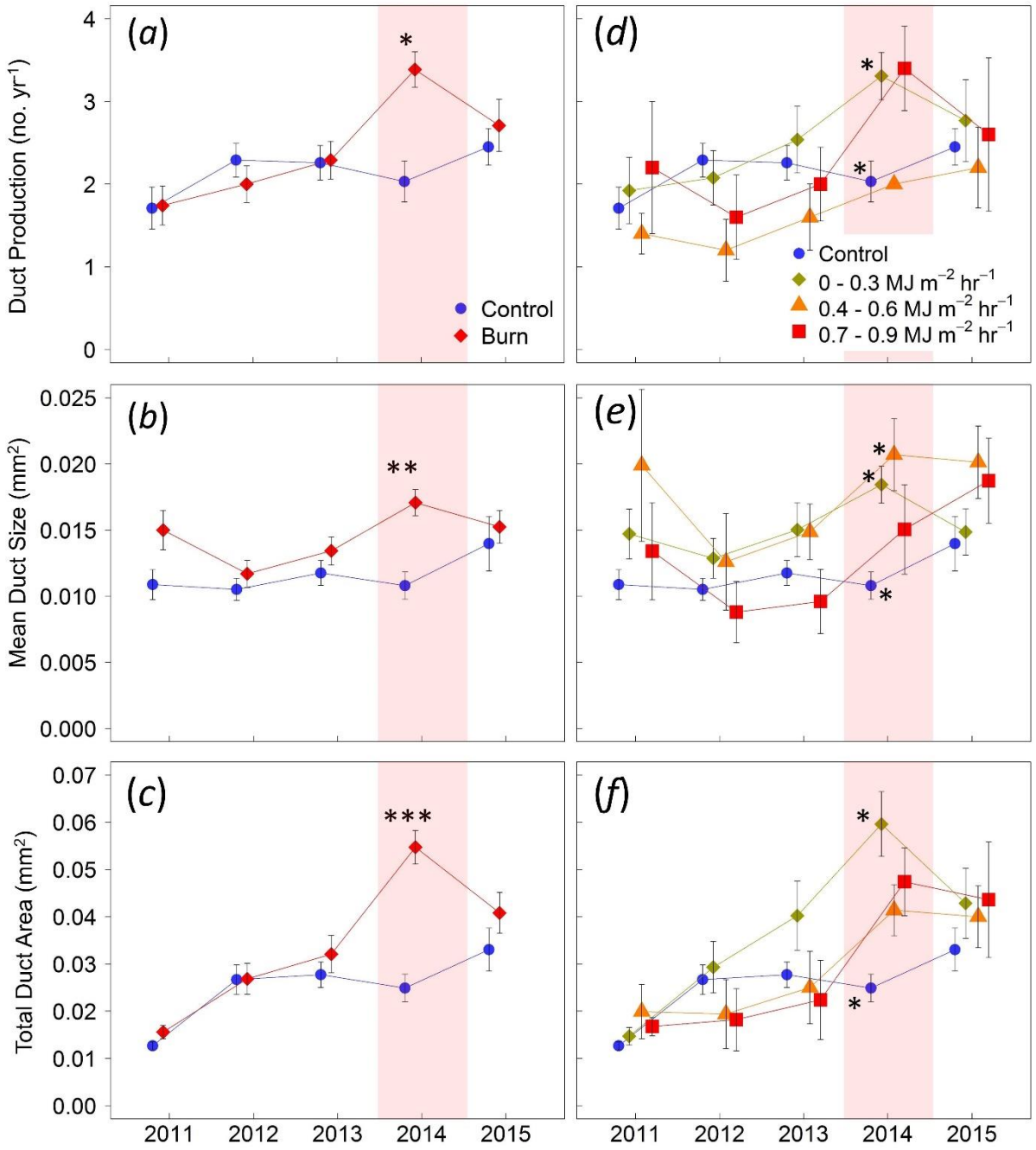

Figure 5. *Pinus ponderosa* resin duct production (mean ± SE) by treatment (a) and normalized average Fire Radiative Flux Density ($FRFD_\mu$) class (d), mean resin duct size by treatment (b) and $FRFD_\mu$ class (e), and total resin duct area by treatment (c) and $FRFD_\mu$ class (f). Red highlight indicates year that prescribed fires were conducted. Asterisks indicate significant differences: * $p<0.05$; ** $p<0.01$; *** $p<0.001$.

Chapter 4

Lasting impacts of fire intensity on post-fire temperate coniferous forest net primary productivity

Abstract

Fire is an extensive ecological disturbance in temperate forests and impacts the carbon cycle through direct combustion emissions, tree mortality, and by impairing the ability of surviving trees to sequester carbon. While sapling-based studies have demonstrated that fire intensity is a determinant of post-fire net primary productivity, wildland fires at landscape to regional scales have largely been assumed to cause tree mortality, or conversely, cause no physiological impact in a binary framework. Our objective was to understand how fire intensity affects post-fire net primary productivity in conifer-dominated forested ecosystems at the spatial scale of large wildland fires. We examined the relationship between fire radiative power (FRP) and net primary productivity (NPP) using 16 years of data from the MOderate Resolution Imaging Spectrometer (MODIS) data for 15 large fires in western United States coniferous forests. The greatest NPP post-fire loss occurred one year-post fire and ranged from -63 to -274 g C m^{-2} yr^{-1} (-13 to -52%) across all fires. Forests dominated by species with higher relative fire resistance had the lowest relative NPP reductions compared to forests with less resistant species. Post-fire NPP decreased with increasing ΣFRP and peak FRP regardless of species composition and lasted for many years post-fire. In some cases, this dose-response relationship remained beyond a decade post-fire, highlighting a legacy effect of fire intensity on post-fire C dynamics in these forests.

Introduction

Forested ecosystems cover ~30% of Earth's land surface and serve as one of the largest terrestrial carbon (C) sinks (Bonan 2008; IPCC 2013). Dynamic ecological processes such as wildfires impact this sink through direct C emissions from combustion, loss of C uptake through tree mortality, decomposition processes, and sequestration of black C within forest soils (Bowman et al. 2009; Brewer et al. 2013; Tinkham et al. 2016). Recent research has demonstrated that increases in fire intensity impair the ability of surviving trees to photosynthesize (Smith et al. 2016, 2017). However, at larger spatial scales, while many

studies have examined and projected post-fire trends in forest productivity (Hicke et al. 2003; Kashian et al. 2006; Goetz et al. 2007; Romme et al. 2011), few have evaluated relationships between the fire intensity and those trends. Characterization of such relationships is essential given lower fuel moisture (Gergel et al. 2017) and higher fire activity (intensity, frequency, and size) are predicted in North American forested ecosystems under anthropogenic climate change (Balshi et al. 2009; Spracklen et al. 2009; IPCC 2013; Barbero et al. 2015; Abatzoglou and Williams 2016; Bowman et al. 2017).

Recent studies have observed relationships between the quantity of fire radiative energy (FRE: J) and peak fire radiative power (FRP: W) incident on trees and reduced tree growth and mortality (Sparks et al. 2016, 2017; Smith et al. 2017). FRP is the instantaneous radiative flux, which is strongly related to common field-based fire intensity metrics (Kremens et al. 2012; Sparks et al. 2017) and its temporal integral is FRE. These are two of the most commonly used metrics to quantify fire intensity from satellite remote sensing products. Under controlled experiments on saplings, a toxicological "dose-response" relationship was observed, whereby increasing FRE resulted in decreasing net photosynthesis in surviving *Pinus contorta* and *Larix occidentalis* saplings (Smith et al. 2016, 2017) and increased mortality 1-year post-fire (Sparks et al. 2016). Furthermore, Sparks et al. (2017) observed decreasing radial growth in mature *Pinus ponderosa* 1.5 years post-fire with increasing peak FRP. These findings suggest that there is a strong link between measures of fire intensity and subsequent vegetation productivity and mortality.

Prior studies have been limited to the individual plant spatial scale and only up to ~1.5 years following fire treatments. They have also not evaluated how relative fire resistance, or the ability of a tree species to withstand and survive heat-induced damage from fire (Starker 1934; VanderWeide and Hartnett 2011), affects the observed dose-response relationship. Numerous studies have linked morphological traits to post-fire survival. Thicker bark, deep rooting depth, and a high, open tree crown have all been identified as characteristics that increase a tree's relative fire resistance (Starker 1934; Fischer and Bradley 1987; Ryan and Reinhardt 1988; VanderWeide and Hartnett 2011; Keeley 2012; He et al. 2012; Harrington 2013). However, the vast majority of studies assume a binary response regarding fire impacts on vegetation: either mortality or no physiological effect at all (Smith et al. 2017). Consequently, there is a need to investigate if dose-response relationships can be quantified

at larger spatial and temporal scales and across forest stands dominated with species of varying levels of fire resistance.

Active and post-fire observations from MODIS provide an avenue to expand previous dose-response studies to a landscape spatial scale and across decadal temporal scales. MODIS-derived FRP has been used in the characterization of fire regimes globally (Giglio et al. 2006; Archibald et al. 2010; Freeborn et al. 2014). Terra and Aqua satellites can observe active fires up to four times daily at 1 km pixels (Justice et al. 2002), enabling the coarse integration of FRP over the duration of a fire, described as fire radiative energy (Boschetti and Roy 2009; Kumar et al. 2011). However, the relatively low temporal resolution results in significant underestimations of FRE when compared with higher temporal resolution sensors (Kumar et al. 2011). Recent studies have used the sum of FRP (ΣFRP) over variable time periods to characterize fire regimes (Williamson et al. 2013; Bowman et al. 2017). MODIS observations have also enabled global estimations of Gross Primary Production (GPP) and Net Primary Production (NPP) when used in tandem with local meteorological data (Running et al. 2004; Zhao and Running 2010). These measurements have been critical to understanding of C fluxes and forest disturbances over large spatial extents (Zhao and Running 2010, Bright et al. 2013).

Given the lack of landscape scale studies that quantify fire intensity and species composition impacts on post-fire C dynamics, the objective here was to understand how fire intensity affects post-fire productivity in conifer-dominated forested ecosystems. Our results provide further insight into post-fire C dynamics and a framework for spatiotemporal assessments of fire effects. In this study we sought to answer the following questions:

1. What are the relationships between FRP and post-fire forest NPP at spatial scales of large wildland fires?
2. How do these relationships vary over time?
3. How do these relationships vary with species composition?

Methodology

Wildland fire selection

Fifteen wildland fires in the Northern Rocky Mountains, U.S., were selected for this study (Figure 1). Fires were chosen to represent coniferous forest stands ranging from those

dominated by highly resistant species (resistors) to those dominated by less resistant species (avoiders). To assess the pre-fire dominant forest cover for each fire, we used the LANDFIRE Existing Vegetation Type (EVT) 30-m product (LANDFIRE 2013). Fire selection was based on the following criteria:

(i) Located in northwestern United States forests to minimize latitudinal climatological gradients;

(ii) Located completely within a designated wilderness or other protected area to minimize confounding factors such as land management disturbance;

(iii) Occur in a closed canopy (mean canopy cover > 60%), conifer-dominated forest to minimize mixed pixels; and

(iv) Within forests where majority of area has not been observed to have burned in the last ~30 years.

Canopy cover for each fire was determined by aggregating 30 m National Land Cover Database (NLCD) Percent Tree Canopy product (Homer et al. 2007) to the 1 km spatial resolution of the MODIS products. We used the Monitoring Trends in Burn Severity (MTBS) fire polygons to estimate whether a forest had burned in the last ~30 years (Eidenshink et al. 2007). Summary information for each fire is given in Table 1.

MODIS Datasets

For each fire, we assessed post-fire NPP trajectories as a function of co-located FRP using MODIS collection 5 NPP and FRP products. We used the 1-km MOD17A3 version 055 NPP product (kg C m-2 yr-1) to characterize changes in productivity within and between our study fires. The NPP product is detailed in Running et al. (2004) and Hasenauer et al. (2012). MODIS reflectance products (fraction of photosynthetically active radiation (FPAR), leaf area index (LAI), and land cover classification) are used in tandem with meteorological data (incoming PAR, stress scalars for high vapor pressure deficit and temperature) and physiological parameters for different vegetation types (Biome Parameter Lookup Table) to calculate daily GPP. NPP is calculated as the sum of GPP over a year minus maintenance and growth respiration. We acquired the NPP product from the Numerical Terradynamic Simulation Group (NTSG) at the University of Montana. NPP data for years 2000-2015 were downloaded from the NTSG FTP site and analyzed in their native Sinusoidal projection.

To calculate FRP metrics co-located with each NPP pixel we used the MODIS Collection 5 global monthly 1-km fire location product, MCD14ML (Giglio 2010), which is derived from the MODIS active fire product (Giglio et al. 2003). MODIS FRP is derived from an empirical relationship between mid-infrared brightness temperature and FRP (Kaufman et al. 1998) and is affected by several factors, including fire background characterization and atmospheric water vapor (Wooster et al. 2005). The MCD14ML product provides the geographic location (centroid coordinates), date, time, FRP, scan angle and other data for each fire pixel detected by MODIS on the Terra and Aqua satellite platforms (Giglio 2010). Following Giglio et al. (2006) and Freeborn et al. (2011), we excluded any fire detections at scan angles greater than 40º due to significant errors that arise from increasing pixel areas at scan edges (Heward et al. 2013). At 40º, the scan-to-scan overlap is ~25%, which can result in oversampling at scan edges due to the MODIS bow-tie effect (Freeborn et al. 2011) and additional uncertainty. The resulting range of FRP was comparable to FRP observed in other closed-canopy temperate forests (Heward et al. 2013). We used MTBS fire perimeters to validate that fire detections were co-located with recorded fire events spatially and temporally. Fire detections outside the MTBS perimeter were included if they were closer than 1000 m from the MTBS fire boundary (as fires can occur anywhere in the 1-km FRP product).

Data Analysis

FRP data was co-located with the nearest NPP pixel centroid coordinates. We calculated FRP metrics (e.g. peak FRP, ΣFRP) for each fire-affected pixel that have been demonstrated to have a dose-response relationship with conifer growth and mortality (Smith et al. 2016, 2017; Sparks et al. 2017). Fire-affected pixels were grouped by peak FRP and ΣFRP percentile classes (0-25, 25-50, 50-75, 75-100) for each fire. By excluding detections above 40º, ΣFRP values in this study underestimate the true ΣFRP observed by MODIS, and this effect should be considered when interpreting our results. Unburned pixels (*n*unburned = *n*FRP percentile group) outside the MTBS fire perimeter with no significant difference in NPP from pre-fire fire-affected pixels were selected as ‘control’ pixels. Pre- and post-fire NPP were used to calculate the percent deviation from mean pre-fire NPP, or relative NPP, for each pixel (i,j) and year (t), which was calculated with the equation:

$$\text{Relative NPP (\%)} = \frac{\left(NPP_{i,j,t} - \overline{NPP_{prefire\ (i,j)}}\right)}{\overline{NPP_{prefire\ (i,j)}}}$$

To account for interannual variability in NPP not caused by the fires we subtracted the unburned (control) pixel values from the burned pixel values (Goetz et al. 2006; Bright et al. 2013). After confirming normality and homogeneity of variances, differences between FRP percentile classes were assessed using ANOVA with a post hoc Tukey's honest significant difference test ($\alpha = 0.05$). Recovery time for the fire affected pixels was also assessed and was defined as the time necessary for post-fire total NPP to equal or surpass mean pre-fire NPP at the same location.

Results

Increasing FRP dose leads to lasting reductions in post-fire NPP

Across all fires, increasing ΣFRP and peak FRP magnitude led to decreasing post-fire NPP response (Figures 2,3). This dose-response relationship was strongest one year post-fire, where mean relative NPP across all fires decreased with increasing peak FRP (Figure 3a) and ΣFRP (Figure 3b). Generally, there were more significant differences between ΣFRP percentile class relative NPP than between peak FRP percentile class relative NPP (Figures 3a-b). At six years post-fire, the longest time period for which there was data for most fires (all fires except the 2011 Saddle fire), the dose-response relationship was not as clear (fewer differences between FRP percentile classes)(Figure 3). While both ΣFRP and peak FRP percentile class relative NPP values were significantly different from the control, there were fewer differences between the percentile classes (Figure 3).

The dose-response relationship was affected by species composition. There were stronger dose-response relationships between ΣFRP/peak FRP percentile class relative NPP for forests dominated by avoider (Figure 4e-f) and mixed species (Figure 4c-d) than those dominated by resistor species (Figure 4a-b). While mean relative NPP was lower than control values, there were no differences between ΣFRP or peak FRP percentile class mean relative NPP in resistor dominated forests. Similar to the relationship for all fires, there were more significant differences between ΣFRP percentile classes than between peak FRP percentile classes. At six years post-fire there were fewer differences between ΣFRP/peak

FRP percentile class relative NPP, but all classes were lower than the control relative NPP (Figures 4).

Maximum relative NPP loss occurred at one year post-fire and differed by species composition. Generally, mixed stands consisting of fire avoiders and resistors had the largest relative post-fire NPP losses with an average loss of -41.4% (-218.3 g C m^{-2} yr^{-1}), followed by stands that were dominated by avoider species with an average loss of -33.9% (-152.8 g C m^{-2} yr^{-1}). Stands dominated by fire resistant species had the smallest average loss of -21.4% (-114.0 g C m^{-2} yr^{-1}).

Recovery and trajectories of post-fire NPP

Post-fire observations ranged from 4-12 years post-fire (average 8.4 years) for the fifteen fires, however, only the lowest FRP class of one fire (2006 South Fork Fire) had recovered to pre-fire NPP levels at the end of the observational period (~9 years post-fire). Generally, recovery trajectories were linear for all fire resistance groups, except for a few fires where NPP started decreasing around 2011 (Figures S1, S2).

Discussion

Increasing FRP dose leads to lasting reductions in post-fire NPP

To date, research has largely analyzed post-fire forest productivity with fire as a binary predictor variable (presence-absence). In the current study, we applied a dose-response methodology that has been demonstrated at the tree-scale (Smith et al. 2016, 2017; Sparks et al. 2016, 2017) to large fires using landscape remote sensing datasets. A dose-response relationship between ΣFRP/peak FRP and NPP was shown across all study fires and lasted for many years post-fire (Figures 3,4). In some cases, this dose-response relationship remained for greater than a decade post-fire (S1, S2). There were differences in the magnitude of post-fire NPP loss between forests with differing species composition (Figure 4). Generally, forests dominated by fire resistant species had lower post-fire relative NPP losses and fewer differences between ΣFRP/peak FRP percentile classes (Figures 4a-b). This is similar to relationships at the tree scale where trees that do not develop fire resistant traits, such as thick bark, have a higher probability of fire-induced damage and mortality (Ryan and Reinhardt 1988; VanderWeide and Hartnett 2011). Across all fires, the maximum NPP loss 1-year post-fire across all fires (63-274 g C m^{-2} yr^{-1}) is comparable to post-fire NPP

losses (60-260 g C m^{-2} yr^{-1}) observed using landscape remote sensing data and modeling in boreal forest (Hicke et al. 2003).

There was considerable variability in the dose-response relationships within each fire resistance grouping, which could potentially be attributed to differences in stand structure and age as well as differing proportions of burned and unburned area within each NPP pixel (mixed pixels). Previous studies have indicated that smaller trees are more susceptible to fire-induced mortality than larger trees (Hood et al. 2007). Additionally, there is evidence that similar FRP doses can lead to widely different growth responses across tree ages (Smith et al. 2017; Sparks et al. 2017). For example, 2.5-year-old *Pinus contorta* and *Larix occidentalis* saplings exposed to highly controlled laboratory surface fires (peak FRP ranged from 4.1-12.9 kW m^{-2}) had radial growth at 1 year post-fire that was -2.5 to -20% of unburned saplings (Smith et al. 2017). In contrast, prescribed fires in 34-year-old *Pinus ponderosa* stands produced a similar range of peak FRP (0.2-16.3 kW m^{-2}), but resulted in tree radial growth that was -10 to -45% of unburned tree radial growth at 1.5 years post-fire (Sparks et al. 2017). Additionally, previous studies have quantified unburned proportions within MTBS perimeters ranging from ~20-25% of within perimeter area (Meddens et al. 2016), which could lead to more mixed pixels (pixels containing burned and unburned forest). The forests analyzed in this study likely had heterogeneous stand structures and ages within each 1 km MODIS pixel. These sub-pixel differences could lead to widely different patterns of mortality and recovery and mask any pixel-scale dose-response relationship.

The observed dose-response relationship was also affected by variability in canopy cover and number of MODIS FRP observations per pixel. Fires that displayed a clear dose-response relationship (more differences between FRP percentile group relative NPP) had higher mean canopy cover (86.6 ± 8.5%) compared to fires that showed a weak dose-response relationship (83.4 ± 10.7%). Forests with higher mean canopy cover likely have a lower number of mixed pixels, or pixels that contain a significant areal proportion of non-forest cover (e.g. understory vegetation, non-vegetated areas). Higher areal proportions of understory vegetation could lead to a smaller NPP reduction post-fire if understory vegetation regenerates quickly after the fire (Bright et al. 2013). In addition to canopy cover, the dose-response relationship was stronger as the average number of MODIS FRP observations per pixel increased. The mean number of FRP observations per pixel decreased

from fires with a clear dose-response relationship (2.6 ± 0.6 obs. pixel^{-1}) to those with weak relationship (1.8 ± 0.1 obs. pixel^{-1}). This pattern could be attributed to the long temporal intervals between consecutive satellite overpasses (maximum 4 overpasses day-1) and consequently, a poorer overall characterization of the fire behavior for a particular pixel (Giglio 2007). This factor could also account for the differences observed between ΣFRP and peak FRP as the long intervals between consecutive satellite overpasses have a high probability of missing increased fire activity associated with peak FRP (Giglio 2007).

Recovery and trajectories of post-fire NPP

Despite an average post-fire observational period of 8.4 years across all fires, only the lowest ΣFRP/peak FRP percentile class of one fire (2006 South Fork Fire) had recovered to pre-fire NPP levels ~9 years post-fire. Other studies that have used remote sensing observations reported recovery time ranging from 5 years (Goetz et al. 2006) to 9 years (Hicke et al. 2003) in boreal forests. Likewise, chronosequence studies in boreal forest have estimated recovery to be ~10 years (Amiro et al. 2010). The results from this study are consistent with observations showing large differences in productivity between burned and unburned forest stands at time periods greater than 10 years post-fire (Dore et al. 2008).

The dose-response relationship for these fires diminished with time (fewer differences between FRP percentile groups). At six years post-fire, relative NPP for most of the FRP percentile classes was significantly different than the control, but there were few differences between FRP percentile class relative NPP (Figure 3). The convergence of NPP trajectories could be attributed to rapid recovery and colonization of fire affected areas by understory species (Goetz et al. 2006). The forests in the current study occur in areas where rapid post-fire colonization by shrub and herbaceous species is common (Jorgensen and Jenkins 2011), which could make NPP appear to recover more rapidly in areas where the forest overstory has been removed (Bright et al. 2013).

Conceptual framework for assessing spatiotemporal post-fire recovery

The results presented in this work, building upon previous tree-scale studies, provide a framework that links fire intensity to post-fire changes in individual tree and forest growth/productivity (Figure 5). In this conceptual system, several post-fire recovery pathways exist for trees/forests depending on the initial fire intensity. We hypothesize that higher intensity fires cause trees to incur more damage, which can lead to rapid mortality if

trees have insufficient resources to repair physiological function in the weeks and months following a fire. The highest fire intensity pathways lead to the greatest losses in physiological function and net primary productivity in surviving trees (Smith et al. 2017; Sparks et al. 2017) as well as the highest probability of delayed mortality in the years after a fire (Sparks et al. 2016). Moderate levels of fire intensity cause enough damage to decrease growth/productivity and alter a tree's vulnerability to secondary mortality agents (e.g. insects, disease and drought). Vulnerability may be lessened if permanent defensive structures, such as resin ducts in *Pinus* species used for expelling bark beetles, are induced by the fire (Hood et al. 2015; Sparks et al. 2017). On the contrary, fire may make trees more susceptible to secondary mortality agents if the photosynthetic potential of trees is sufficiently impaired (Davis et al. 2012). Trees experiencing low intensity fires will likely have reduced growth, but a higher probability of surviving than trees subjected to higher fire intensities. For any post-fire pathway, trees in better physiological condition or those exposed to fewer environmental stressors will likely experience a lower impact to post-fire growth and a lower probability of mortality.

Limitations

The dose-response relationship we observed between ΣFRP/peak FRP and post-fire NPP does not necessarily mean this methodology can now be directly applied to the characterization of landscape-scale C dynamics; several limitations are obvious. First, this study analyzed fires that occurred in forests with little-to-no management disturbance. Applying this methodology to managed forests may produce significantly different results as land management disturbances (e.g. timber harvest, urban development) may alter the dose-response relationship between FRP and NPP. Secondly, in forests with canopy cover <100%, MODIS observes reflectance from overstory and understory forest vegetation. Understory vegetation that recovers rapidly could alter the magnitude of post-fire NPP drop and make it appear to recover more or less quickly. Thirdly, due to the fact that MODIS FRP observations per pixel were generally low for fires in this region (mean = 2.2 observations $pixel^{-1}$), caution should be used when interpreting results and comparing to other ground and remote sensing based measurements. Finally, by excluding detections above 40º, ΣFRP values in this study underestimate the true ΣFRP observed by MODIS, and this effect should be considered when interpreting our results.

Conclusions

Through the use of remotely sensed fire radiative power and net primary productivity, we demonstrate that increasing doses of ΣFRP/peak FRP lead to decreasing post-fire net primary productivity in coniferous forests. This dose-response relationship has a legacy effect on C dynamics, in some cases lasting for greater than a decade post-fire. Species composition influenced the magnitude of post-fire NPP loss, highlighting the importance of relative fire resistance of forest species in accounting for post-fire C dynamics. Despite post-fire observations ranging up to 12 years, most of the forests had not recovered to pre-fire productivity levels, which agrees with field observations showing large differences in productivity between burned and unburned temperate forest stands up to a decade post-fire (Dore et al. 2008). Ultimately, this study extends prior tree-scale dose-response studies and presents a framework for using fire radiative metrics to quantifying long-term post-fire effects, such as reduction and recovery of NPP, at the landscape spatial scale.

Acknowledgements

Partial funding for this research for Sparks, Kolden, and Smith was provided by the National Science Foundation under Hazards SEES award #1520873. Partial funding for Sparks was provided by the Joint Fire Science Program under GRIN Award 16-2-01-09.

References

Abatzoglou, J.T. and Williams, A.P., 2016. Impact of anthropogenic climate change on wildfire across western US forests. *Proceedings of the National Academy of Sciences*, 113(42), pp.11770-11775.

Amiro, B.D., Barr, A.G., Barr, J.G., Black, T.A., Bracho, R., Brown, M., Chen, J., Clark, K.L., Davis, K.J., Desai, A.R., Dore, S., Engel V., Fuentes J.D., Goldstein A.H., Goulden M.L., Kolb T.E., Lavigne M.B., Law B.E., Margolis H.A., Martin T., McCaughey J.H., Misson L., Montes-Helu M., Noormets A., Randerson J.T., Starr G., and Xiao J. 2010. Ecosystem carbon dioxide fluxes after disturbance in forests of North America. *Journal of Geophysical Research: Biogeosciences*, 115(G4).

Archibald S, Scholes RJ, Roy DP, Roberts G, Boschetti L (2010) Southern African fire regimes as revealed by remote sensing. *International Journal of Wildland Fire* 19, 7, 861-878.

Balshi, M.S., McGuire, A.D., Duffy, P., Flannigan, M., Kicklighter, D.W. and Melillo, J., 2009. Vulnerability of carbon storage in North American boreal forests to wildfires during the 21st century. *Global Change Biology*, 15(6), pp.1491-1510.

Barbero, R., Abatzoglou, J.T., Larkin, N.K., Kolden, C.A. and Stocks, B., 2015. Climate change presents increased potential for very large fires in the contiguous United States. *International Journal of Wildland Fire*, 24(7), pp.892-899.

Barrett, K. and Kasischke, E.S., 2013. Controls on variations in MODIS fire radiative power in Alaskan boreal forests: implications for fire severity conditions. *Remote Sensing of Environment*, 130, pp.171-181.

Bonan, G.B., 2008. Forests and climate change: forcings, feedbacks, and the climate benefits of forests. *Science*, 320(5882), pp.1444-1449.

Bowman, D.M., Balch, J.K., Artaxo, P., Bond, W.J., Carlson, J.M., Cochrane, M.A., D'Antonio, C.M., DeFries, R.S., Doyle, J.C., Harrison, S.P. and Johnston, F.H., 2009. Fire in the Earth system. *science*, 324(5926), pp.481-484.

Bowman, D.M., Williamson, G.J., Abatzoglou, J.T., Kolden, C.A., Cochrane, M.A. and Smith, A.M., 2017. Human exposure and sensitivity to globally extreme wildfire events. *Nature Ecology & Evolution*, 1, p.0058.

Brewer, N.W., Smith, A., Hatten, J.A., Higuera, P.E., Hudak, A.T., Ottmar, R.D. and Tinkham, W.T., 2013. Fuel moisture influences on fire-altered carbon in masticated fuels: An experimental study. *Journal of Geophysical Research: Biogeosciences*, 118(1), pp.30-40.

Bright, B.C., Hicke, J.A. and Meddens, A.J., 2013. Effects of bark beetle-caused tree mortality on biogeochemical and biogeophysical MODIS products. *Journal of Geophysical Research: Biogeosciences*, 118(3), pp.974-982.

Chmura, D.J., Anderson, P.D., Howe, G.T., Harrington, C.A., Halofsky, J.E., Peterson, D.L., Shaw, D.C. and Clair, J.B.S., 2011. Forest responses to climate change in the northwestern United States: ecophysiological foundations for adaptive management. *Forest Ecology and Management*, 261(7), pp.1121-1142.

Davis, R.S., Hood, S. and Bentz, B.J., 2012. Fire-injured ponderosa pine provide a pulsed resource for bark beetles. *Canadian Journal of Forest Research*, 42(12), pp.2022-2036.

Dore, S., Kolb, T.E., Montes-Helu, M., Sullivan, B.W., Winslow, W.D., Hart, S.C., Kaye, J.P., Koch, G.W. and Hungate, B.A., 2008. Long-term impact of a stand-replacing fire on ecosystem CO2 exchange of a Ponderosa pine forest. *Global Change Biology*, 14(8), pp.1801-1820.

Dunnette, P.V., Higuera, P.E., McLauchlan, K.K., Derr, K.M., Briles, C.E. and Keefe, M.H., 2014. Biogeochemical impacts of wildfires over four millennia in a Rocky Mountain subalpine watershed. *New Phytologist*, 203(3), pp.900-912.

Eidenshink, J., Schwind, B., Brewer, K., Zhu, Z., Quayle, B. and Howard, S., 2007. A project for monitoring trends in burn severity. Fire Ecology 3 (1): 3-21. *Fire Ecology Special Issue* Vol, 3, p.4.

Fire Effects Information System (FEIS), [Online]. U.S. Department of Agriculture, Forest Service, Rocky Mountain Research Station, Missoula Fire Sciences Laboratory (Producer). Available: https://www.fs.fed.us/database/feis/plants/fern/polmun/all.html [2017, February 3].

Freeborn, P.H., Wooster, M.J. and Roberts, G., 2011. Addressing the spatiotemporal sampling design of MODIS to provide estimates of the fire radiative energy emitted from Africa. *Remote Sensing of Environment*, 115(2), pp.475-489.

Freeborn, P.H., Cochrane, M.A. and Wooster, M.J., 2014. A decade long, multi-scale map comparison of fire regime parameters derived from three publically available satellite-based fire products: a case study in the Central African Republic. *Remote Sensing*, 6(5), pp.4061-4089.

Gergel, D.R., Nijssen, B., Abatzoglou, J.T., Lettenmaier, D.P. and Stumbaugh, M.R., 2017. Effects of climate change on snowpack and fire potential in the western USA. *Climatic Change*, pp.1-13, doi:10.1007/s10584-017-1899-y.

Giglio, L., Csiszar, I. and Justice, C.O., 2006. Global distribution and seasonality of active fires as observed with the Terra and Aqua Moderate Resolution Imaging Spectroradiometer (MODIS) sensors. *Journal of Geophysical Research: Biogeosciences*, 111(G2).

Giglio, L., 2007. Characterization of the tropical diurnal fire cycle using VIRS and MODIS observations. *Remote Sensing of Environment*, 108(4), pp.407-421.

Giglio L (2010) 'MODIS Collection 5 Active Fire product User's Guide Version 2.5'. University of Maryland: College Park, MD).

Goetz, S.J., Fiske, G.J. and Bunn, A.G., 2006. Using satellite time-series data sets to analyze fire disturbance and forest recovery across Canada. *Remote Sensing of Environment*, 101(3), pp.352-365.

Goetz, S.J., Mack, M.C., Gurney, K.R., Randerson, J.T. and Houghton, R.A., 2007. Ecosystem responses to recent climate change and fire disturbance at northern high latitudes: observations and model results contrasting northern Eurasia and North America. *Environmental Research Letters*, 2(4), p.045031.

Hasenauer, H., Petritsch, R., Zhao, M., Boisvenue, C. and Running, S.W., 2012. Reconciling satellite with ground data to estimate forest productivity at national scales. *Forest Ecology and Management*, 276, pp.196-208.

Heinsch, F.A., Zhao, M., Running, S.W., Kimball, J.S., Nemani, R.R., Davis, K.J., Bolstad, P.V., Cook, B.D., Desai, A.R., Ricciuto, D.M. and Law, B.E., 2006. Evaluation of remote sensing based terrestrial productivity from MODIS using regional tower eddy flux network observations. *IEEE Transactions on Geoscience and Remote Sensing*, 44(7), pp.1908-1925.

Heward, H., Smith, A.M., Roy, D.P., Tinkham, W.T., Hoffman, C.M., Morgan, P. and Lannom, K.O., 2013. Is burn severity related to fire intensity? Observations from landscape scale remote sensing. *International Journal of Wildland Fire*, 22(7), pp.910-918.

Hicke, J.A., Asner, G.P., Randerson, J.T., Tucker, C., Los, S., Birdsey, R., Jenkins, J.C. and Field, C., 2002. Trends in North American net primary productivity derived from satellite observations, 1982–1998. *Global Biogeochemical Cycles*, 16(2).

Hicke, J.A., Asner, G.P., Kasischke, E.S., French, N.H., Randerson, J.T., James Collatz, G., Stocks, B.J., Tucker, C.J., Los, S.O. and Field, C.B., 2003. Postfire response of North American boreal forest net primary productivity analyzed with satellite observations. *Global Change Biology*, 9(8), pp.1145-1157.

Homer, C., Dewitz, J., Fry, J., Coan, M., Hossain, N., Larson, C., Herold, N., McKerrow, A., VanDriel, J.N., and Wickham, J. 2007. Completion of the 2001 National Land Cover Database for the Conterminous United States. *Photogrammetric Engineering and Remote Sensing*, Vol. 73, No. 4, pp 337-341.

Hood, S.M., McHugh, C.W., Ryan, K.C., Reinhardt, E. and Smith, S.L., 2007. Evaluation of a post-fire tree mortality model for western USA conifers. *International Journal of Wildland Fire*, 16(6), pp.679-689.

Hood, S., Sala, A., Heyerdahl, E.K. and Boutin, M., 2015. Low-severity fire increases tree defense against bark beetle attacks. *Ecology*, 96(7), pp.1846-1855.

IPCC (2013). The Fifth Assessment Report (AR5) of the United Nations Intergovernmental Panel on Climate Change (IPCC), Climate Change 2013: The Physical Science Basis, IPCC WGI AR5. Tech. rep., Intergovernmental Panel on Climate Change (IPCC).

Jorgensen, C.A. and Jenkins, M.J., 2011. Fuel complex alterations associated with spruce beetle-induced tree mortality in Intermountain spruce/fir forests. *Forest Science*, 57(3), pp.232-240.

Kashian, D.M., Romme, W.H., Tinker, D.B., Turner, M.G. and Ryan, M.G., 2006. Carbon storage on landscapes with stand-replacing fires. *BioScience*, 56(7), pp.598-606.

Kaufman, Y.J., Justice, C.O., Flynn, L.P., Kendall, J.D., Prins, E.M., Giglio, L., Ward, D.E., Menzel, W.P. and Setzer, A.W., 1998. Potential global fire monitoring from EOS-MODIS. *Journal of Geophysical Research: Atmospheres*, 103(D24), pp.32215-32238.

Kremens, R.L., Dickinson, M.B. and Bova, A.S., 2012. Radiant flux density, energy density and fuel consumption in mixed-oak forest surface fires. *International Journal of Wildland Fire*, 21(6), pp.722-730.

LANDFIRE: LANDFIRE Existing Vegetation Type layer. (2013, June - last update). U.S. Department of Interior, Geological Survey. [Online]. Available: http://landfire.cr.usgs.gov/viewer/ [2013, May 8].

Meddens, A.J., Kolden, C.A. and Lutz, J.A., 2016. Detecting unburned areas within wildfire perimeters using Landsat and ancillary data across the northwestern United States. *Remote Sensing of Environment*, 186, pp.275-285.

Neumann, M., Zhao, M., Kindermann, G. and Hasenauer, H., 2015. Comparing modis net primary production estimates with terrestrial national forest inventory data in Austria. *Remote Sensing*, 7(4), pp.3878-3906.

Romme, W.H., Boyce, M.S., Gresswell, R., Merrill, E.H., Minshall, G.W., Whitlock, C. and Turner, M.G., 2011. Twenty years after the 1988 Yellowstone fires: lessons about disturbance and ecosystems. *Ecosystems*, 14(7), pp.1196-1215.

Running, S.W., Nemani, R.R., Heinsch, F.A., Zhao, M., Reeves, M. and Hashimoto, H., 2004. A continuous satellite-derived measure of global terrestrial primary production. *Bioscience*, 54(6), pp.547-560.

Schoennagel, T., Veblen, T.T. and Romme, W.H., 2004. The interaction of fire, fuels, and climate across Rocky Mountain forests. *BioScience*, 54(7), pp.661-676.

Smith, A.M.S., A.M. Sparks, C.A. Kolden, J.T. Abatzoglou, A.F. Talhelm, D.M. Johnson, L. Boschetti, J.A. Lutz, K.G. Apostol, K.M. Yedinak, W.T. Tinkham and R.J. Kremens (2016), Towards a new paradigm in fire severity research using dose-response experiments, *International Journal of Wildland Fire*, dx.doi.org/10.1071/WF15130.

Smith, A.M.S., A.F. Talhelm, D.M. Johnson, A.M. Sparks*, C.A. Kolden, K.M. Yedinak, K.G. Apostol, W.T. Tinkham, J.T. Abatzoglou, J.A. Lutz, A.S. Davis, K.S. Pregitzer, H.D. Adams, and R.L. Kremens (2017), Effects of fire radiative energy density doses on *Pinus contorta* and *Larix occidentalis* seedling physiology and mortality, *International Journal of Wildland Fire*, WF16077.

Spanner, M.A., Pierce, L.L., Peterson, D.L. and Running, S.W., 1990. Remote sensing of temperate coniferous forest leaf area index: The influence of canopy closure, understory

vegetation and background reflectance. *International Journal of Remote Sensing*, 11(1), pp.95-111.

Sparks, A.M., C.A. Kolden, A.F. Talhelm, A.M.S. Smith, K.G. Apostol, D.M. Johnson and L. Boschetti (2016), Spectral indices accurately quantify changes in seedling physiology following fire: toward mechanistic assessments of post-fire carbon cycling, *Remote Sensing*, 8, 7, 572.

Sparks, A.M., A.M.S. Smith, A.F. Talhelm, C.A. Kolden, K.M. Yedinak and D.M. Johnson (2017), Impacts of fire radiative flux on mature *Pinus ponderosa* growth and vulnerability to secondary mortality agents, *International Journal of Wildland Fire*, doi:10.1072/WF16139.

Starker, T.J., 1934. Fire resistance in the forest. Journal of Forestry, 32(4), pp.462-467.

Tinkham, W.T., Smith, A.M., Higuera, P.E., Hatten, J.A., Brewer, N.W. and Doerr, S.H., 2016. Replacing time with space: using laboratory fires to explore the effects of repeated burning on black carbon degradation. *International Journal of Wildland Fire*, 25(2), pp.242-248.

Turner, D.P., Ritts, W.D., Cohen, W.B., Gower, S.T., Running, S.W., Zhao, M., Costa, M.H., Kirschbaum, A.A., Ham, J.M., Saleska, S.R. and Ahl, D.E., 2006. Evaluation of MODIS NPP and GPP products across multiple biomes. *Remote Sensing of Environment*, 102(3), pp.282-292.

VanderWeide, B.L. and Hartnett, D.C., 2011. Fire resistance of tree species explains historical gallery forest community composition. *Forest Ecology and Management*, 261(9), pp.1530-1538.

Westerling, A.L., Turner, M.G., Smithwick, E.A., Romme, W.H. and Ryan, M.G., 2011. Continued warming could transform Greater Yellowstone fire regimes by mid-21st century. *Proceedings of the National Academy of Sciences*, 108(32), pp.13165-13170.

Williamson, G.J., Price, O.F., Henderson, S.B. and Bowman, D.M., 2013. Satellite-based comparison of fire intensity and smoke plumes from prescribed fires and wildfires in south-eastern Australia. *International Journal of Wildland Fire*, 22(2), pp.121-129.

Zhao, M. and Running, S.W., 2010. Drought-induced reduction in global terrestrial net primary production from 2000 through 2009. *Science*, 329(5994), pp.940-943.

Tables

Table 2. Summary of the fifteen fires analyzed in this study.

Fire Name	Size (ha)	Location	Dominant Conifer Species	Ignition Date
Ahorn	18,778	Montana	Mix	June 28, 2007
Arnica	4,556	Wyoming	Avoiders	September 23, 2009
Bridge	15,116	Idaho	Avoiders	July 18, 2007
Columbine	7,115	Wyoming	Avoiders	August 9, 2007
East	7,145	Wyoming	Avoiders	August 8, 2003
Fawn Peak	31,870	Washington	Mix	June 30, 2003
Fool Creek	22,186	Montana	Avoiders	June 28, 2007
Little Salmon	13,598	Montana	Mix	July 18, 2003
Meriwether	7,762	Montana	Resistors	July 21, 2007
North Fork	6,774	Oregon	Resistors	August 1, 2009
Saddle	12,706	Idaho	Mix	August 18, 2011
Sawmill	6,015	Montana	Resistors	July 13, 2007
Shower Bath	19,911	Idaho	Resistors	July 17, 2007
South Fork	11,494	Idaho	Resistors	August 7, 2006
Tatoosh	20,185	Washington	Mix	August 22, 2006

Figures

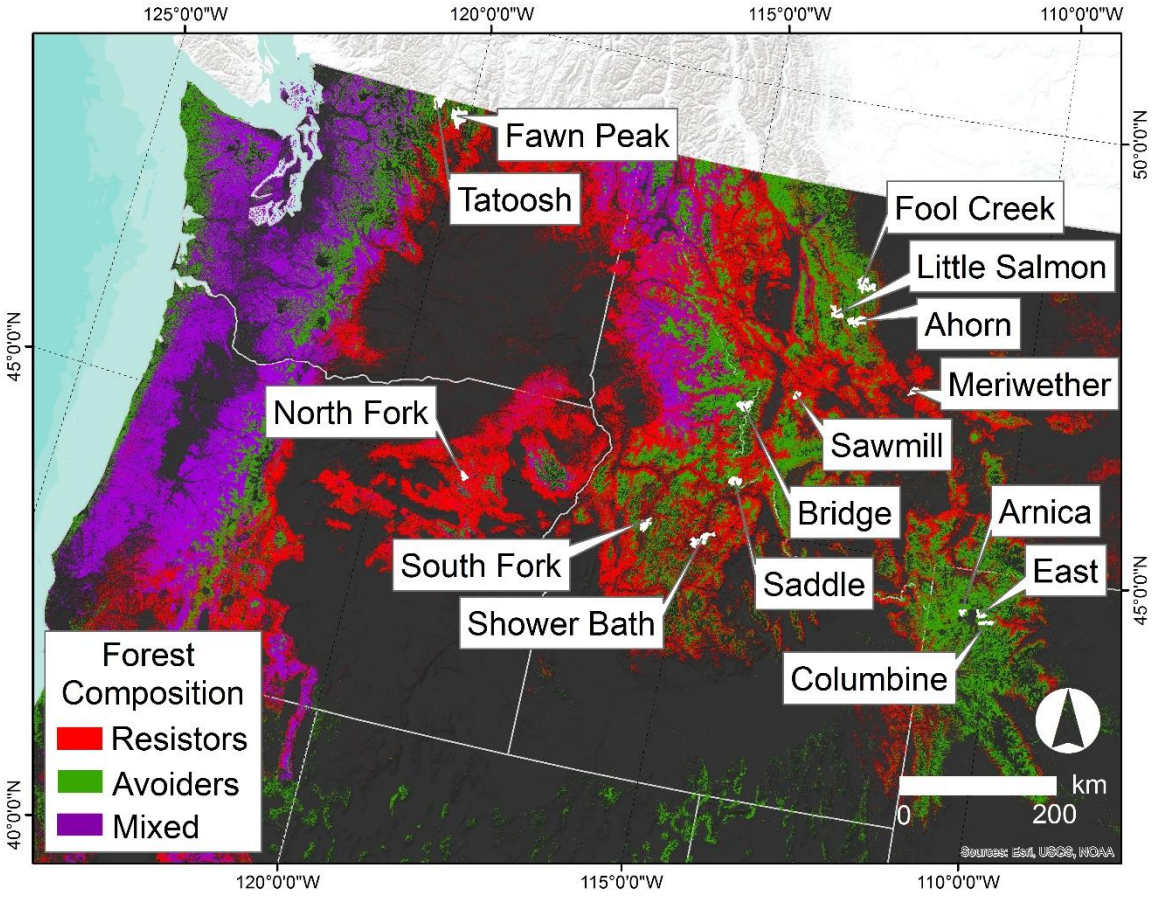

Figure 1. Location of study fires overlaid on current distribution of U.S. forest type classified using relative fire resistance information in the literature.

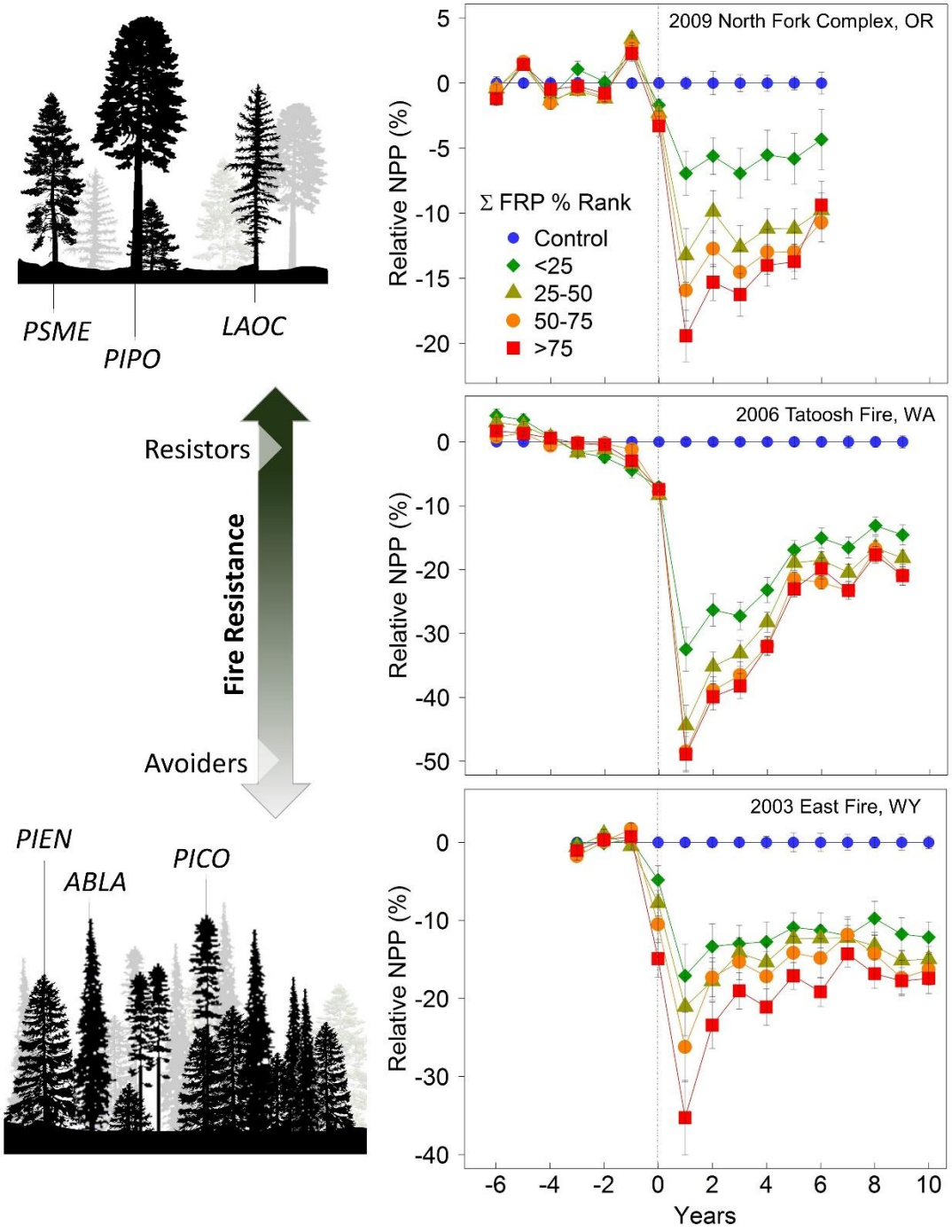

Figure 2. ΣFRP dose impacts on net primary productivity response observed in forest stands dominated by species varying from highly resistant (resistors) to less resistant (avoiders) (top – bottom row). Four letter codes represent typical conifer species in northwestern United States forests: PSME, *Pseudotsuga menziesii*; PIPO, *Pinus ponderosa*; LAOC, *Larix occidentalis*; PIEN, *Picea engelmannii*; ABLA, *Abies lasiocarpa*; PICO, *Pinus contorta*. Grey dotted line marks fire year.

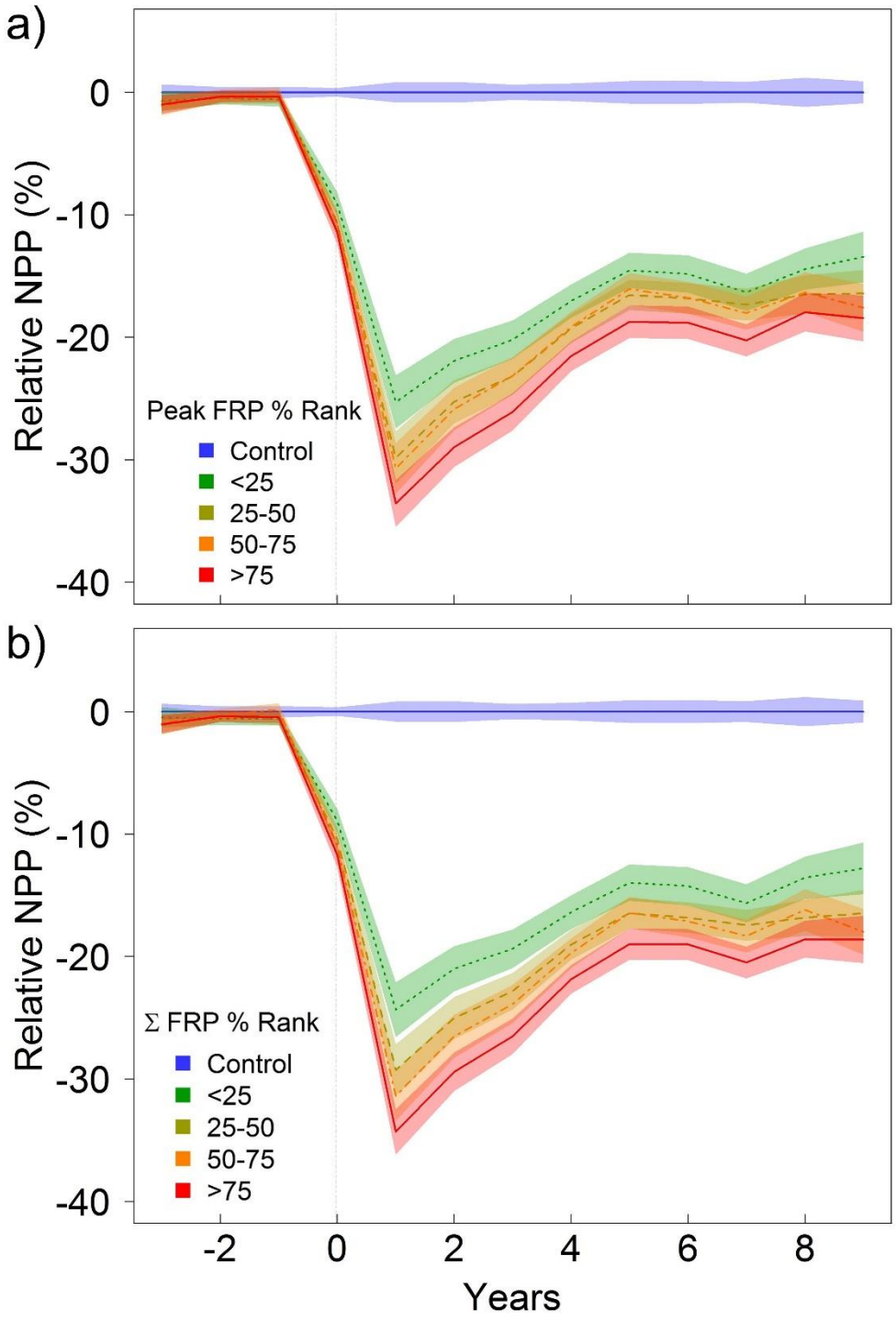

Figure 3. FRP impacts on net primary productivity response across all study fires by: a) peak FRP percentile class and b) ΣFRP percentile class. Shading represents 95% confidence intervals and vertical grey dotted line marks fire year.

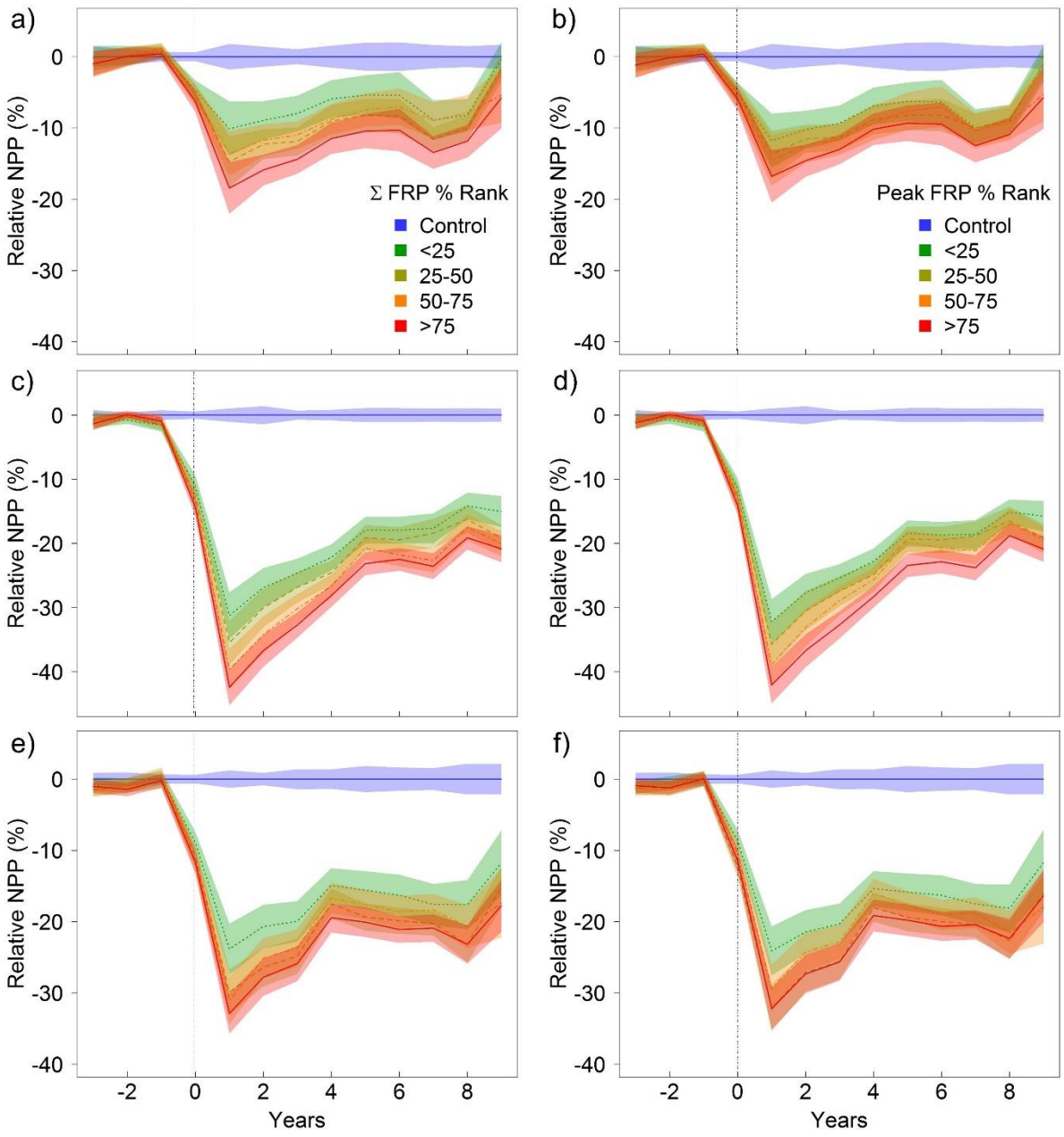

Figure 4. FRP impacts on net primary productivity response by ΣFRP percentile class (left column) and peak FRP percentile class (right column). NPP response shown for forests dominated by species varying from highly resistant (a,b) to mixed (c,d) to less resistant (e,f). Shading represents 95% confidence intervals and vertical grey dotted line marks fire year.

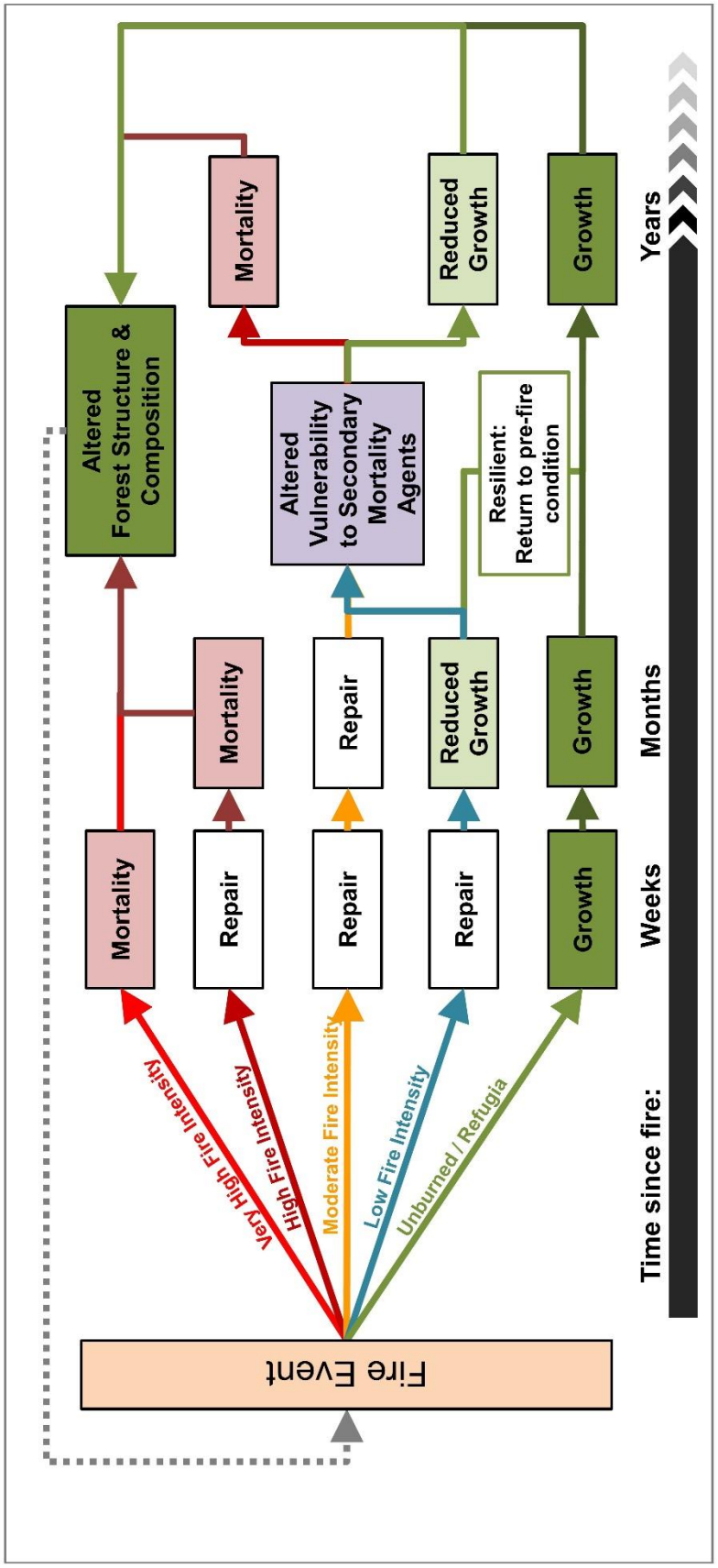

Figure 5. Conceptual framework for quantifying impacts of fire intensity on physiology, growth, and vulnerability of coniferous forests.

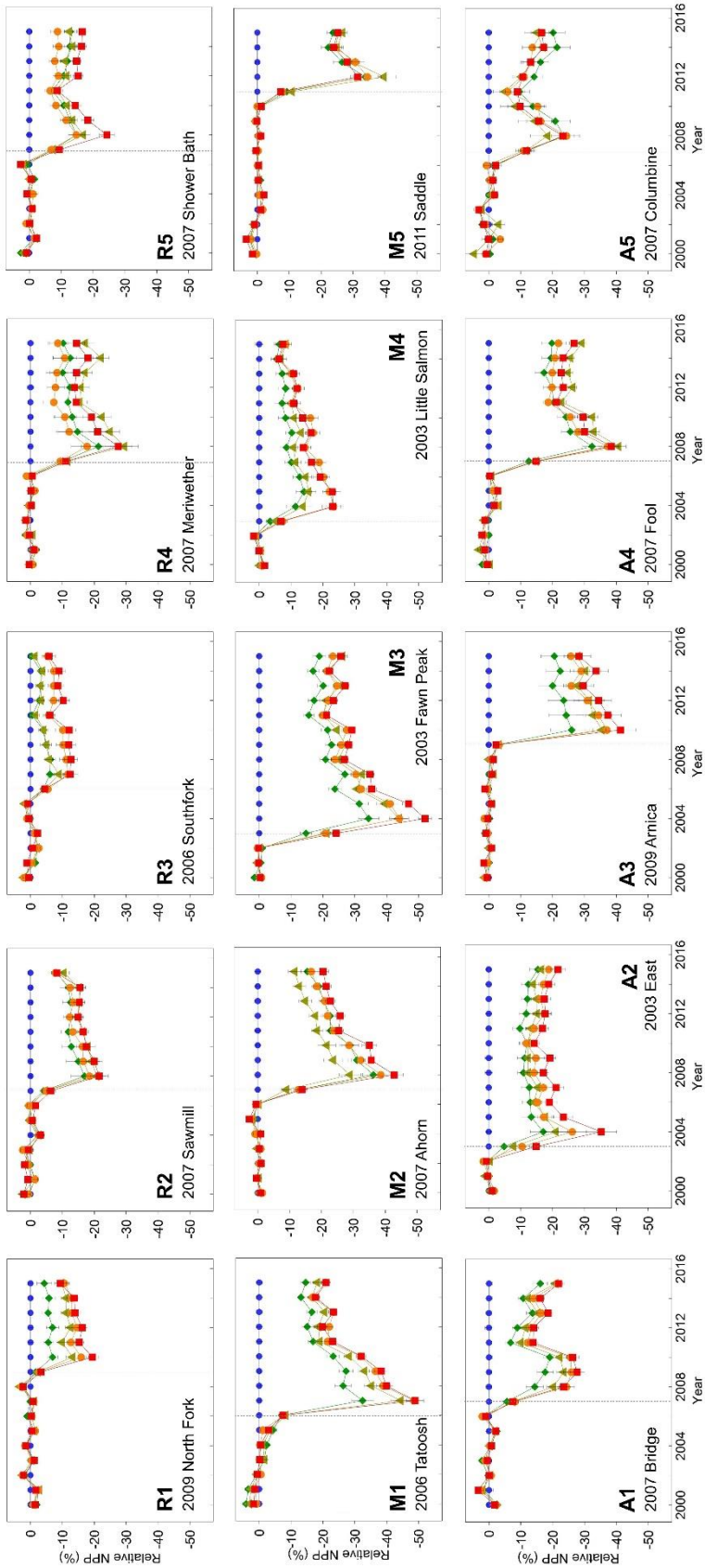

Supplemental Figure 1. ΣFRP dose impacts on NPP response observed in forest stands dominated with species across the fire resistance continuum. Resistor dominated forests (R1-R5), mixed forests (M1-M5), and avoider dominated forests (A1-A5) are shown. Grey dotted line marks fire year; colors as in figure 2.

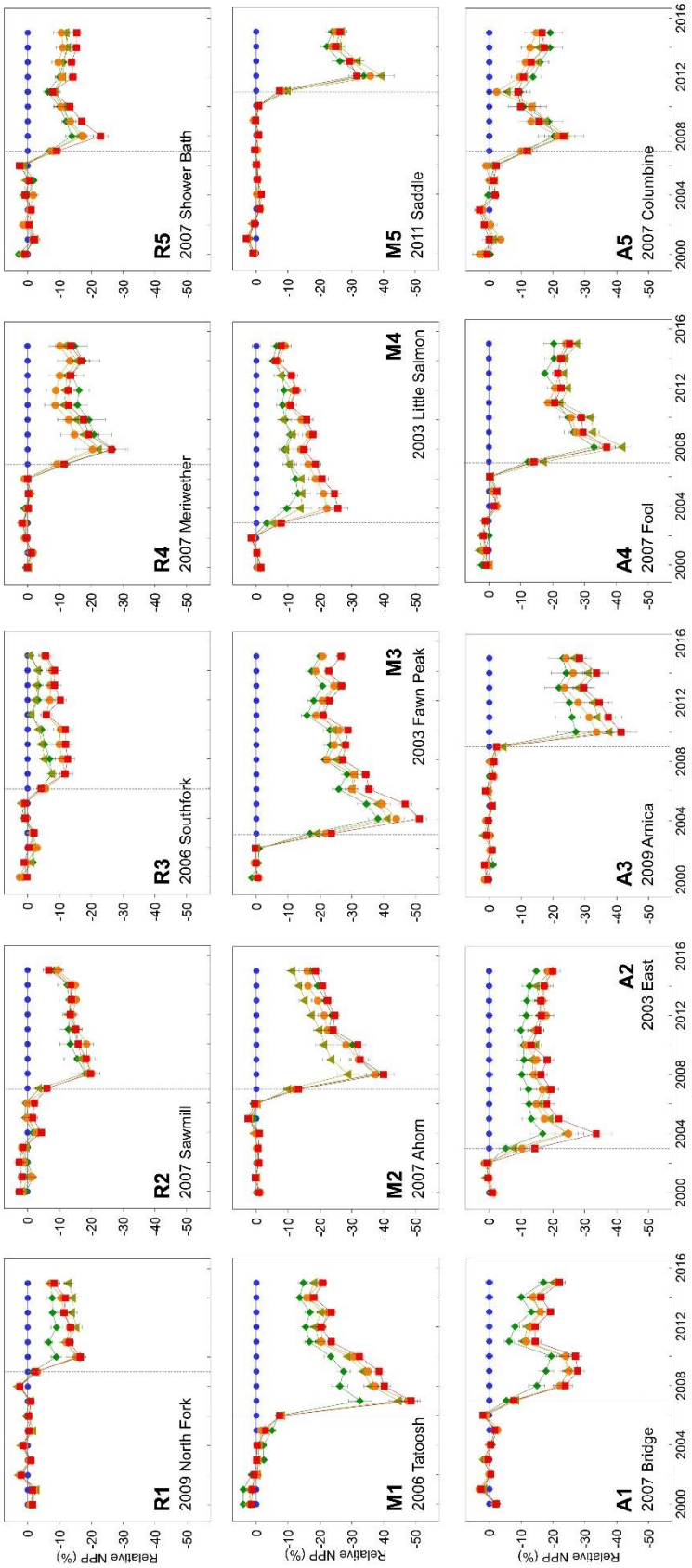

Supplemental Figure 2. Peak FRP dose impacts on NPP response observed in forest stands dominated with species across the fire resistance continuum. Resistor dominated forests (R1-R5), mixed forests (M1-M5), and avoider dominated forests (A1-A5) are shown. Grey dotted line marks fire year; colors as in figure 2.

Chapter 5

Conclusions and Future Research Avenues

In this PhD dissertation I sought to improve our understanding of fire impacts on conifer physiology, mortality and vulnerability and develop a spatiotemporal framework to quantify these impacts. Specifically, the research in this dissertation sought to quantify relationships between fire intensity and tree physiological processes, growth, and mortality at individual tree and landscape spatial scales. Laboratory, field, and satellite data were used to help quantify these relationships at multiple spatial and temporal scales.

In Chapter 2, highly controlled laboratory surface fires were used to quantify relationships between fire radiative metrics and post-fire seedling physiology and mortality. Increasing doses of fire radiative energy led to greater reductions in physiological function (e.g. net photosynthesis, chlorophyll fluorescence) and higher mortality at one year post-fire. Physiological change was accurately quantified by the dNDVI spectral index, indicating the potential of spectral indices for quantification of post-fire carbon processes. All spectral indices returned to baseline values at one year post-fire suggesting that initial severity assessments may be more useful than extended assessments. This work has implications for both land managers and researchers seeking to quantify and predict mortality and recovery of surviving seedlings post-fire. Additionally, this chapter provides critical information for interpreting spectral index values in terms of physiological change over time.

Chapter 3 used prescribed fires in *Pinus ponderosa* stands to quantify relationships between fire radiative metrics and mature *Pinus ponderosa* growth and vulnerability post-fire. Increasing fire radiative power led to decreases in radial growth of fire affected *Pinus ponderosa*. Unlike chapter 2, there was no relationship between fire radiative energy and tree growth. This discrepancy is potentially due to differences in fire behavior; in chapter 2 fire behavior was flaming dominated and in chapter 3 fire behavior was dominated by smoldering combustion. Results suggest that other modes of heat transfer (e.g. convection) associated with higher intensity fire behavior (e.g. higher fireline intensity and fire radiative power) may be responsible for reductions of growth post-fire. Increased resin duct density, average size, and total area per growth ring occurred regardless of fire intensity, indicating that *Pinus ponderosa* may have reduced vulnerability to secondary mortality agents, such as bark beetles, post-fire. This work has implications for both land managers and researchers

seeking to quantify and predict impacts of prescribed and wildland fires on mature tree growth and vulnerability post-fire. This chapter also highlights the importance of quantifying fine-scale fire behavior (instead of average fire behavior for entire fire spatial extent and duration) for determining fire effects.

Chapter 4 used landscape remote sensing observations from fifteen large wildfires in the northwestern United States to quantify relationships between fire radiative power and coniferous forest productivity. Similar to observations at the tree scale, forest net primary productivity decreased with increasing fire intensity, regardless of species composition. This dose-response relationship has a legacy effect on C dynamics, in some cases lasting for greater than a decade post-fire. Forests with higher fire resistant species displayed lower reductions in post-fire net primary productivity, highlighting the importance of species composition in accounting for post-fire carbon dynamics. This work has implications for both land managers and researchers seeking to quantify and predict impacts of prescribed and wildland fires on coniferous forests at the landscape spatial scale and decadal temporal scale. The conceptual framework presented in this work demonstrates a model for future spatiotemporal post-fire recovery assessments.

The ultimate goal of this dissertation was to build a spatiotemporal framework that could either predict fire effects using active fire observations from field/remotely sensed data, predictable fire behavior metrics (e.g. fire radiative power, fire radiative energy), or post-fire remotely sensed data. While the research in this dissertation made large advances toward that goal, our knowledge regarding impacts of fires on trees is far from complete and there are an uncountable number of questions that need to be explored in future research. A few of the questions that arose during the completion of this dissertation were: Are there dose-response relationships between other modes of heat transfer (e.g. conduction, convection) and post-fire tree mortality/physiology/growth? How does duration of heat flux dose impact vegetation response post-fire (i.e. vegetation response to heat flux dose over a long time versus same dose distributed over a short time)? Are trees most affected by heat induced damage to roots, stem, or crown? Is there a particular age or size where trees that develop fire resistant features (e.g. thick bark, high crown base height) respond to fire differently than less resistant species? How does plant stress (e.g. water and nutrient stress) affect the observed dose-response relationship in seedlings and mature trees? How do multiple

disturbances (e.g. fire + bark beetles, fire + drought, fire + human land management) affect the dose-response relationship between fire behavior and tree mortality? The initial trajectory of my future research will be guided by these unanswered questions.

Appendix A

Relationships between fuel properties, biomass consumed, and energy release in heterogeneous woody fuels

Abstract

Several relationships between fire radiative power (FRP: W) and rate of biomass consumed (g s^{-1}) are available in the scientific literature. Although fuel moisture has been demonstrated to impact these relationships in pine needle fuelbeds, the role of this and other factors including particle size and fuelbed bulk density in wood dominated fuels is not well understood. Controlled laboratory experiments were used to explore relationships between biomass consumed (BC: kg m^{-2}), FRP, and fire radiative energy per unit area (FRE: J m^{-2}). Experiments were conducted using both idealized wood dowels and irregular natural woody fuels burned under varying levels of fuel water content, particle surface-area-to-volume ratio (SA/V: m^{-1}), and fuelbed bulk density (kg m^{-3}). Results demonstrate that fuels with greater SA/V generally produce larger peak fire radiative power values. Linear relationships between BC and peak FRP in dry fuelbeds indicates that peak FRP can potentially be modeled from BC in uniform or mixed fuelbeds. Particle SA/V and fuelbed bulk density were not observed to be significant drivers of the amount of biomass consumed per Joule of FRE emitted; a metric often referred to as the combustion factor (CF: kg J^{-1}). While not significant, the ambient fuel water content particles exhibited consistently higher combustion factors than their dry counterparts. These results demonstrate that FRE can be used to estimate biomass consumed in heterogeneous woody fuels. The results also further confirmed a previous theoretical biomass consumed model that linked FRE and fuel water content and demonstrated its broad applicability across fuel types.

Introduction

Fires are critical to human civilization and Earth system processes (Bowman *et al.* 2009; Smith *et al.* 2016a). Estimates of biomass consumed from global wildland fires are important in quantifying impacts on regional air quality and climate-altering large-scale atmospheric chemistry processes (Seiler and Crutzen 1980; Andreae and Merlet 2001; van der Werf *et al.* 2010; Hyde *et al.* in review). A common approach to inferring biomass

consumed from wildland fires is through the application of biomass conversion factors (Wooster *et al.* 2005; Schroeder *et al.* 2014) which relate observations of fire radiative power (FRP, units: W) to the rate of biomass consumed (Freeborn *et al.* 2008; Kaiser *et al.* 2012; Kremens *et al.* 2012; Smith *et al.* 2013; Hudak *et al.* 2015). Fire radiative energy (FRE, units: J), the time integral of FRP, is linearly related to total biomass combusted in many different fuel types (Wooster *et al.* 2005; Freeborn *et al.* 2008; Smith *et al.* 2013). This relationship, termed the combustion factor (CF), is the amount of biomass consumed per Joule of FRE emitted (kg MJ^{-1}) for a given fuel type. Several universal combustion factors have been proposed to aid global emission estimates (Wooster *et al.* 2005; Kaiser *et al.* 2012), however, limited research has examined the associated uncertainties (Freeborn *et al.* 2008; Smith *et al.* 2013).

FRP and FRE have been used for quantifying emissions from fires globally. Bottom-up trace gas and aerosol emissions can be estimated using the product of biomass consumption from FRP/FRE derived CFs with trace gas and aerosol emission factors (Freeborn *et al.* 2008; Wooster *et al.* 2011; Konovalov *et al.* 2011; Kaiser *et al.* 2012; McCarty *et al.* 2012; Zhang *et al.* 2012; Schroeder *et al.* 2014), or by directly relating emission rates and total flux to FRP or FRE (emission ratios: g MJ^{-1}) (Ichoku and Kaufman 2005; Freeborn *et al.* 2008; Mebust *et al.* 2011; Konovalov *et al.* 2014). Recent research has demonstrated that assuming a constant CF across fuel types can significantly impact emissions estimates (Schroeder *et al.* 2014). Likewise, emission fluxes derived from emission ratios may be subject to large errors if seasonal changes in combustion efficiency and trace gas emissions are not considered (Hoffa *et al.* 1999; Korontzi *et al.* 2003; Lapina *et al.* 2008; Mebust and Cohen 2013). In addition to fire emissions, there are an increasing number of studies using FRP metrics (e.g. peak FRP values) to characterize fire behavior (Kremens *et al.* 2012; Hudak *et al.* 2016), fire severity (Heward *et al.* 2013), post-fire vegetation response and mortality (Sparks *et al.* 2017), fire regimes (Archibald *et al.* 2010; Andela *et al.* 2015), and assessing global susceptibility to wildfires (Bowman *et al.* in review).

Several studies have identified sources of uncertainty associated with FRP and FRE including: sensor viewing angle (Freeborn *et al.* 2008; Frankman *et al.* 2013; Paugam *et al.* 2013; Freeborn *et al.* 2014; Dickinson *et al.* 2016), temporal sampling issues (Boschetti and Roy, 2009; Kumar *et al.* 2011; Hudak *et al.* 2015), obscuration by clouds, smoke (Schroeder

et al. 2014), and tree cover (Hudak *et al.* 2015; Mathews *et al.* 2016), combustion phase (Freeborn *et al.* 2008), radiative fraction (f_r) (Kremens *et al.* 2010, 2012), emission and absorption by trace gas combustion products (Kremens *et al.* 2012; Dickinson *et al.* 2016), fire diurnal cycles (Andela *et al.* 2015), and fuel water content (Smith *et al.* 2013). While many studies have proposed that fuel type (Kremens *et al.* 2012; Schroeder *et al.* 2014) and fuel bed heterogeneity (Simeoni *et al.* 2011; Cannon *et al.* 2014; Andela *et al.* 2015) may be a significant source of uncertainty in estimating FRE and CFs, few have specifically tested these assumptions. Table 1 presents a synthesis of the wide range of observed and modeled CFs found in the literature.

Fuel particle size and shape, which have not been widely researched, are additional potential sources of uncertainty in FRP and FRE characterization. Fuel particle research has indicated that particle size and shape as well as porosity of the entire fuelbed can significantly influence combustion properties including: conduction, convection, and radiation heat transfer rates (Finney *et al.* 2013; Santoni *et al.* 2014; Al-Shemmeri *et al.* 2015), moisture evaporation rate (Yang *et al.* 2005), and volatile yields (Lu *et al.* 2010). Specifically, fuelbeds with smaller particles have been observed to have higher moisture evaporation rates (Yang *et al.* 2005) and higher volatile yields, regardless of particle shape (Lu *et al.* 2010). An additional source of uncertainty arises in wood-dominated fuelbeds. Specifically, particle water content, which is known to impact f_r (Smith *et al.* 2013), can vary dramatically due to the vertical and horizontal arrangement in the fuelbed. Additionally, highly compacted fuels within the fuelbed will exhibit very different water content characteristics than surface fuels that are subjected to higher degrees of solar heating (Kreye *et al.* 2012). Although most CF relationships have been produced assuming constant water content, a theoretical biomass consumed model using FRE that incorporated varying water content has been proposed (Smith *et al.* 2013).

Clearly, the assessment of FRP, FRE, and biomass consumed can be particularly challenging when dealing with highly heterogeneous fuelbeds such as sites with large quantities of downed woody debris. In such fuel complexes, destructive quadrat sampling may not be realistic given the large potential mass of fuel per typical field sampling unit (e.g. 1 m^2). Therefore, the objectives of this study were to: (1) Characterize FRP per unit area (W m^{-2}), which is sometimes referred to as fire radiative flux density (FRFD), and FRE

per unit area (J m^{-2}), often referred to as FRED (Kremens *et al.* 2012; Hudak *et al.* 2016), released as a function of particle surface-area-to-volume ratio (SA/V: m^{-1}) under dry and ambient fuel water content, (2) characterize FRP and FRE in both idealized and natural woody fuel beds under a range of fuelbed bulk densities, and (3) test whether a theoretical biomass consumed model using FRE, that includes water content and was developed on pine needle fuelbeds, transfers to the combustion of woody fuels.

Methodology

Fuelbed characterization

Laboratory burn experiments were conducted at the combustion laboratory associated with the Idaho Fire Institute for Research and Education (IFIRE) detailed in Smith *et al.* (2013, 2016b) and Sparks *et al*. (2016). Two fuel types with three significantly different mean SA/V's were burned: 1) cylindrical birch dowels (diameters: 0.32, 0.79, and 1.27 cm) cut into ~1 cm sections, and 2) recently chipped *Pinus ponderosa* Dougl. ex Laws. (ponderosa pine) chips (Figure 1). Dowels were chosen to represent a theoretically uniform-SA/V fuelbed. Chipped *Pinus ponderosa* chips were sorted into three SA/V groups using coarse mesh (~2.54 cm pore size) and fine mesh (~1.27 cm pore size) sieves following the methodology presented in Brewer *et al.* (2013). Volume (m^3) and surface area (m^2) were estimated from a simple random sample (n=50) from each sorted group. Sample size represented the number of observations necessary to estimate each group mean within less than ±15% at the 95% confidence level. Volume and surface area of dowels were calculated using particle length and diameter. Average (±SE) SA/V (m^{-1}) for the dowel groups was 1390 (4.5), 659 (1.1), and 469 (0.6). Volume of chipped particles was determined using water displacement methodology presented in Fasth *et al.* (2010). Surface area of chipped particles was determined via a planar area approach as the majority of chipped particles were fractured into flat-faced triangular or rectangular prisms. Planar area methods have been shown to be more appropriate for characterizing porous, irregularly shaped objects than wetted layer techniques (e.g. Fernandes and Rego 1998) that use changes in mass from immersion of object into water or other substance (Bergey and Getty 2006). We acknowledge that a downside of the planar area approach is that it underestimates surface area for particles that have rough surface texture (Bergey and Getty 2006). Images of each

particle face were acquired with a 16 mega-pixel tripod-mounted camera with a known field-of-view and classified using the Hartigan-Wong K-means clustering algorithm (Hartigan and Wong 1979) within R statistical software version 3.2.1 (R Core Team 2014). The total surface area of a chipped particle was calculated to be the sum of each classified particle face. Average (±SE) SA/V (m^{-1}) for the chipped groups was 1082 (41.5), 666 (27.8), and 395 (23.7).

Fuelbeds were created by combining dry *Pinus monticola* needles and dowel/chipped woody particles such that there was a uniform mixture of wood particles and needles (Figure 1). *Pinus monticola* needles were used to facilitate fire spread, as fire would not spread in pure wood fuelbeds. *Pinus monticola* needles were used instead of *Pinus ponderosa* needles as the combustion characteristics are well understood (Smith *et al.* 2013, 2016b; Sparks *et al.* 2016), whereas we observed that *Pinus ponderosa* needles exhibited high variability of heat release at fuel water content < 0.06, potentially due to the presence of oils. The fuel water content, W_C, was calculated and controlled following the methodology presented in Smith *et al.* (2013).

$$W_C = \frac{W_M}{D_M + W_M} \quad (1)$$

where, W_C (dimensionless, 0-1) is the fuel water content, W_M (kg) is the water mass, and D_M (kg) is the dry mass of the fuel sample. Fuelbeds were compressed with a steel plate to a desired depth and measured at four locations (center and edges) to the nearest 0.1 cm to ensure uniformity of fuelbed bulk density. To examine biomass consumed to FRE relationships, a total of 36 dry (W_C <0.01) fuelbeds were burned (2 fuel types * 3 SA/V groups * 2 fuelbed bulk densities * 3 replicates). To test the combined influence of SA/V and W_C, an additional 30 fuelbeds were burned (2 fuel types * 3 SA/V groups * 1 fuelbed bulk density * 5 replicates) at ambient W_C, 0.09 ± 0.007 (mean ± SE). Fuelbeds were burned at fuelbed bulk densities of: 50 and 70 kg m^{-3} for dry dowels, 30 and 40 kg m^{-3} for dry chipped particles, 64 kg m^{-3} for ambient dowels, 50 kg m^{-3} for ambient chipped particles. Fifty grams of needles were used for all fuelbeds except the ambient dowel burns, where 100 g were used.

Theoretical Heat Budget

Following the methodologies of Kremens *et al.* (2012) and Smith *et al.* (2013), the following approximate heat budget was used to account for the relationship between FRE and biomass consumed as a function of the fuel water content:

$$\frac{FRE}{BC} = f_r\left[H_c - W_c\left(H_c + H_{vap} + C_W(373 - T_a) + H_D\right)\right] \quad (2)$$

where W_c and FRE are already defined, BC is the biomass consumed (kg m^{-2}), H_c is the high heat of combustion of the fuels (MJ kg^{-1}), H_{vap} is the enthalpy of water vaporization at atmospheric pressure (2.257 MJ kg^{-1}), C_W is the heat capacity of water (0.0042 MJ kg^{-1}), T_a is the ambient temperature (300 K), and H_D is the heat of desorption (0.1 MJ kg^{-1}). The fraction of total energy released in the form of radiation (f_r) was then derived by dividing the observed FRE (MJ m^{-2}) by the product of the heat of combustion (MJ kg^{-1}) and the total biomass consumed (kg m^{-2}). Wood and pine needle high heat of combustion values were measured using a Parr plain jacket calorimeter (Parr Instrument Company, Moline, IL, USA). Average (±SE) H_C (MJ kg^{-1}) values for the needles, dowels, and chipped *Pinus ponderosa* were 21.7 (0.16), 19.5 (0.46), and 19.5 (0.26), respectively.

To model BC, while accounting for W_C, we followed the derivation outlined in Smith et al. (2013) where equation (2) is rearranged and substituted by (1) and normalized for biomass consumed:

$$BC = \frac{FRE}{(b - m * W_c)} \quad (3)$$

where m is the bias in the FRE emitted per unit biomass consumed as a function of W_C, and b (MJ kg^{-1}) is the FRE emitted per unit of biomass consumed for dry fuel (0 W_C). Therefore, b is the reciprocal of CF on a dry fuel basis. The constant m is derived by calculating the slope coefficient from linear regression analysis between FRE/BC (dependent variable) and W_C (independent variable). For the purpose of this assessment, the value of m presented in Smith *et al.* (2013) of 5.32 is applied. Although this value was calculated for *Pinus monticola* needles, it was used in this study to evaluate the broad transferability of this method.

Experimental Burns

For each burn, 1-2 g of butane was applied to the edge of each fuelbed to promote a uniform flaming front. FRP was calculated via dual-band thermometry (Dozier 1981) using a dual-band infrared radiometer detailed in Kremens *et al.* (2012) and Smith *et al.* (2013). The 52º field-of-view radiometer was positioned at nadir, 0.68 m above the center of each 0.28 m^2 circular fuelbed and recorded data at 2 Hz from several minutes pre-ignition to burn completion. Each burn was considered complete when FRP values reached mean pre-fire values. After each burn, charred wood particles and ash were sifted using a fine sieve (~2 mm pore size), oven dried, and weighed to obtain separate consumption estimates for the wood particles and pine needles and calculate FRE per unit biomass consumed (FRE/BC: MJ kg^{-1}). FRE values for the wood particles were calculated by subtracting pine needle FRE from total FRE. Pine needle FRE for dry fuels (W_C <0.01) was obtained by using a previously calculated biomass consumed to FRE relationship, FRE = BC / 0.331 (Smith *et al.* 2013). This calculation was performed with the assumption that the majority of radiation emitted from combusting pine needles in the sensor field-of-view was not blocked or absorbed by wood particles. This assumption should be reasonable as the construction of our fuelbeds resulted in minimal layering of pine needles and wood.

Data Analysis

To assess whether SA/V had a significant effect on peak FRP, the relationship between FRP and BC for each SA/V group was characterized using linear regression. For comparison purposes, data from Smith *et al.* (2013) was used to assess this relationship for pure *Pinus monticola* fuelbeds. A SA/V estimate of 9050 m^{-1} was used for *Pinus monticola* needles (Brown 1970). Linear regression was also used to characterize the relationships between FRE and BC for each SA/V and fuelbed bulk density group. The regressions between FRP/FRE and biomass consumed for each of the different SA/V and fuelbed bulk density groups were compared using analysis of covariance (ANCOVA) to determine whether the slope coefficients were significantly different ($p < 0.05$). Relationship 'goodness of fit' between explanatory and response variables was assessed using the coefficient of determination (r^2) and standard error (SE).

Results and Discussion

Peak FRP values increased linearly as BC increased for both fuel types at 0.0 W_C (Figure 2). In pure *Pinus monticola* fuelbeds, peak FRP was linearly related with BC (r^2 = 0.99, SE=0.77 kW m^{-2}, $p<0.001$) (Figure 2). Likewise, all woody fuelbeds (dowels and chipped fuels) at 0.0 W_C displayed strong linear relationships ($r^2 > 0.9$, SE < 2.5 kW m^{-2}, $p<0.001$) between BC and peak FRP. The results of the ANCOVA analysis identified significant interactions between all woody fuelbeds and pure *Pinus monticola* fuelbeds, indicating that the regression slope coefficients were significantly different (i.e. pure *Pinus monticola* fuelbeds produce greater peak FRP values than the woody fuelbeds at a given BC value). Slope coefficients for the woody fuelbeds generally increased with increasing SA/V for both fuel types, but were only significant between the largest dowel SA/V group (1390 m^{-1}) and the two other dowel SA/V groups (659 and 469 m^{-1}). Increasing heat release with increasing SA/V was also observed by Santoni *et al.* (2014) in dry pine needle fuelbeds burned in a forced flow combustion chamber. Specifically, modeled heat release rate (kW m^{-2}) increased as surface-area-to-volume ratio increased in needles from three *Pinus* species. Santoni *et al.* (2014) also identified fuelbed permeability as a significant driver of heat release, which is affected by the orientation and compactness of fuel particles. This factor could account for some of the variability in BC to peak FRP relationships in the current study. These observations may provide useful information and guidance for studies using FRP to characterize fire behavior (e.g. Kremens *et al.* 2012; Cannon *et al.* 2014; Hudak *et al.* 2016), post-fire vegetation response and mortality (e.g. Smith *et al.* 2017; Sparks *et al.* 2017), and fire regimes (e.g. Archibald *et al.* 2010; Andela *et al.* 2015). However, further work is necessary at the forest stand (e.g. Kremens *et al.* 2012; Sparks *et al.* 2017) and landscape spatial scales to confirm if and how these relationships scale.

There was little variation in observed combustion factors, even when considering all SA/V groups, fuelbed bulk densities, and fuel water content conditions (Figure 3a,b). There were no significant interactions between SA/V groups or between fuelbed bulk density groups, indicating that the regression slope coefficients (CFs) were not significantly different. Although dry and ambient laboratory derived CFs were not significantly different, ambient SA/V groups produced CFs consistently higher than their dry counterparts (Figure 3a,b). In the current study, the CF for fuels burned at <0.01 W_C was slightly lower than that

for fuels burned at 0.09 W_C (dry CF: 0.216 kg MJ^{-1}; ambient CF: 0.232 kg MJ^{-1}). This is mirrored in the literature where CFs are consistently higher across studies with wetter fuels (Freeborn *et al.*, 2008; Smith *et al.* 2013) and lower across studies with drier fuels (Wooster *et al.* 2005; Smith *et al.* 2013) (Table 1). The CF derived in Kremens *et al.* (2012) is slightly lower than expected for the reported fuel moisture content and could possibly be explained by the dry wood added to the fuelbeds during their experiments. Notably, biomass consumed estimates calculated using the universal CF from Kaiser *et al.* (2012) more than double those estimated with the next highest laboratory derived CF for extremely wet ($W_C > 0.25$) fuels (Smith *et al.* 2013). Ultimately, our data supports previous experiments highlighting moisture effects on biomass consumed estimates from FRE (Smith *et al.* 2013). Observed consumption was in strong agreement with modeled consumption (Figure 3c) using the water content adjusted biomass consumed to FRE relationship described in Smith *et al.* (2013).

Conclusions

Woody fuel CFs derived from this study have been presented over a range of fuel SA/V and loadings. SA/V did not have a significant impact on FRE derived from fuelbeds at dry or ambient fuel water content. Unlike FRE, peak values of FRP generally increased as SA/V increased. Linear relationships between biomass consumed and peak FRP in uniform and mixed fuelbeds at 0.0 W_C indicates that peak FRP could be modeled from biomass consumed estimates with further study. Although CFs have been observed to vary with changes in fuel water content in pine needles (Smith *et al.* 2013), woody fuels seem to be insensitive to small changes in fuel water content. CFs derived from our ambient woody fuels were slightly higher than dry fuels, but were within the margin of error for the CF derived from all fuels. This indicates that robust estimates of biomass consumed and carbon loss can be quantified using FRP and FRE methodology in fire prone ecosystems with significant woody fuels (e.g. boreal and temperate forest). Future work is needed to confirm these results in other fuel types and spatial scales to improve our understanding of CF uncertainty and characterization of wildland fires.

Acknowledgements

Equipment was provided by the Idaho Fire Initiative for Research and Education (IFIRE). We would like to thank the University of Idaho's Experimental Forest 2014 research crew and students from the College of Natural Resources for helping collect fuels and conduct laboratory fires. Partial funding for Sparks was provided by the Joint Fire Science Program under awards 13-1-05-7 and GRIN Award 16-2-01-09, and through the Idaho Space Grant Consortium which is funded by the National Aeronautics and Space Administration (NASA). This work was also partially funded by NASA under awards NNX11AO24G and NNX14AF96G and the National Science Foundation under grant no. DMS-1520873.

References

Al-Shemmeri TT, Yedla R, Wardle D (2015) Thermal characteristics of various biomass fuels in a small-scale biomass combustor. *Applied Thermal Engineering* **85**, 243-251.

Andela N, Kaiser JW, van der Werf GR, Wooster MJ (2015) New fire diurnal cycle characterizations to improve fire radiative energy assessments made from MODIS observations. *Atmospheric Chemistry and Physics* **15**, 8831-8846.

Andreae MO, Merlet P (2001) Emission of trace gases and aerosols from biomass burning, *Global Biogeochemical Cycles* **15**, 4, 955-966.

Archibald S, Scholes RJ, Roy DP, Roberts G, Boschetti L (2010) Southern African fire regimes as revealed by remote sensing. *International Journal of Wildland Fire* **19**, 7, 861-878.

Bergey EA, Getty GM (2006) A review of methods for measuring the surface area of stream substrates. *Hydrobiologia* **556**, 1, 7-16.

Boschetti L, Roy DP (2009) Strategies for the fusion of satellite fire radiative power with burned area data for fire radiative energy derivation. *Journal of Geophysical Research-Atmospheres* **114**, (D20).

Bowman DMJS, Balch JK, Artaxo P, Bond WJ, Carlson JM, Cochrane MA, D'Antonio CM, DeFries RS, Doyle JC, Harrison SP, Johnston FH, Keeley JE, Krawchuk MA, Kull CA, Marston JB, Moritz MA, Prentice IC, Roos CI, Scott AC, Swetnam TW, van der Werf GR, Pyne SJ (2009) Fire in the earth system. *Science* **324**, 5926, 481-484, doi:10.1126/science.1163886.

Bowman DMJS, Williamson G, Kolden CA, Abatzoglou, JT Cochrane MA, Smith AMS. Human exposure and sensitivity to globally extreme wildfire events, *Nature: Ecology and Evolution, in review.*

Brewer NW, Smith AMS, Hatten JA, Higuera PE, Hudak AT, Ottmar RD, Tinkham WT (2013) Fuel moisture influences on fire-altered carbon in masticated fuels: An experimental study. *Journal of Geophysical Research* **118**, 30-40, doi:10.1029/2012JG002079.

Brown JK (1970) Ratios of surface area to volume for common fine fuels. *Forest Science* **16**, 1, 101-105.

Cannon J, O'Brien J, Loudermilk E, Dickinson M, Peterson C (2014) The influence of experimental wind disturbance on forest fuels and fire characteristics. *Forest Ecology and Management* **330**, 294–303.

Dickinson MB, Hudak AT, Zajkowski T, Loudermilk EL, Schroeder W, Ellison L, Kremens RL, Holley W, Martinez O, Paxton A, Bright BC (2016) Measuring radiant emissions from entire prescribed fires with ground, airborne and satellite sensors–RxCADRE 2012. *International Journal of Wildland Fire* **25**, 1, 48-61.

Dozier J (1981) A method for satellite identification of surface temperature fields of subpixel resolution. *Remote Sensing of Environment* **11**, 221-229.

Fasth B, Harmon ME, Woodall CW, Sexton J (2010) Evaluation of techniques for determining the density of fine woody debris. Research Paper NRS-11, USDA Forest Service, Northern Research Station, Newton Square, PA.

Fernandes PM, Rego FC (1998) A new method to estimate fuel surface area-to-volume ratio using water immersion. *International Journal of Wildland Fire* **8**, 2, 59-66.

Finney MA, Cohen JD, McAllister SS, Jolly WM (2013) On the need for a theory of wildland fire spread. *International Journal of Wildland Fire* **22**, 1, 25-36.

Frankman D, Webb BW, Butler BW, Jimenez D, Forthofer JM, Sopko P, Shannon KS, Hiers JK, Ottmar RD (2013) Measurements of convective and radiative heating in wildland fires. *International Journal of Wildland Fire* **22**, 2, 157-167.

Freeborn PH, Wooster MJ, Hao WM, Ryan CA, Nordgren BL, Baker SP, Ichoku SPC (2008) Relationships between energy release, fuel mass loss, and trace gas and aerosol emissions during laboratory biomass fires. *Journal of Geophysical Research-Atmospheres* **113**, D1, 1-17, doi: 10.1029/2007JD008679.

Freeborn PH, Wooster MJ, Roy DP, Cochrane MA (2014) Quantification of MODIS fire radiative power (FRP) measurement uncertainty for use in satellite-based active fire

characterization and biomass burning estimation. *Geophysical Research Letters* **41**, 6, 1988-1994.

Hartigan JA, Wong MA (1979) A K-means clustering algorithm. *Applied Statistics* **28**, 100–108.

Heward H, Smith AMS**,** Roy DP, Tinkham WT, Hoffman CM, Morgan P, Lannom KO (2013) Is burn severity related to fire intensity? Observations from landscape scale remote sensing. *International Journal of Wildland Fire* **9**, 910-918, doi: 10.1071/WF12087.

Hudak AT, Dickinson MB, Bright BC, Kremens RL, Loudermilk EL, O'Brien JJ, Hornsby BS and Ottmar RD (2016) Measurements relating fire radiative energy density and surface fuel consumption-RxCADRE 2011 and 2012. *International Journal of Wildland Fire* **25**, 1, 25-37, doi:10.1071/WF14159.

Hyde JC, Yedinak K, Talhelm AF, Smith AMS, Bowman DMJS, Johnson F, Lahm P, and Fitch M**.** A review of United States air quality policy considering smoke from wildland fires, *International Journal of Wildland Fire, in review.*

Ichoku C, Kaufman YJ (2005) A method to derive smoke emission rates from MODIS fire radiative energy measurements. *Geoscience and Remote Sensing, IEEE Transactions on* **43**, 11, 2636-2649.

Kaiser JW, Heil A, Andreae MO, Benedetti A, Chubarova N, Jones L, Morcrette J, Razinger M, Schultz MG, Suttie M, Werf GR (2012) Biomass burning emissions estimated with a global fire assimilation system based on observed fire radiative power. *Biogeosciences* **9**, 527-554. doi:10.5194/bg-9-527-2012.

Konovalov IB, Beekmann M, Kuznetsova IN, Yurova A, Zvyagintsev AM (2011) Atmospheric impacts of the 2010 Russian wildfires: integrating modelling and measurements of the extreme air pollution episode in the Moscow megacity region. *Atmospheric Chemistry and Physics* **11**, 4, 12141-12205.

Konovalov IB, Berezin EV, Ciais P, Broquet G, Beekmann M, Hadji-Lazaro J, Clerbaux C, Andreae MO, Kaiser JW, Schulze ED (2014) Constraining CO_2 emissions from open biomass burning by satellite observations of co-emitted species: a method and its application to wildfires in Siberia. *Atmospheric Chemistry and Physics* **14**, 10383-10410.

Korontzi S, Ward DE, Susott RA, Yokelson RJ, Justice CO, Hobbs PV, Smithwick EAH, Hao WM (2003) Seasonal variation and ecosystem dependence of emission factors for selected trace gases and PM2.5 for southern African savanna fires. *Journal of Geophysical Research-Atmospheres* **108**, (D24).

Kremens RL, Smith AMS, Dickinson MB (2010) Fire Metrology: Current and Future Directions in Physics-Based Measurements. *Fire Ecology* **6**, 13-35. doi:10.4996/fireecology.0601013.

Kremens RL, Dickinson MB, Bova A (2012) Radiant flux density, energy density and fuel consumption in mixed-oak forest surface fires. *International Journal of Wildland Fire* **21**, 722, doi:10.1071/WF10143.

Kreye JK, Varner JM, Knapp EE (2012) Moisture desorption in mechanically masticated fuels: effects of particle fracturing and fuelbed compaction. *International Journal of Wildland Fire* **21**, 7, 894-904.

Kumar SS, Roy DP, Boschetti L, Kremens R (2011) Exploiting the power law distribution properties of satellite fire radiative power retrievals: A method to estimate fire radiative energy and biomass burned from sparse satellite observations. *Journal of Geophysical Research-Atmospheres* **116**, (D19).

Lapina K, Honrath RE, Owen RC, Val Martin M, Hyer EJ, Fialho P (2008) Late summer changes in burning conditions in the boreal regions and their implications for NOx and CO emissions from boreal fires. *Journal of Geophysical Research-Atmospheres* **113**, (D11).

Lu H, Ip E, Scott J, Foster P, Vickers M, Baxter LL (2010) Effects of particle shape and size on devolatilization of biomass particle. *Fuel* **89**, 5, 1156-1168.

Mathews B.J., E.K. Strand, A.M.S. Smith, A.T. Hudak, M.B. Dickinson, and R.L. Kremens (2016), Laboratory experiments to estimate interception of infrared radiation by tree canopies, *International Journal of Wildland Fire* **25**, 9, 1009-1014, doi: 10.1071/WF16007.

McCarty JL, Ellicott EA, Romanenkov V, Rukhovitch D, Koroleva P (2012) Multi-year black carbon emissions from cropland burning in the Russian Federation. *Atmospheric Environment* **63**, 223-238.

Mebust AK, Russell AR, Hudman RC, Valin LC, Cohen RC (2011) Characterization of wildfire NOx emissions using MODIS fire radiative power and OMI tropospheric NO2 columns. *Atmospheric Chemistry and Physics* **11**, 5839-5851.

Mebust AK, Cohen RC (2013) Observations of a seasonal cycle in NOx emissions from fires in African woody savannas. *Geophysical Research Letters* **40**, 7, 1451-1455.

Paugam R, Wooster MJ, Roberts G (2013) Use of handheld thermal imager data for airborne mapping of fire radiative power and energy and flame front rate of spread. *Geoscience and Remote Sensing, IEEE Transactions on* **51**, 6, 3385-3399.

R Core Team (2014) R: A Language and Environment for Statistical Computing (Vienna, Austria: R Foundation for Statistical Computing).

Santoni PA, Bartoli P, Simeoni A, Torero JL (2014) Bulk and particle properties of pine needle fuel beds–influence on combustion. *International Journal of Wildland Fire* **23**, 8, 1076-86.

Schroeder W, Ellicott E, Ichoku C, Ellison L, Dickinson M, Ottmar R, Clements C, Hall D, Ambrosia V, Kremens R (2014) Integrated active fire retrievals and biomass burning emissions using complementary near-coincident ground, airborne and spaceborne sensor data. *Remote Sensing of Environment* **140**, 719-730, doi:10.1016/j.rse.2013.10.010.

Seiler W, Crutzen PJ (1980) Estimates of gross and net fluxes of carbon between the biosphere and the atmosphere from biomass burning. *Climatic Change* **2**, 3, 207-247.

Simeoni A, Salinesi P, Morandini F (2011) Physical modelling of forest fire spreading through heterogeneous fuel beds. *International Journal of Wildland Fire* **20**, 5, 625-632.

Smith AMS, Tinkham WT, Roy DP, Boschetti L, Kumar S, Sparks AM, Kremens RL, Falkowski MJ (2013) Quantification of fuel moisture effects on biomass consumed derived from fire radiative energy retrievals. *Geophysical Research Letters* **40**, 23, 6298-6302, 10.1002/2013GL058232.

Smith AMS, Kolden CA, Paveglio TB, Cochrane MA, Bowman DM, Moritz MA, Kliskey AD, Alessa L, Hudak, Hoffman CM, Lutz JA, Queen LP, Goetz SJ, Higuera PE, Boschetti L, Flannigan M, Yedinak KM, Watts AC, Strand EK, Wagtendonk JWV, Anderson JW, Stocks BJ, Abatzoglou JT (2016a) The Science of Firescapes: Achieving Fire-Resilient Communities. *BioScience* **66**, 130-146.

Smith AMS, Sparks AM, Kolden CA, Abatzoglou JT, Talhelm AF, Johnson DM, Boschetti L, Lutz JA, Apostol KO, Yedinak KM, Tinkham WT (2016b) Towards a new paradigm in fire severity research using dose-response experiments. *International Journal of Wildland Fire* **25**, 2, 158–166.

Smith AMS, Talhelm AF, Johnson DM, Sparks AM, Yedinak KM, Apostol KG, Tinkham WT, Kolden CA, Abatzoglou JT, Lutz JA, Davis AS, Pregitzer KS, Adams HD, Kremens RL. (2017) Impacts of fire radiative energy density doses on *Pinus contorta* and *Larix occidentalis* seedling physiology and mortality, *International Journal of Wildland Fire,* doi 10.1072/WF16077.

Sparks AM, Kolden CA, Talhelm AF, Smith AMS, Apostol KG, Johnson DM, Boschetti L (2016) Spectral indices accurately quantify changes in tree physiology following fire: toward mechanistic assessments of landscape post-fire carbon cycling. *Remote Sensing* **8**, 7, 572.

Sparks AM, Smith AMS, Talhelm AF, Kolden CA, Yedinak KM, Johnson DM (2017), Impacts of fire radiative flux on mature Pinus ponderosa growth and vulnerability to secondary mortality agents. *International Journal of Wildland Fire* **26**, 95-106, doi:10.1072/WF16139.

Van der Werf GR, Randerson JT, Giglio L, Collatz GJ, Mu M, Kasibhatla PS, Morton DC, DeFries RS, Jin YV, van Leeuwen TT (2010) Global fire emissions and the contribution of deforestation, savanna, forest, agricultural, and peat fires (1997–2009). *Atmospheric Chemistry and Physics* **10**, 23, 11707-35.

Wooster MJ, Roberts G, Perry G, Kaufman YJ (2005) Retrieval of biomass combustion rates and totals from fire radiative power observations: calibration relationships between biomass consumption and fire radiative energy release. *Journal of Geophysical Research* **110**, D24, doi: 10.1029/2005JD006018.

Wooster MJ, Freeborn PH, Archibald S, Oppenheimer C, Roberts GJ, Smith TEL, Govender N, Burton M, Palumbo I (2011) Field determination of biomass burning emission ratios and factors via open-path FTIR spectroscopy and fire radiative power assessment: headfire, backfire and residual smoldering combustion in African savannahs. *Atmospheric Chemistry and Physics* **11**, 22, 11591-11615.

Yang YB, Ryu C, Khor A, Yates NE, Sharifi VN, Swithenbank J (2005) Effect of fuel properties on biomass combustion. Part II. Modelling approach—identification of the controlling factors. *Fuel* **84**, 16, 2116-2130.

Zhang X, Kondragunta S, Ram J, Schmidt C, Huang HC (2012) Near-real-time global biomass burning emissions product from geostationary satellite constellation. *Journal of Geophysical Research-Atmospheres* **117**, (D14).

Tables

Table 1. Combustion factors (CF: kg MJ^{-1}) and radiative fraction (f_r) derived from lab and field experimental studies and modeling. Fuel moisture content (FMC, calculated on dry weight basis) is used for comparison to other studies.

Fuel Type	FMC (%)	CF (kg MJ^{-1})		f_r (%)		Reference
Observed						
Grass, wood, shrub mix		0.195				Frankman *et al.* 2013
Pinus ponderosa, birch wood	<1	0.216	± 0.041	25	± 5	*This study*
Pinus ponderosa, birch wood	10	0.232	± 0.046	23	± 1	*This study*
Grass		0.261				Schroeder *et al.* 2014
Oak savannah litter	7.3 - 27.4	0.299		17	± 3	Kremens *et al.* 2012
Pinus monticola needles	<1	0.325	± 0.008	15	± 1.0	Smith *et al.* 2013
Miscanthus grass	12	0.368	± 0.015	13	± 3.0	Wooster *et al.* 2005
Grass, wood, shrub mix	7.1 - 44.8	0.453	± 0.068	11.7	± 2.4	Freeborn *et al.* 2008
Modeled						
AGOS[a]		0.13				Kaiser *et al.* 2012
SAOS[a]		0.26				Kaiser *et al.* 2012
AG[a]		0.29				Kaiser *et al.* 2012
Grass		0.3-0.31	± 0.37-0.38			Konovalov *et al.* 2014
Forest		0.3-0.52	± 0.33-0.56			Konovalov *et al.* 2014
EF[a]		0.49				Kaiser *et al.* 2012
Pinus monticola needles	>25	0.59	± 0.065	8	± 1.0	Smith *et al.* 2013
Forest		0.66-0.85	± 0.81-1.05			Konovalov *et al.* 2014
Grass		0.69-0.86	± 1.13-1.24			Konovalov *et al.* 2014
SA[a]		0.78				Kaiser *et al.* 2012
TF[a]		0.96				Kaiser *et al.* 2012
Universal		1.37				Kaiser *et al.* 2012
EFOS[a]		1.55				Kaiser *et al.* 2012
Peat		5.87				Kaiser *et al.* 2012

[a]Land cover class: AGOS: agriculture with organic soil, SAOS: savannah with organic soil, AG: agriculture, EF: extratropical forest, SA:savannah, TF: tropical forest, EFOS: extratropical forest with organic soil

Figures

Figure 1. Birch dowels and chipped *Pinus ponderosa* wood particles displayed by surface-area-to-volume ratio (SA/V: m-1) group. Horizontal dotted lines represent mean SA/V 95% confidence intervals. Right panes show typical dowel (upper right) and chipped (lower right) laboratory fuelbeds consisting of a uniform mix of wood particles and *Pinus monticola* needles.

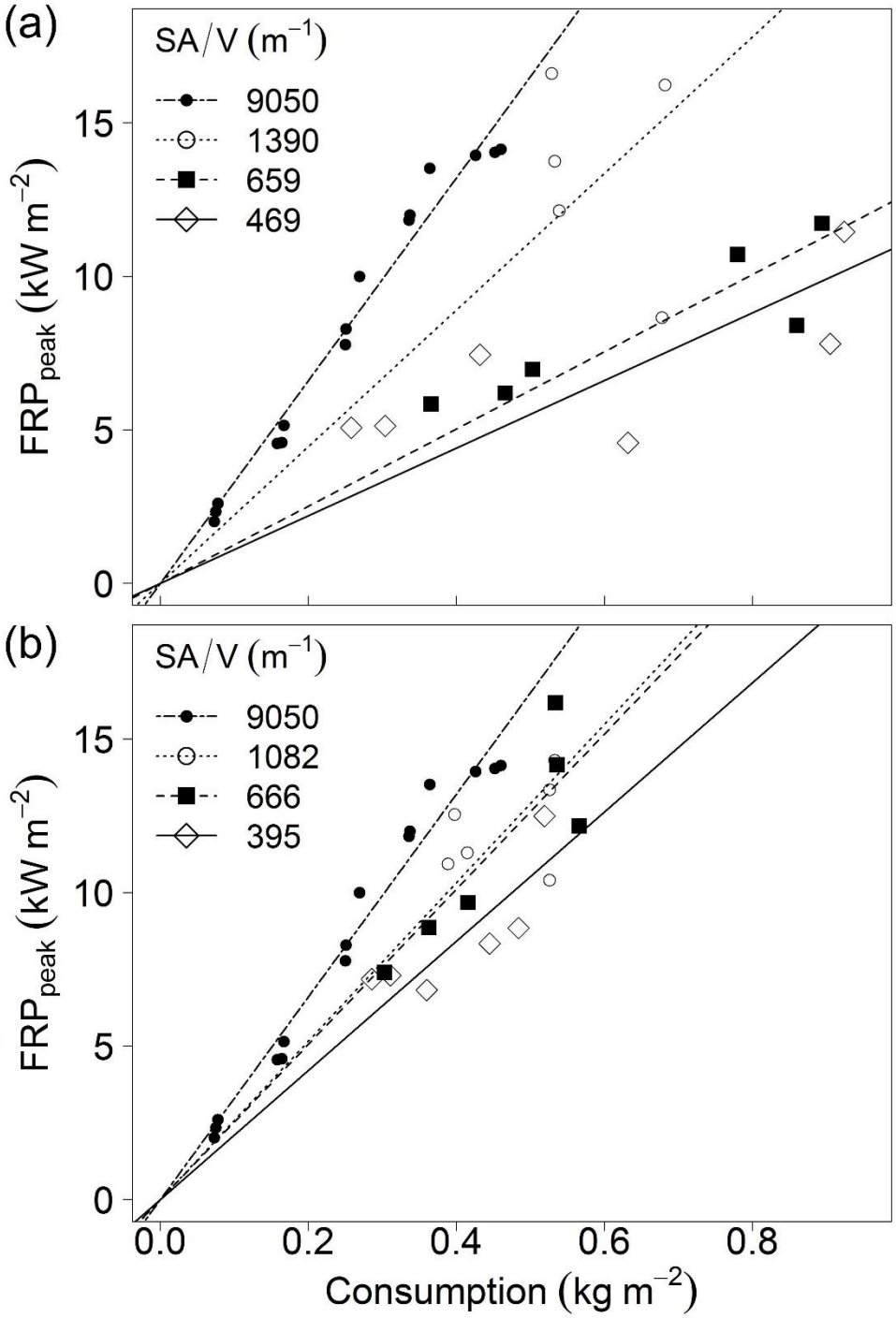

Figure 2. Relationships between biomass consumed (BC) and peak fire radiative power (FRP) for all surface-area-to-volume ratio (SA/V) groups for, a) dowel fuelbeds at 0.0 fuel water content (WC), and b) chipped *Pinus ponderosa* fuelbeds at 0.0 WC. The relationship for pure *Pinus monticola* (SA/V: 9050 m-1) fuelbeds (data from Smith et al. (2013)) is also shown in both panes for comparison purposes. Lines represent the ordinary least squares (OLS) linear best fit through the origin between consumption and peak FRP for each SA/V group.

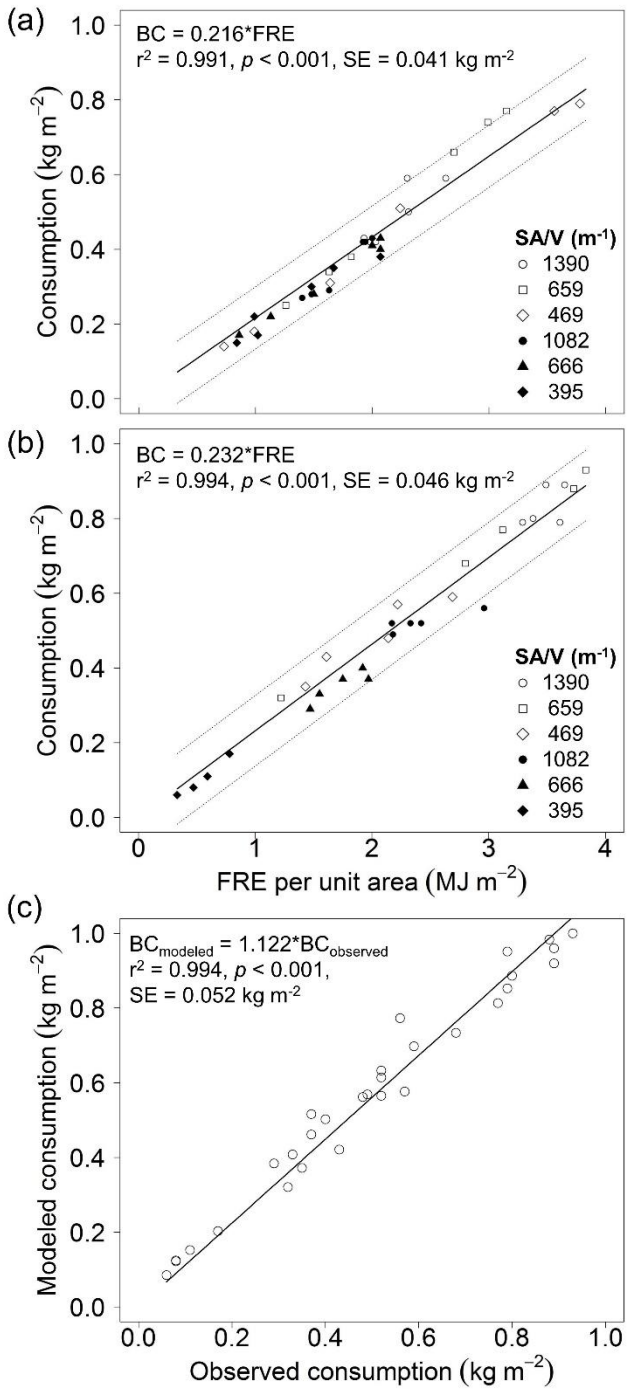

Figure 3. Relationship between fire radiative energy (FRE) and biomass consumed (BC) for all surface-area-to-volume ratio (SA/V) groups for dry fuels (a) and ambient water content fuels (b). Hollow markers represent dowels and solid markers represent chipped wood particles. The relationship between observed and predicted consumption using the water content adjusted biomass consumed-to-FRE model from Smith *et al.* (2013) is also shown (c). In all panes, the solid line represents the ordinary least squares (OLS) linear best fit through the origin between consumption and FRE and the dashed lines represent the 95% prediction interval.

Appendix B

Copyright Statements

MDPI Open Access Information and Policy

Remote Sensing

All articles published by MDPI are made immediately available worldwide under an open access license. This means:

- everyone has free and unlimited access to the full-text of all articles published in MDPI journals, and
- everyone is free to re-use the published material if proper accreditation/citation of the original publication is given.
- open access publication is supported by the authors' institutes or research funding agencies by payment of a comparatively low Article Processing Charge (APC) for accepted articles.

CSIRO Publishing Copyright Statement

International Journal of Wildland Fire

To protect the significant investment by both parties, CSIRO Publishing requires an exclusive, worldwide Licence to Publish that clearly stipulates our rights and the specific rights retained by our authors. Authors retain the right to: Use the work for non-commercial purposes within their institution subject to the usual copyright licensing agency arrangements. Use the work for further research and presentations at meetings and conferences. Use the illustrations (line art, photographs, figures, plates) and research data in their own future works. Share print or digital copies of their work with colleagues for personal use or study. Include the work in part or in full in a thesis provided it is not published for commercial gain. Place his/her pre-publication version of the work on a pre-print server. Place his/her pre-publication version of the work on a personal website or institutional repository on condition that there is a link to the definitive version on the CSIRO Publishing web site. Authors may also order hardcopy reprints of their papers at the time they complete author corrections. Authors may create links to their papers from their personal webpages.

CSIRO Publishing supplies the corresponding authors with a free PDF of their paper upon publication. This file can be used to:

- send to individual colleagues for non-commercial purposes
- print out and distribute to colleagues attending any conference presentation you make
- include in a course pack, subject to the usual copyright licensing agency arrangements.

However, the PDF may not be included on any website or on any server, including an institutional repository without prior approval. Authors are expected to clear all third party intellectual property rights and obtain formal permission from their respective institutions before submission, where necessary.